

# TI Designs Temperature Sensor Interface Module for Programmable Logic Controllers (PLC)



## TI Designs

TI Designs provide the foundation that you need including methodology, testing and design files to quickly evaluate and customize the system. TI Designs help you accelerate your time to market.

## Design Resources

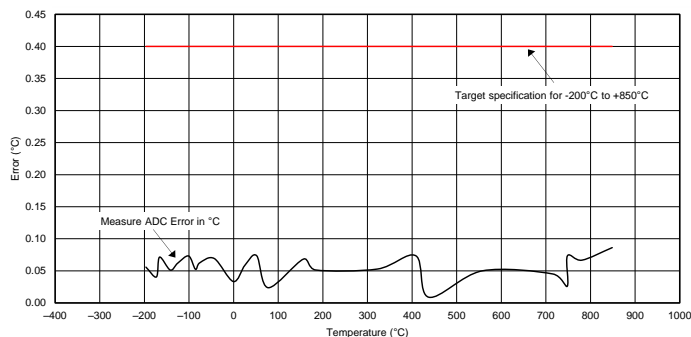
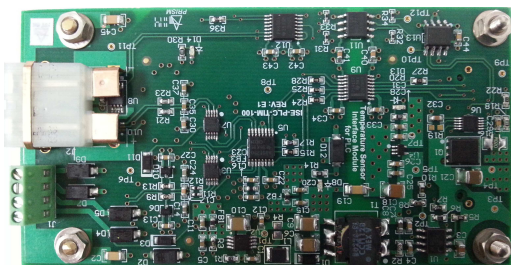
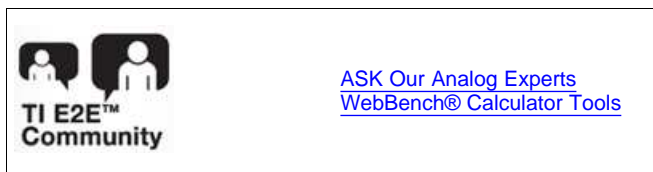
<a href="#">TIDA-00018</a>	Tool Folder Containing Design Files
<a href="#">ADS1220</a>	Product Folder
<a href="#">LM5017</a>	Product Folder
<a href="#">LM5069</a>	Product Folder
<a href="#">ISO7141CC</a>	Product Folder
<a href="#">ISO1540</a>	Product Folder
<a href="#">TPS71533</a>	Product Folder
<a href="#">TPS7A4901</a>	Product Folder
<a href="#">TCA6408A</a>	Product Folder
<a href="#">LM94022</a>	Product Folder
<a href="#">LMP275</a>	Product Folder
<a href="#">TS5A23159</a>	Product Folder

## Design Features

- Two Different Sensor Input Channels:
  - K-Type Thermocouple Input with CJC
  - Compatible to 2-, 3-, or 4-Wire RTD Probes
- Ratiometric Measurement for RTD
- Measurement Accuracy for Thermocouple  $\pm 1^{\circ}\text{C}$
- Measurement Accuracy for RTD  $\pm 0.4^{\circ}\text{C}$
- Sensor Open Circuit/Signal Out-of-Range Detection
- Digital Isolation for I/O Controller Interface
- 24 V  $\pm 20\%$  Input Power Supply Operation
- IEC-61000-4-4: EFT Up to  $\pm 1$  KV at 5 KHz on Signal Ports
- IEC-61000-4-2: ESD Up to 4-KV Contact and 8-KV Air Discharge
- IEC-61000-4-5: Surge Up to  $\pm 1$ -KV Line-Earth (CM) on Signal Ports

## Featured Applications

- Programmable Logic Controllers
- Factory Automation and Process Control
- Portable Instrumentation
- Data Acquisition Systems
- Industrial Robotics



**Measured Error of RTD Input  
across Temperature Range of  $-200^{\circ}\text{C}$  to  $850^{\circ}\text{C}$**

All trademarks are the property of their respective owners.



An IMPORTANT NOTICE at the end of this TI reference design addresses authorized use, intellectual property matters and other important disclaimers and information.

## 1 Design Specifications and Features

Table 1 shows the design specifications of the *Temperature Sensor Interface Module for Programmable Logic Controllers (PLC)* reference design:

Table 1.

PARAMETER	SPECIFICATIONS and FEATURES
Inputs	Two channels
Sensor Types	K-Types thermocouple 2-, 3-, and 4-wire PT100 RTD probes (Hardware supports RTDs with resistance up to 2 kΩ, whereas existing TIVA MCU software is implemented for PT100 RTD only)
Overall Measurement Accuracy (excluding sensor errors)	<b>For thermocouple channel:</b> ±1.0°C; Over the entire TC temperature Range: –200°C to 1372°C <b>For RTD channel:</b> ±0.4°C; Over the entire RTD temperature Range: –200°C to 850°C
Resolution	<b>For thermocouple channel:</b> 0.1°C <b>For RTD channel:</b> 0.025°C
Cold Junction Compensation (CJC) Type	On-board local temperature sensor IC
Cold Junction Compensation Temperature Range	0°C to 60°C
Measurement Type	Ratiometric for RTD
Sensor Linear Interpolation	PT100 RTD (–200°C to 850°C) and Thermocouple (–200°C to 1372°C) lookup tables implemented in TIVA™ MCU software
Module Calibration	ADC's offset and gain calibration
Power Supply Range	18 V to 32-V DC
Isolation	250-V DC (Continuous), Basic isolation 1500-V AC for one minute
ESD Immunity	<b>IEC 61000-4-2:</b> 4 kV contact discharges, 8 kV air discharges
EFT Immunity	<b>IEC 61000-4-4:</b> ±1 kV at 5 kHz on signal ports
Surge Transient Immunity	<b>IEC 61000-4-5:</b> ±1 kV line-earth (CM) on signal ports
Operating Temperature Range	0°C to 60°C
Storage Temperature	–40°C to 85°C
Temperature, Surrounding Air	60°C
Connector(s)	50-pin connector pluggable to <i>PLC I/O Module Front-End Controller Using a Tiva C Series ARM® Cortex™-M4 MCU (TIDU191)</i> 4-pin screw terminal block for 2-, 3-, and 4-wire RTD probes 2-pin dedicated K-type thermocouple connector
Form Factor (L x W)	90.0 mm x 50.8 mm (Small industrial form factor)

## 2 Overview

The sole objective of this reference design is to focus on the complete circuit design guidelines that help engineers and system architects to develop high precision temperature measurement solutions using 24-bit delta-sigma ADC and most widely used temperature sensors like thermocouples and Resistance Temperature Detectors (RTDs). This reference design addresses sensor signal conditioning, thermocouple cold junction compensation, ratiometric measurement technique for RTDs, recommended software flow, sensor linearization, sensor diagnostics, transient protection, PCB layout, and other practical design considerations for achieving high-precision robust design for temperature measurement in industrial applications.

The Temperature Sensor Interface Module is a fully isolated design which is essential for small sensor signal measurement. The signal chain and power line galvanic isolation barrier between the host controller side and the measurement side have been achieved using digital isolators and a flyback transformer, respectively. The heart of this reference design is the ADS1220 device, a 24-bit delta-sigma ADC, which provides a high resolution, high integration, low noise, and low cost complete sensor analog front-end for DC sensing applications. This design is also suitable to interface with different types of sensors. This design saves on board space, reduces design efforts, reduces time to market, and reduces cost. This reference design also demonstrates other TI products, such as hot swap and in-rush current limit controller, isolated Fly-Buck™ controller, low noise LDO, digital isolators, local temperature sensors, analog switch and I<sup>2</sup>C to GPIO expander that can be used in the entire PLC signal processing chain.

Furthermore, external protection circuitry is deployed in-place. This circuitry has been successfully tested and verified for compliance with regulatory IEC61000-4 standards: EFT, ESD, and Surge requirements. EMC compliance with standard IEC61000-4 is necessary to ensure that the design not only survives but also performs as intended in harsh or noisy industrial environments.

All the relevant design files like Schematics, BOM, Layer Plots, Altium Files, Gerber, and TIVA™ C-Series MCU software are executable with an easy-to-use Graphical User Interface (GUI). Users may download the files at [TIDA-00018](http://TIDA-00018).

## 3 Block Diagram

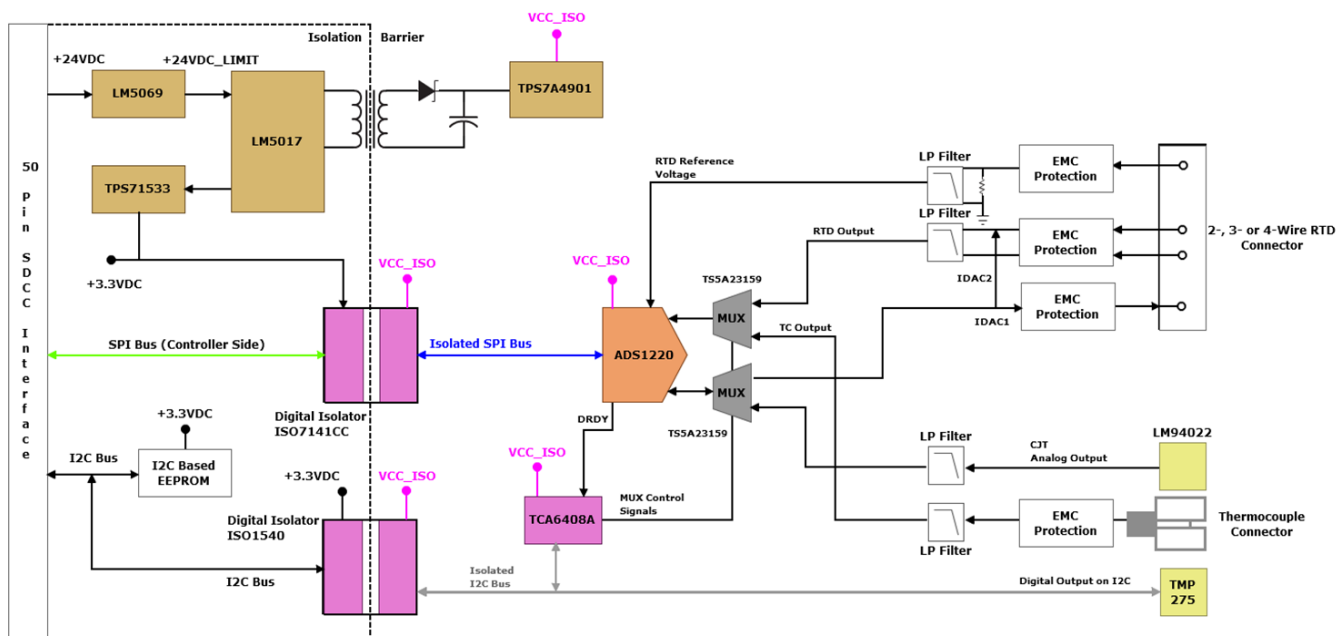


Figure 1. Block Diagram of Temperature Sensor Interface Module for PLC

## 4 System Description

The Temperature Sensor Interface Module provides two differential input channels to take measurements from two different sensors. One channel supports 2-, 3-, and 4-wire RTD. The other channel supports K-Type thermocouple temperature sensors. The design uses a single ADS1220 24-bit delta-sigma ADC with an external TS5A23159 dual channel 2 x 1 analog multiplexer. The multiplexer switches the two differential analog inputs to share the same ADC. The host controller communicates with TCA6408A - I<sup>2</sup>C to the GPIO expander over an I<sup>2</sup>C bus, crossing the isolation barrier via the ISO1540 bi-directional I<sup>2</sup>C digital isolator. TCA6408A in-turn controls TS5A23159 to route one of the two inputs to the ADC for measurement. The input channel selection is done in software.

Any signal coming in or going out of the module is protected against high voltage fast transient events, which are often expected in industrial environments. The protection circuitry makes use of TVS and ESD diodes. The temperature sensors (especially thermocouples) produce output in the millivolt range, which makes sensors prone to noise pickups. The RC low-pass differential and common mode filters are used on each analog input before it reaches the ADS1220. The filters effectively eliminates any high frequency noise pickup which may be present.

The design provides two local temperature sensor ICs to sense the cold junction (or reference junction) temperature. LM94022 is a multi-gain analog output type temperature sensor fed to ADS1220 after passing through a low pass filter and one additional TS5A23159 dual channel 2 x 1 analog multiplexer. Another local temperature sensor IC is the TMP275, which is a two-wire digital output temperature sensor directly interfaced to the I<sup>2</sup>C bus.


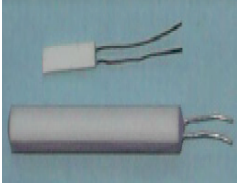
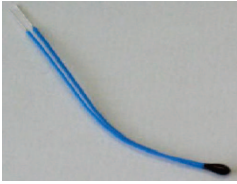

The data ready signal (DRDY) from ADS1220 reports the conversion status, which connects to the GPIO pin of TCA6408A, configured as input. Before reading the converted sensor data, the host controller polls for the data ready status latched inside the input port register of TCA6408A over the I<sup>2</sup>C bus.

## 5 Theory of Operation

Temperature is one of the oldest known physical quantities. Temperature is the most essential factor that needs continuous measurement, monitoring, and control in various processes in industry. Today, industry demands accurate, repeatable, and reliable measurement of temperature, because temperature can have significant impact on product cost, quality, efficiency and safety. All temperature sensors measure temperature by sensing some change in material physical characteristics as a function of temperature. Temperature sensors are available in a wide variety such as:

- Thermocouple
- Resistance Temperature Detector (RTD)
- Thermistor
- Semiconductor Temperature Sensor IC

**Table 2. Comparison of Different Temperature Sensors**

	THERMOCOUPLE	RESISTANCE TEMPERATURE DETECTOR (RTD)	THERMISTOR	SEMICONDUCTOR TEMPERATURE SENSOR IC
Range	-270°C to 2000°C	-200°C to 850°C	-50°C to 300°C	-55°C to 200°C
Changing Physical Characteristic	Voltage	Resistance	Resistance	Voltage or current
Excitation	Self-powered	Current excitation	Current excitation	Power Supply (µA)
Cost	Low	High	Low to moderate	Low
Response	Medium to fast	Medium	Medium to fast	Medium to fast
Accuracy	Less	Best	Good	Better
Repeatability	Reasonable	Excellent	Fair to Good	Good to excellent
Ruggedness	Very high (Can withstand high shock and vibration)	Less	High	Medium
Special Requirements	Amplification, Filtering, Cold junction compensation, Linearization	Lead Compensation, Filtering	Linearization	Power supply, Self-contained
Sensitivity at 20°C	Low (40 µV per °C for K-Type)	Medium	Very high	High (Typically 10 mV/°C)
Self-Heating	No	Very low to low	High	Very low to low
Lead Wire Resistance	Not a problem	Problematic	Not a problem	Not a problem
Interchangeability	Good	Excellent	Poor to fair	Better
Long Term Stability	Poor	Stable over long period; Typically Less than 0.1°C per year	Poor	Good
Noise Susceptibility	High	Medium	Low	Medium
Linearity	Fair	Good	Poor (Logarithmic)	Good
Size	Small to large	Medium to small	Small to medium	Small to medium but limited package choices
				

Among different types of temperature sensors, the most frequently used ones in industrial applications are thermocouples and resistance temperature detectors (RTDs).

5.1 Thermocouple Input Channel

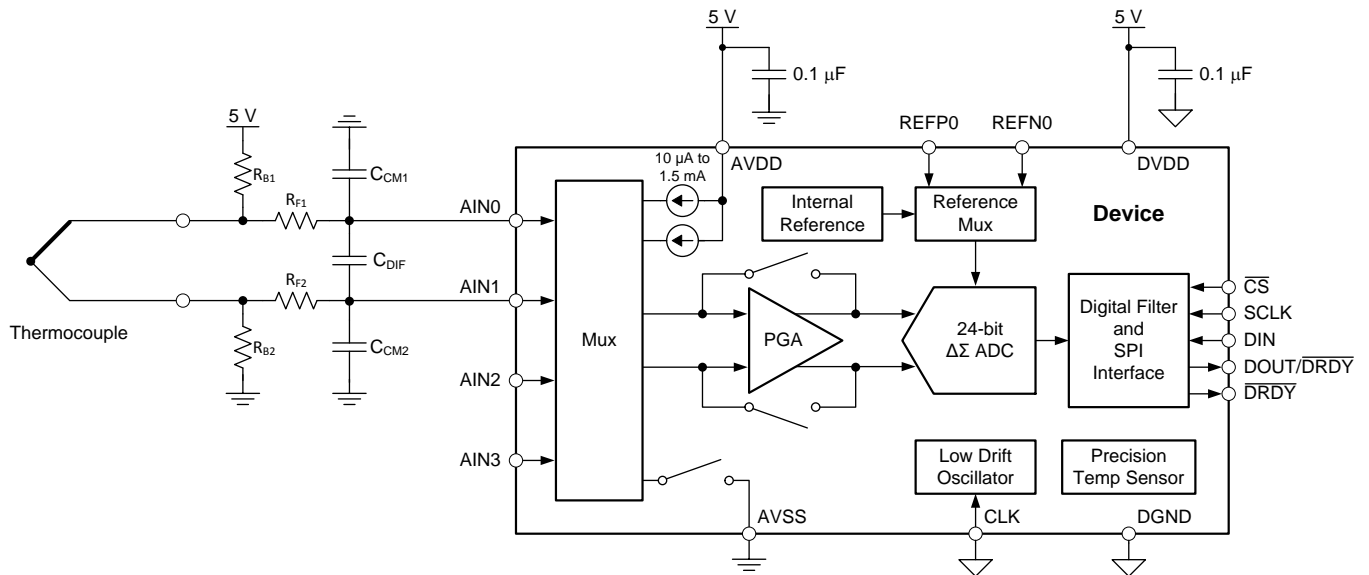


Figure 2. Thermocouple Measurement Circuit Using ADS1220

5.1.1 Thermocouple Fundamentals – “Back to Basics”

**NOTE:** Any conductor subjected to thermal gradient will generate a voltage between its ends.

A simple metal bar produces a voltage when there is a temperature difference between the two ends. The electrons at the hot end are more thermally agitated than the electrons at the cooler end. The more thermally agitated electrons on the hot end begin to diffuse towards the cooler end. The redistribution of electrons creates a negative charge at the cooler end and an equal positive charge at the hotter end. This process produces an electrostatic voltage between the two ends. The open circuit voltage produced in this way is known as “**Seebeck Voltage.**” The phenomenon is called the “**Seebeck Effect.**” The Seebeck Effect was first discovered by German scientist Thomas Johann Seebeck in 1821. Direct measurement of Seebeck Voltage of a single metal bar is impossible. Another similar metal bar will also produce the same Seebeck Voltage, cancelling each other and resulting in 0 V at the measuring point. However, a single wire does not form as a thermocouple. A thermocouple is formed when two dissimilar metals are bonded together electrically to form two junctions as shown in Figure 4.

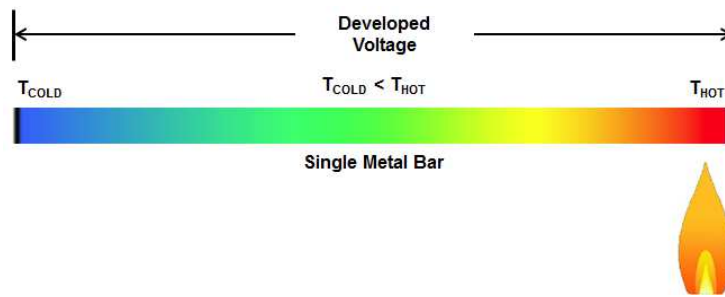


Figure 3. Voltage Developed Due to Temperature Gradient

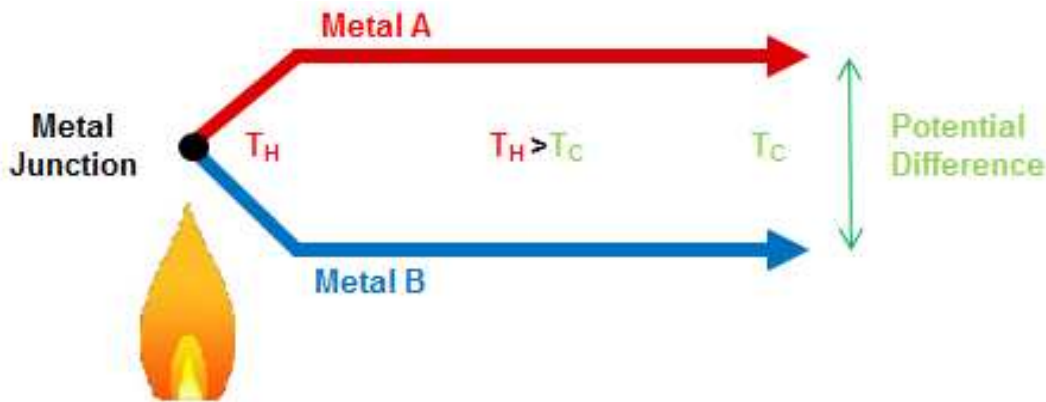


Figure 4. Thermocouple

The magnitude and direction of open circuit voltage developed between the two ends is proportional to the temperature difference, as shown in Figure 4 and Equation 1.

$$\Delta V = S \times (T_{HOT} - T_{COLD}) \tag{1}$$

where S is the **Seebeck coefficient** or **thermoelectric sensitivity**

When designing with thermocouples, it is important to understand that thermocouples are bipolar. Bipolar means thermocouples can produce a positive or a negative voltage, depending on whether or not the measured temperature is higher or lower than the system temperature, respectively.

The most misunderstood important point about a thermocouple is that virtually no voltage is developed at the junction. The junction is basically an electrical bond between two metals which complete the circuit, so that current flow can take place. Voltage is developed across each wire as temperature changes, as shown in Figure 5. The voltage difference is observed at the measuring end, because two dissimilar metals have different Seebeck coefficients.

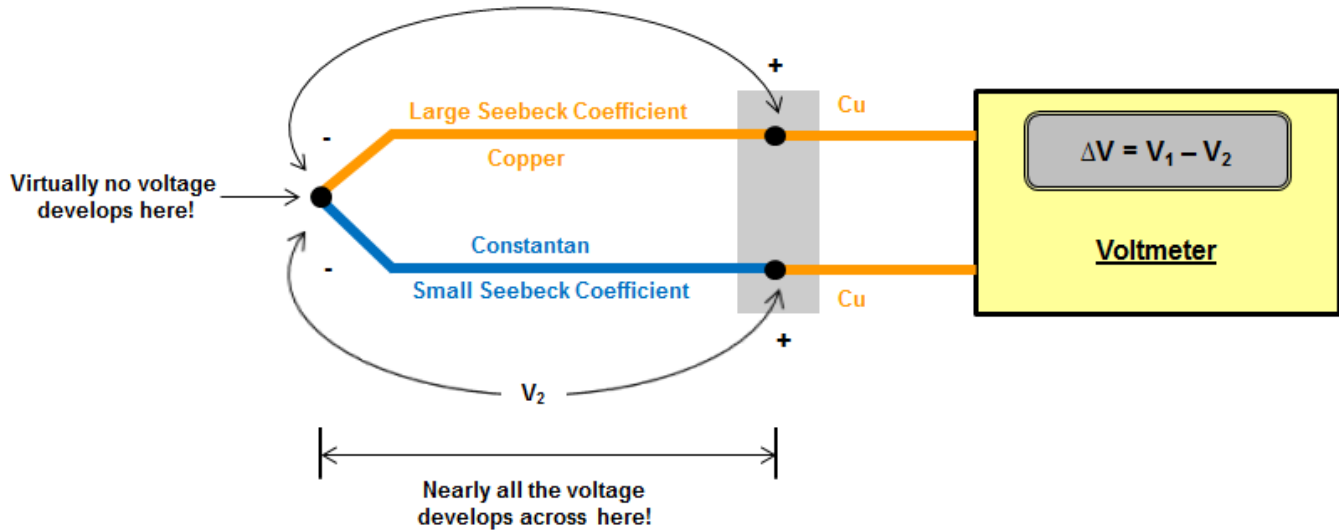


Figure 5. Thermocouple and Developed Voltage

Depending on the required temperature range, vibration resistance, chemical resistance, response time, and installation and equipment requirements, the designer can choose the appropriate thermocouple. Thermocouples are available in different combinations of metals and calibrations as given in Table 3.

Table 3. Types of Thermocouple

TYPE	TYPE E	TYPE K	TYPE J	TYPE R	TYPE S	TYPE T
Junction Material	Nickel –10% Chromium versus Constantan	Nickel –10% Chromium versus Nickel –5% Aluminum Silicon	Iron versus Constantan	Platinum –13%, Rhodium versus Platinum (–)	Platinum –10%, Rhodium versus Platinum (–)	Copper versus Constantan
Seebeck Coefficient at 20°C	62 μV/°C	40 μV/°C	62 μV/°C	7 μV/°C	7 μV/°C	40 μV/°C
Temperature Range	–100°C to 1000°C	0°C to 1370°C	0°C to 760°C	0°C to 1450°C	0°C to 1750°C	–160°C to 400°C
General Application	Cryogenic use; non-magnetic use	General purpose	Higher Sensitivity	High Resistance to oxidation and corrosion, calibration purposes	Standard for calibration for the melting point of gold	Often used in differential measurements



Each thermocouple sensor has its own sensitivity ( $\mu\text{V}/^\circ\text{C}$ ), a temperature range, and a nonlinear voltage curve over that temperature range, depending on its metals and calibration type. Thermocouple voltage curves are nonlinear over their operating temperature ranges, as can be seen in Figure 6.

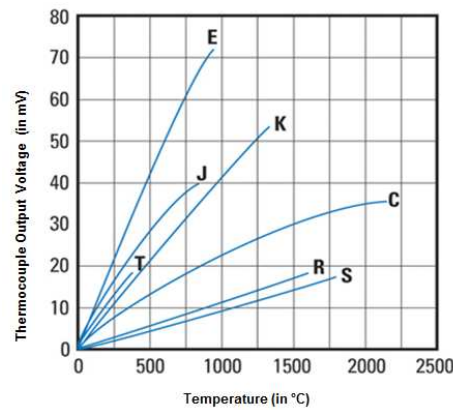


Figure 6. Thermocouple Output as a Function of Temperature

The Seebeck coefficient is a nonlinear function of temperature and causes the output voltages of thermocouples to be nonlinear over their operating temperature ranges. **Thermocouples are not perfectly linear across temperature.** As a best practice, always choose a thermocouple having less variation in its Seebeck coefficient.

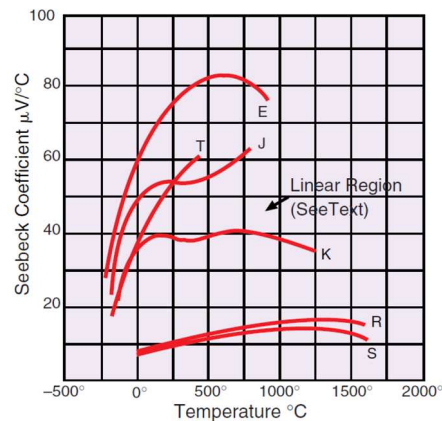


Figure 7. Temperature versus Seebeck Coefficient

### 5.1.2 Cold Junction Compensation (CJC)

A thermocouple measures the temperature difference between hot and cold junctions. Thermocouples do not measure the absolute temperature at one junction as illustrated in Figure 8. The cold junction is also sometimes referred to as the reference junction.

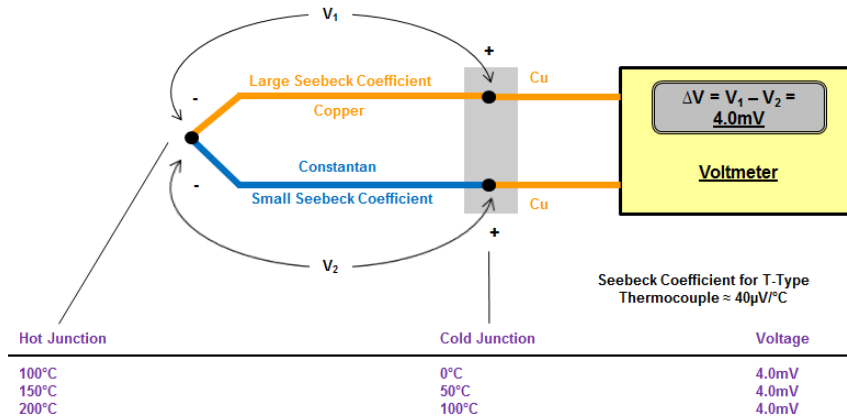


Figure 8. Simplified View of Cold Junction Compensation

The voltmeter measures the same voltage for all three example cases where 100°C temperature difference between hot and cold junctions always generates 4 mV. Connecting a voltmeter to measure the thermocouple output creates one more junction, J2. This junction also creates a small voltage and the difference between the two voltages is measured by the voltmeter. Figure 9 shows a unique case of a T-Type thermocouple (for simplicity, where the copper-to-copper connection does not form another junction). But when thermocouples other than T-Type are employed, two parasitic (unwanted) thermocouples are created with leads at the meter connection. In the PCB, these unwanted thermocouples are one of the biggest concerns. Each dissimilar metal connection creates a new thermocouple when proceeding from the measuring end to the wire connector, to the solder, to the copper PCB trace, to the IC pin, to the bonding wire, and to the chip or die contact. However, if the signal is differential (and each of the thermocouple pairs are at the same temperature), the thermocouple voltages will cancel (and have no net effect on the measurement). Therefore, the net voltage error added by these connections is zero.

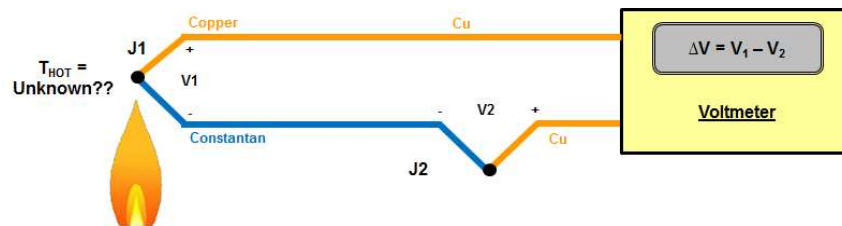


Figure 9. Unwanted Thermocouple Junction

Equation 2 shows how to calculate the temperature ( $T_{HOT}$ ) of measuring junction J1.

$$T_{HOT} = \frac{\Delta V}{S} + T_{COLD} \quad (2)$$

Equation 2 shows that to determine the temperature of a thermocouple hot junction, the temperature of the cold junction must be known. Classically, the cold junction of a thermocouple is kept in an ice bath as shown in Figure 10 to keep the cold junction at the known reference temperature of 0°C. The low 0°C temperature is another reason this junction is called the cold junction. In reality, it is impractical and inconvenient in most applications to provide a true ice point reference. The National Institute of Standards and Technology (NIST) thermocouple reference tables also assume that the cold junction is at 0°C.

For example, if a T-Type thermocouple produces an open circuit voltage of 3.4 mV with its cold junction reference temperature maintained at 0°C, what would be the temperature of the thermocouple's hot junction? Assume that Seebeck coefficient of the T-Type thermocouple is 40  $\mu\text{V}/^\circ\text{C}$ . The answer is that the temperature of the thermocouple's hot junction would be 85°C, as shown in Equation 3 and Figure 10.

$$T_{\text{HOT}} = \frac{3.4 \text{ mV}}{40 \mu\text{V}/^\circ\text{C}} + 0^\circ\text{C} = 85^\circ\text{C} \quad (3)$$

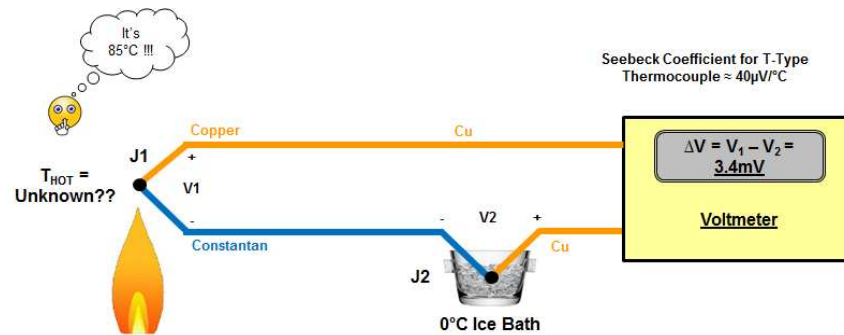


Figure 10. Measuring Absolute Temperature using 0°C Ice Bath

Therefore, in order to determine the correct absolute temperature at the measuring junction, it is necessary to know the cold junction reference temperature. In other words, additional measurement becomes mandatory (to determine the cold junction reference temperature). A more practical and logical approach is to use some other type of direct-reading temperature sensor means capable of absolute (not relative) measurement like RTD, Thermistor, or Sensor IC to measure the temperature at the reference junction. Then, use the temperature at the reference junction to compute the temperature at the measuring junction of thermocouple. This technique is called **Cold Junction Compensation (CJC)**.

Cold junction compensation can be either hardware compensation or software compensation. This reference design discusses and implements only software cold junction compensation. Software cold junction compensation is the most adaptable technique, because changing the type of thermocouple does not call for a change in the hardware. The one disadvantage is that software cold junction compensation requires a small amount of additional time to calculate the reference junction temperature.

The CJC is accomplished on-board by an LM94022 multiple gain analog temperature sensor having an accuracy of  $\pm 1.5^\circ\text{C}$  (max) specified from 0°C to 50°C and an TMP275 2-wire digital output temperature sensor having an accuracy of  $\pm 0.5^\circ\text{C}$  (max) specified from  $-20^\circ\text{C}$  to 100°C. The on-board temperature sensor IC continuously monitors the temperature at the cold junction to minimize reference errors. Only one direct-reading temperature sensor IC is sufficient to perform cold junction compensation. However, this reference design has two different devices so that their individual performances can be evaluated and compared. Accurate measurement of temperature at the cold junction is critical and has a direct impact on overall accuracy of thermocouple temperature measurement. In order to achieve accuracy, thermocouple terminals should have an isothermal connection to the board to minimize any potential temperature gradients. A large amount of copper offers a very good form of isothermal stabilization. An isothermal block or zone can be formed by creating islands of copper-fill in and around the junction on top, bottom, and inner layers, and then stitching the layers together using vias as shown in Figure 11. The local temperature sensor IC must be held isothermal with the thermocouple reference junction for proper compensation.

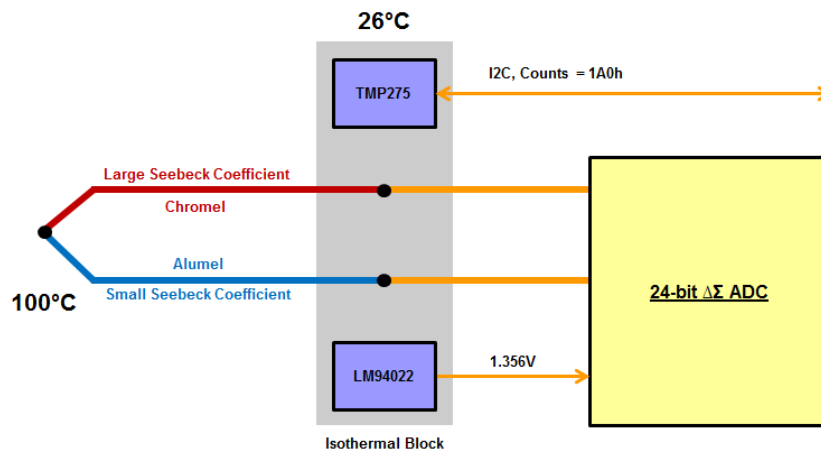


Figure 11. Isothermal Block

### 5.1.3 Piecewise Linear Approximation Method

If the cold junction is in a very stable environment, more periodic cold junction measurements are sufficient. In order to account for the cold junction, the local temperature sensor reading must first be converted to temperature ( $T_{CJ}$ ) by referring to the device lookup table or transfer function. The temperature is again translated to a voltage that is proportional to the thermocouple currently being used, to yield  $V_{CJ}$ . This process is generally accomplished by performing a reverse lookup on the table used for the thermocouple voltage-to-temperature conversion. Adding the two voltages yields the thermocouple-compensated voltage  $V_{ACTUAL}$ , where  $V_{CJ} + V_{TC} = V_{ACTUAL}$ .  $V_{ACTUAL}$  is then converted to temperature using the same lookup table from before, and yields  $T_{ACTUAL}$ . A block diagram showing this process is given in Figure 12.

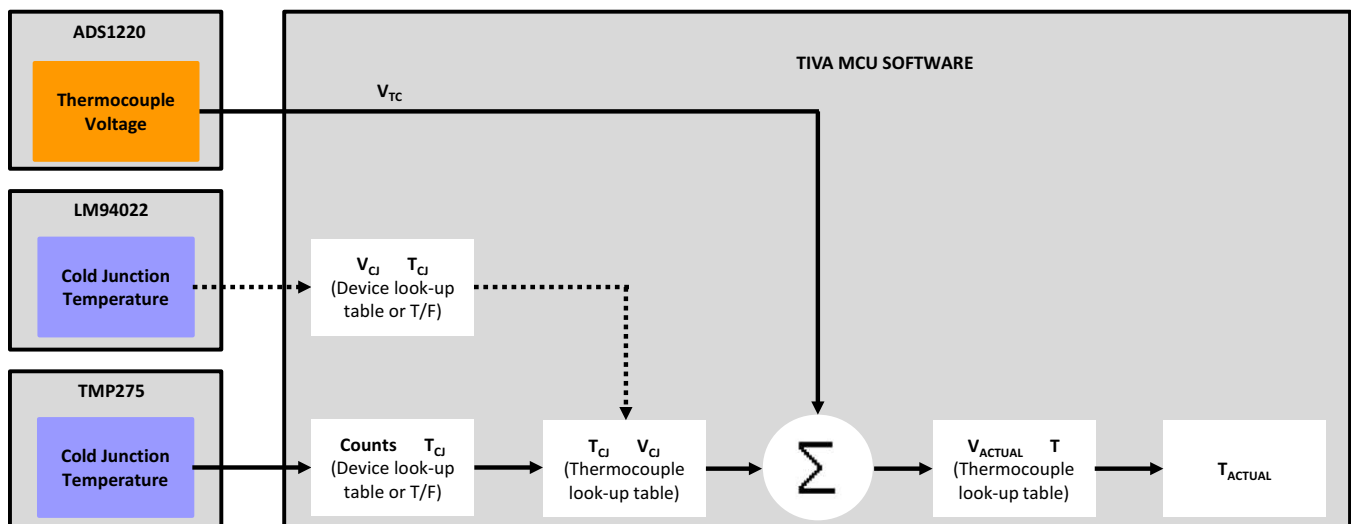
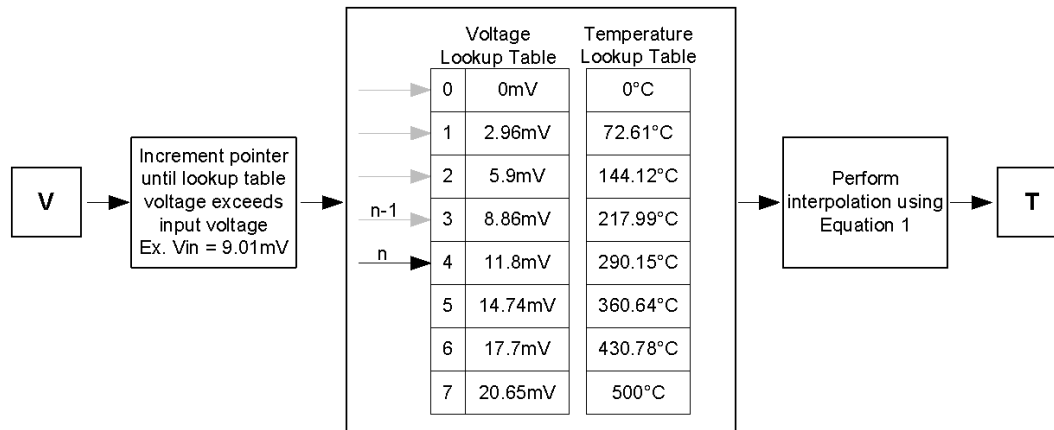


Figure 12. Software Flow Diagram for Thermocouple Linearization

Thermocouple manufacturers usually provide a lookup table that offer excellent accuracy for linearization of a specific type of thermocouple. The granularity on these lookup tables is also very precise—approximately 1°C for each lookup value. To save microcontroller memory and development time, an interpolation technique applied to these values can be used. An example of this method when converting from voltage to temperature with eight lookup table entries is shown in [Figure 13](#).

To perform a linear interpolation using a lookup table, first compare the measured thermocouple voltage to values given in the lookup table, until the lookup table value exceeds the measured value being converted. Then, use [Equation 4](#) to convert the measured thermocouple voltage to temperature, where  $V_{LT}$  is the voltage lookup table array and  $T_{LT}$  is the temperature lookup table array. This operation involves four additions, one multiplication, and one division step, respectively. This operation can be done easily on most 16- and 32-bit microcontrollers. Converting from temperature to voltage is the same, except that the lookup tables and the temperature variables are reversed, as shown in [Equation 4](#).



**Figure 13. V-to-T Conversion Block Diagram for Thermocouple**

$$T = T_{LT}[n-1] + (T_{LT}[n] - T_{LT}[n-1]) \left( \frac{V_{IN} - V_{LT}[n-1]}{V_{LT}[n] - V_{LT}[n-1]} \right)$$

$$V = V_{LT}[n-1] + (V_{LT}[n] - V_{LT}[n-1]) \left( \frac{T_{IN} - T_{LT}[n-1]}{T_{LT}[n] - T_{LT}[n-1]} \right)$$

(4)

Use the following steps for thermocouple linearization using the lookup table:

1. Read the voltage from temperature sensor IC (LM94022 and/or TMP275) placed inside the isothermal block. For example, reading TMP275 will give a count equal to 1A0h, while reading LM94022 will give a voltage output of 1.356 V.
2. Use temperature sensor IC's mV/°C transfer function or lookup table to convert this voltage to temperature. This temperature corresponds to cold junction temperature. For TMP275, a count 1A0h corresponds to 26°C temperature. For LM94022, a voltage output 1.356 V also corresponds to 26°C temperature (which means cold junction temperature is 26°C).
3. Translate this cold-junction temperature reading into the corresponding voltage for a K-type thermocouple at that temperature using lookup. The resulting voltage is  $V_{REF} = 1.041$  mV at 26°C.
4. Read the voltage on thermocouple input channel. For example, the thermocouple voltage measured is  $V = 3.055$  mV.
5. Add the voltage obtained in to the voltage read in step 2 to the voltage read in step 3.  $V_{TC} = V + V_{REF} = 3.055$  mV +  $1.041$  mV =  $4.096$  mV.
6. Translate this voltage reading into the corresponding temperature using the lookup table.  $V_{TC} = 4.096$  mV corresponds to a thermocouple temperature of 100°C.

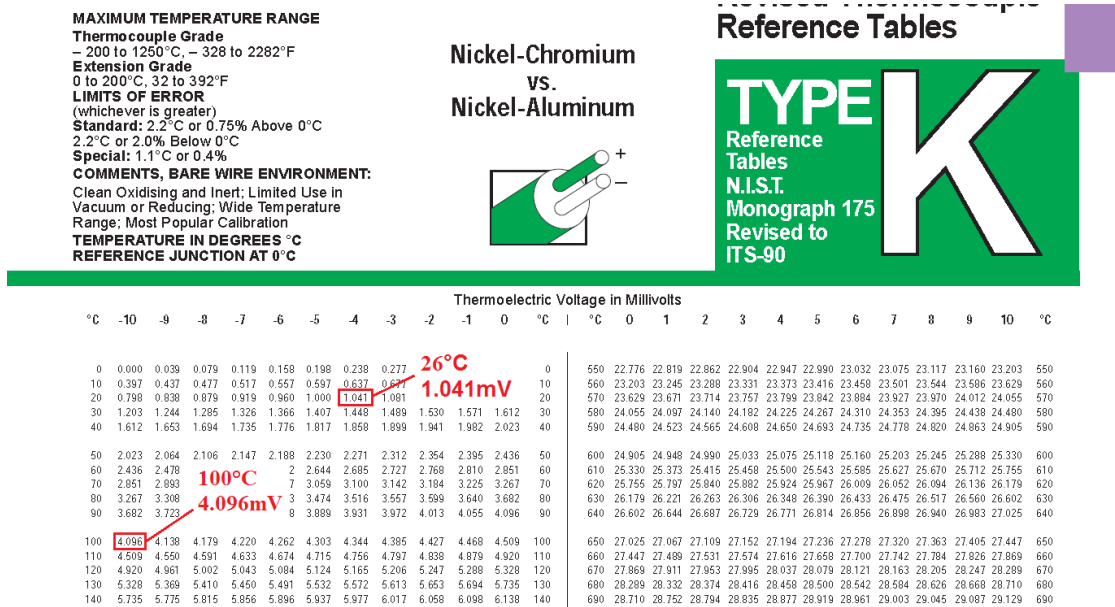


Figure 14. K-Type Thermocouple lookup Table

The mV/°C transfer function and/or the look tables for [LM94022](#) (with hardwired gain = 01) and [TMP275](#) can be found in their respective datasheets.

### 5.1.4 PCB Layout Recommendations

In order to get the best out of cold junction compensation, careful attention must be paid to the following facts:

1. Provide an isothermal block on the board to minimize any temperature gradients across the cold reference junction.
2. Thermocouple connector pins must land inside the isothermal block.
3. Avoid any high voltage traces running close to thermocouple signal traces.
4. The temperature sensor IC must be positioned within close proximity of the reference junction and inside the isothermal block.
5. Place the temperature sensor IC on the same side where the thermocouple connector is placed.
6. Keep the heat sources away from the reference junction and isothermal block.
7. Route the PCB traces together to ensure equal numbers of junctions are maintained on each trace.
8. Keep the module and hardware in a thermally stable environment for optimal performance.
9. If possible, use a dedicated thermocouple connector to minimize parasitic or unwanted thermocouple junction.
10. Choose a temperature sensor IC having very low quiescent current to minimize the self-heating. LM94022 has quiescent current less than 6  $\mu\text{A}$ . TMP275 has a quiescent current less than 50  $\mu\text{A}$  in active mode. However, if TMP275 is operated in on-shot temperature measurement mode with shutdown mode, the current drastically drops to 0.1  $\mu\text{A}$ .

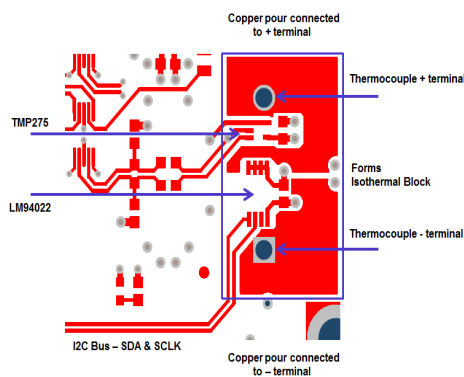


Figure 15. Top Layer

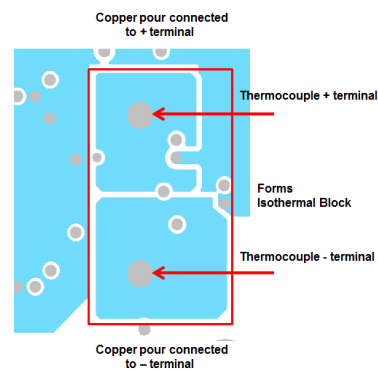


Figure 16. Power Layer

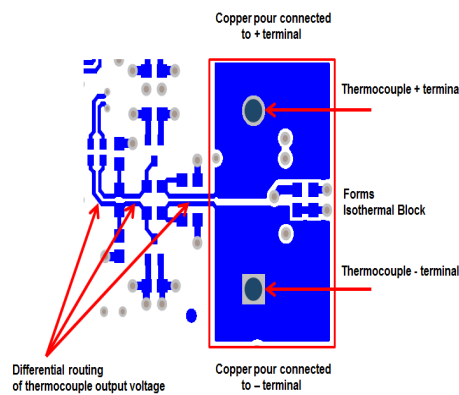


Figure 17. Bottom Layer



### 5.1.5 Filter Calculation

In DC to low-frequency sensing signal-conditioning applications, simply relying on the common-mode rejection ratio (CMRR) of a PGA to provide robust noise rejection in harsh industrial environments could be insufficient. Thermocouple output signals are in the millivolt range and become an easy target of noise. If any high frequency noise is allowed to reach to PGA stage, it will be amplified by high gain and will appear in volts at the PGA output. ADS1220 has an internal FIR digital filter that can be configured to reject 50 Hz or 60 Hz power line frequency pick-up noise or simultaneously reject both only at data rates of 5 SPS and 20 SPS.

Note that inside ADS1220, the input signal is sampled at the modulator clock frequency, not at the output data rate. The filter response of the digital filter repeats at multiples of the sampling frequency ( $F_{MOD}$ ). Signals or noise up to a frequency where filter response repeats are attenuated by the digital filter. However, any frequency components present in the input signal around the modulator frequency or multiples thereof are not attenuated and alias back into the band of interest (unless attenuated by an external analog filter). Some signals are inherently band-limited. For example, the output of a thermocouple cannot be expected to change very quickly and has a bandwidth less than 1 Hz.

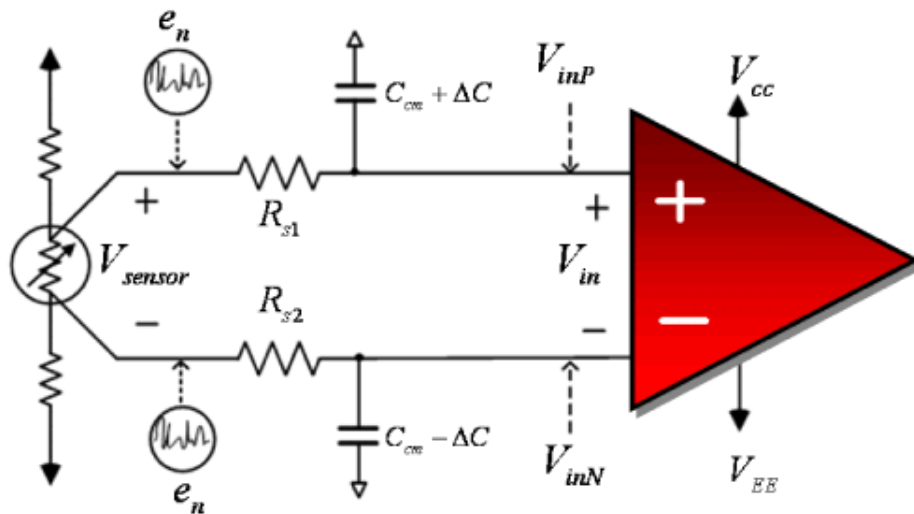
Nevertheless, long thermocouple wires can easily pick up high frequency noise, which can fold back into the frequency band of interest. Therefore, it is generally recommended to implement a simple low-pass, anti-aliasing RC filter at the inputs of the ADC. This implementation sufficiently rejects the high-frequency noises to achieve an acceptable signal to noise ratio (SNR).

For noisy environment applications, a higher order (2<sup>nd</sup>, 3<sup>rd</sup>, or 4<sup>th</sup> order) filter provides more attenuation at high frequencies. When designing an input filter circuit, be sure to take into account the interaction between the filter network and the input impedance of the ADS1220. However, avoid increasing the filter resistance beyond 1 k $\Omega$ . When an excessively large filter resistance is used, this resistance will begin to interact with the ADC's input impedance, resulting in linearity and gain errors.

The thermocouple sensor connects differentially to high input impedance of the ADC through a simple RC low pass filter in each input line. This filter is known as a common mode filter. The important point here is that if the filter components in both the inputs are perfectly matched, the common mode noise will also be attenuated equally. Resistors can be matched closely by choosing 1% tolerance or better. However, capacitors have a typical tolerance of 5% or 10%. Due to this capacitive mismatch, some percentage of common mode noise gets converted to differential noise and becomes a part of the thermocouple input signal.

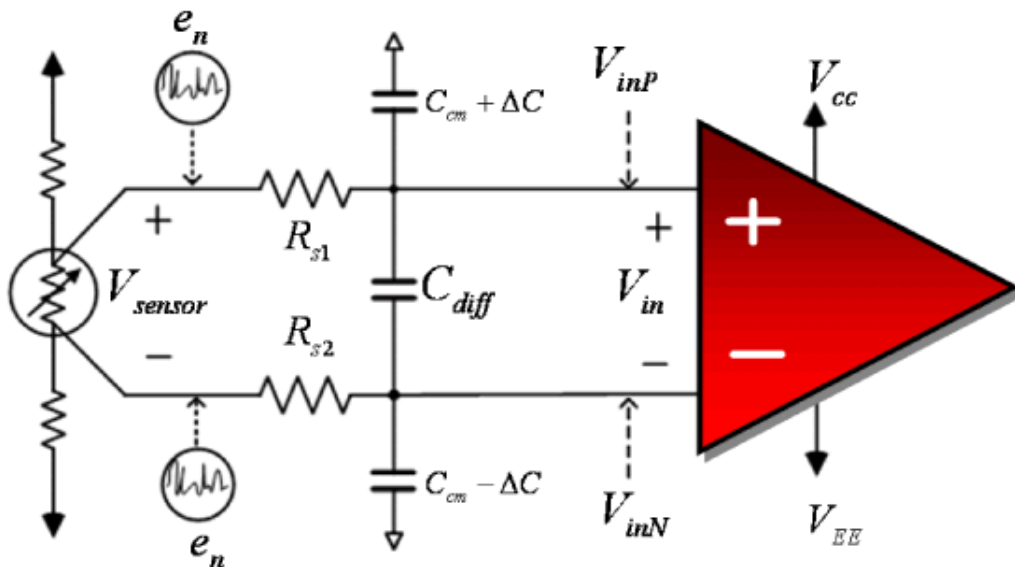
To overcome this problem, a differential capacitor is also added. The filter, formed by  $R_{DIFFA}$ ,  $C_{DIFF}$ , and  $R_{DIFFB}$  is known as a "differential mode filter." Just adding a differential capacitor is not enough, as the following four criteria must be satisfied:

1. The differential cutoff frequency should be sized to provide sufficient attenuation of any noise component around the modulator frequency so that noise does not fold back into the frequency band of interest.
2. Choose the common mode capacitor 10 times smaller than the differential mode capacitor. This 10 times smaller size makes differential voltage translated due to a common mode capacitive mismatch less critical. The differential mode filter cutoff frequency becomes much smaller than common mode filter cutoff frequency.
3. The filter components should be placed symmetrically on the board.
4. The order of the filter must be decided so that the expected direct differential mode noise around the modulator's clock frequency (256 kHz for ADS1220) is suppressed to less than 1 LSB.



$C_{CM} (\pm\Delta C)$  mismatch causes asymmetric  $e_n$  attenuation, resulting in significant differential noise, which is also amplified by PGA gain along with sensor input.

**Figure 18. Common Mode Filter (Undesired)**



$C_{CM} (\pm\Delta C)$  mismatch causes asymmetric  $e_n$  attenuation. As long as  $C_{DIFF} \geq 10 C_{CM}$ , differential noise is attenuated to an insignificant level.

**Figure 19. Common Mode and Differential Mode Filter (Desired)**

$$F_{DM} = \frac{1}{2\pi(R_{47} + R_{45}) \left[ C_{65} + \left( \frac{C_{68} \times C_{61}}{C_{68} + C_{61}} \right) \right]}$$

$$F_{DM} = \frac{1}{2\pi(499 \Omega + 499 \Omega) \left[ 1 \mu\text{F} + \left( \frac{0.1 \mu\text{F} \times 0.1 \mu\text{F}}{0.1 \mu\text{F} + 0.1 \mu\text{F}} \right) \right]}$$

$$F_{DM} \approx 152 \text{ Hz}$$

(5)

$$F_{CM\_1} = \frac{1}{2\pi \times R_{S1} \times C_{CM1}} \quad (6)$$

$$F_{CM\_2} = \frac{1}{2\pi \times R_{S2} \times C_{CM2}}$$

$$F_{CM\_1} = F_{CM\_2} \approx 3.2 \text{ KHz} \quad (7)$$

### 5.1.6 PGA Gain and Common Mode Voltage

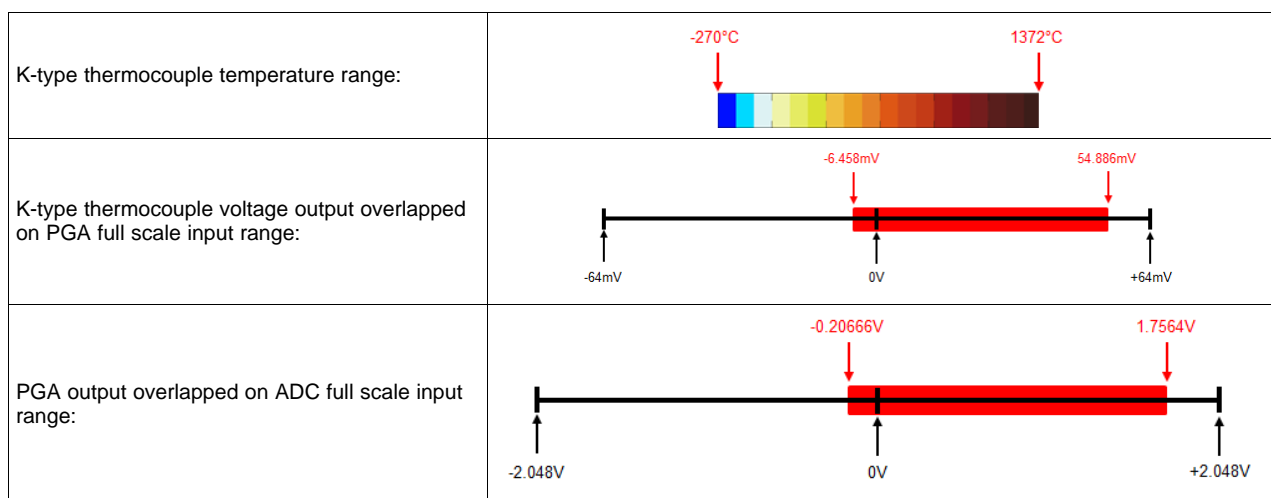
The K-Type thermocouple has a temperature range of  $-270^{\circ}\text{C}$  to  $1372^{\circ}\text{C}$ . The K-Type thermocouple produces a voltage input to the PGA ranges from  $-6.458 \text{ mV}$  to  $54.886 \text{ mV}$ . Therefore, the thermocouple full scale input range ( $V_{TC\_IN\_FS}$ ) is as shown in and Equation 9.

$$V_{TC\_IN\_FS} = [54.886 \text{ mV} - (-6.458\text{mV})] = 61.344 \text{ mV} \quad (8)$$

$$\text{PGA Gain} = \frac{V_{REF}}{V_{IN\_FS}} = \frac{2.048 \text{ V}}{61.344 \text{ mV}} = 33.4 \text{ V/V} \quad (9)$$

The closest PGA gain supported by ADS1220 is 32 V/V.

The differential full scale input voltage ( $V_{FS}$ ) range for the PGA at a gain of 32 V/V is  $\pm 64 \text{ mV}$ . The thermocouple full scale input voltage ( $V_{TC\_IN\_FS}$ ) lies within the PGA full scale input.



The ADC can measure inputs differentially, which means the ADC measures one input with respect to another input with both inputs' active signals. For 5-V single power supply operation,  $A_{IN\_P}$  and  $A_{IN\_N}$  signals should not be allowed to swing below ground. Therefore, it is important to set common mode voltage of the differential signals equal to the mid-supply so that the differential signals swing above and below the common mode voltage and always remain within the valid ADC range as shown below in Figure 20.  $A_1$  and  $A_2$  are not rail-to-rail output amplifiers. Therefore  $ADC\_IN\_P$  and  $ADC\_IN\_N$  have to be within  $(AVSS + 0.2 \text{ V})$  and  $(AVDD - 0.2 \text{ V})$ . Equation 10 shows the most confusing common mode voltage requirement for the inputs:

$$\left( AVSS + 0.2 \text{ V} + \frac{V_{IN} \times \text{PGA}}{2} \right) \leq V_{CM} \leq \left( AVDD - 0.2 \text{ V} - \frac{V_{IN} - \text{PGA}}{2} \right) \quad (10)$$

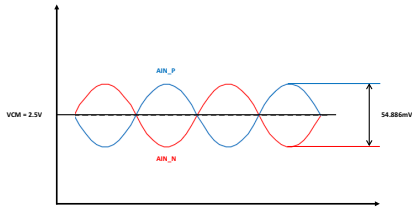
For example,  $AVDD = 5 \text{ V}$ ,  $AVSS = 0 \text{ V}$ ,  $\text{PGA Gain} = 32 \text{ V/V}$  and Internal ADC Reference ( $V_{REF}$ ) = 2.048 V.

Therefore, the maximum possible differential input voltage that can be applied is

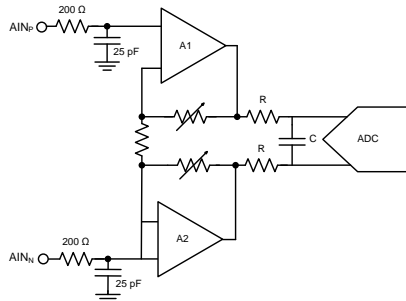
$$\pm \frac{V_{REF}}{\text{PGA Gain}} = \pm \frac{2.048 \text{ V}}{32 \text{ V/V}} = \pm 0.064 \text{ V}$$

So, the allowed common mode voltage range is  $1.224 \text{ V} \leq V_{CM} \leq 3.776 \text{ V}$ .

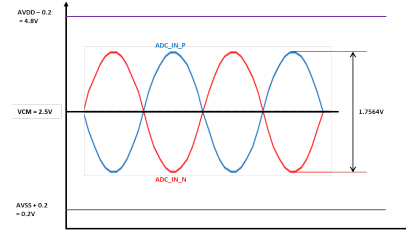
However, the thermocouple sensor output that is connected to the inputs in this design does not make use of the entire full-scale range. Instead, the output is limited to  $V_{IN} = \pm 54.886 \text{ mV}$  (max). Accordingly, this reduced input signal relaxes the  $V_{CM}$  restriction to  $1.078 \text{ V} \leq V_{CM} \leq 3.922 \text{ V}$ .



**Figure 20. Thermocouple Sensor Output = Input to PGA**



**Figure 21. PGA with Gain Programmed to 32 V/V**



**Figure 22. PGA Output = ADC Input**

The thermocouple signal conditioning circuit includes a simple bias generation through  $R_{PU}$  and  $R_{PD}$ , which basically centers the thermocouple between supply and ground. This is often an ideal common-mode input for PGA.  $R_{PU}$  and  $R_{PD}$  should be sized as high as possible to minimize the current flowing through the thermocouple without introducing too much additional noise.

The thermal noise or Johnson noise for a resistor can be given as:

$$V_N = \sqrt{4KTR(BW)}$$

where

- $R = R_{PU} + R_{PD}$
- $K = \text{Boltzmann constant} = 1.38 \times 10^{-23} \text{ J/K}$
- $T = \text{Temperature in Kelvin} = 273.15 + 85^\circ\text{C (max)} = 358.15 \text{ K (max)}$
- $BW = \text{Bandwidth} = \text{External input filter bandwidth} = 152 \text{ Hz}$

(11)

For this design, the variables are sized to restrict their total noise contribution to less than the peak-to-peak input referred noise of the ADC.

$$R_{PU} + R_{PD} \leq \frac{(\text{Peak-to-Peak Input Referred Noise})^2}{4KT(BW)}$$

(12)

A 1 M $\Omega$  resistor each is sufficient to accomplish the task without adding too much noise.

### 5.1.7 Accuracy Calculation

K-Type Thermocouple Voltage at 1372°C temperature produces 54.886 mV.

ADS1220's Full Scale Range = FSR = ±0.064 V = ±64 mV

PGA Gain = 32 V/V

$$\text{ADC Error Contribution} = \sqrt[2]{(\text{INL})^2 + (\text{OFFSET})^2 + (\text{OFFSET DRIFT})^2 + (\text{GAIN})^2 + (\text{GAIN DRIFT})^2} \quad (13)$$

Individual errors using typical ADC specifications are:

INL = ±15 PPM of FSR = ±15 PPM × 55 mV = ±0.385 μV

Offset error = ±10 μV (from datasheet graph)

Error due to offset drift = ±0.08 μV/°C × (60°C – 0) = ±4.8 μV

Gain error = ±300 PPM of FSR = ±300 PPM × 55 mV = ±16.5 μV

Error due to gain drift = ±1 PPM/°C × (60°C – 0) = ±3.3 μV

ADC Error Contribution = ±17.52 μV

$$\text{This yields temperature error} = \frac{\text{ADC Error Contribution}}{\text{Average Thermocouple Sensitivity}} = \frac{17.52 \mu\text{V}}{40.6 \mu\text{V}/^\circ\text{C}} = 0.431^\circ\text{C}$$

ADC Temperature Error ≈ ±0.5°C (Typical)

$$\text{Total Unadjusted Error (TUE)} = \sqrt[2]{(\text{CJC Error})^2 + (\text{ADC Temp Error})^2}$$

For TMP275, the temperature accuracy is ±0.5°C

$$\text{Total Unadjusted Error (TUE)} = \sqrt[2]{(0.5^\circ\text{C})^2 + (0.5^\circ\text{C})^2} = \pm 0.707^\circ\text{C} \text{ (excluding thermocouple sensor error)}$$

For LM94022, the temperature accuracy is ±1.5°C

$$\text{Total Unadjusted Error (TUE)} = \sqrt[2]{(1.5^\circ\text{C})^2 + (0.5^\circ\text{C})^2} = \pm 1.58^\circ\text{C} \text{ (excluding thermocouple sensor error)}$$

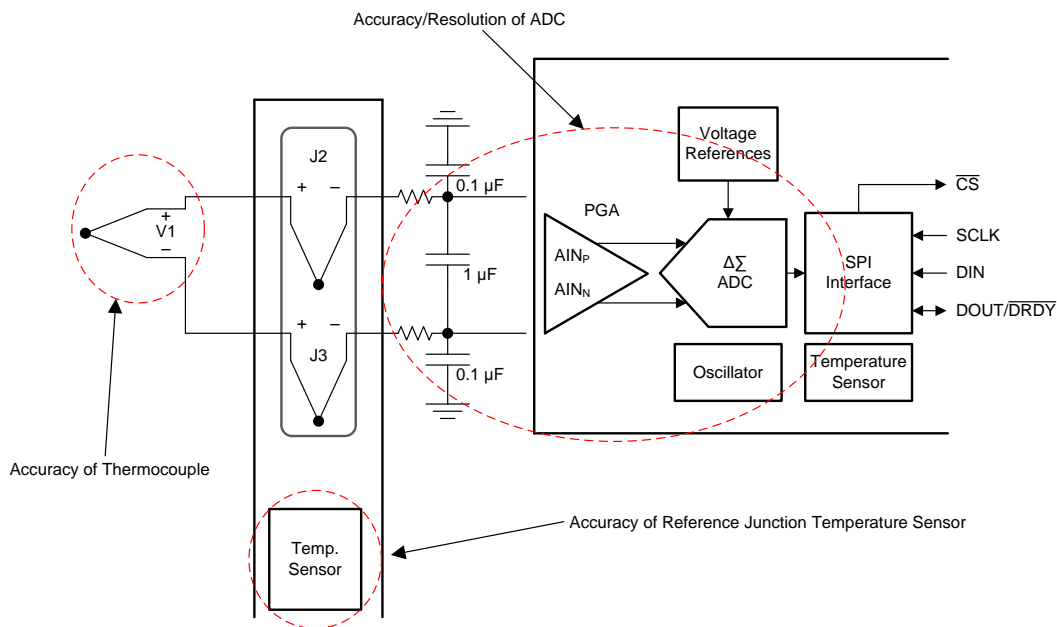
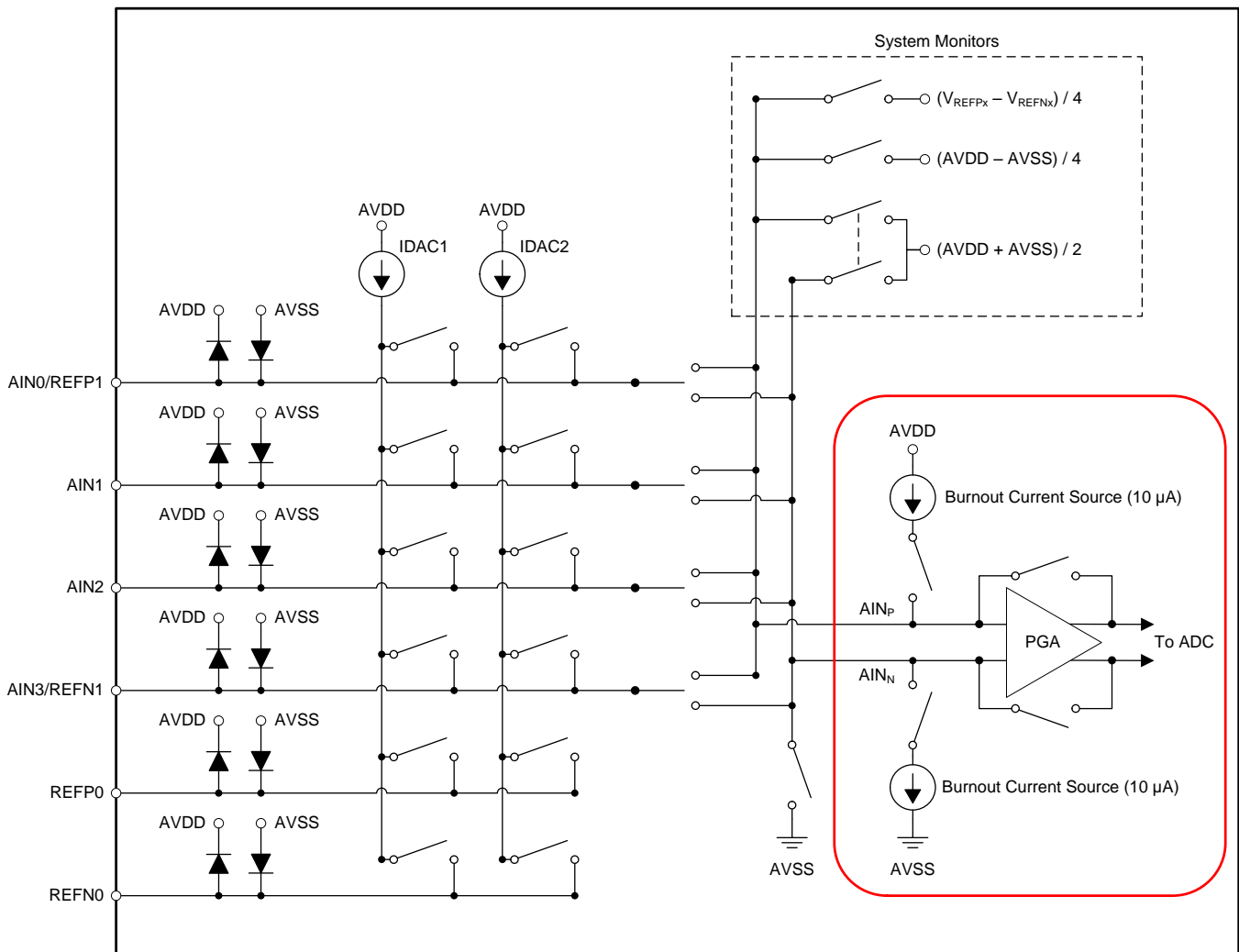


Figure 23. Parts of Circuit Affecting Accuracy

### 5.1.8 Sensor Diagnostics

As thermocouples are exposed to extreme environmental conditions, thermocouple wire tends to break or increase in wire resistance. Therefore, an easy and quick detection of broken or increased resistance is required in critical applications. The second purpose of the 1 MΩ resistors is to offer a weak pull-up and pull-down for sensor open detection. In the event that a sensor is disconnected, the inputs to the ADC extend to supply and ground, and yield a full-scale readout, which indicates a sensor disconnection.

Alternatively, ADS1220 provides internal 10 μA, burn-out current sources which can be enabled by setting the BCS bit in the configuration register. One current source sends current to the selected positive analog input (AIN<sub>P</sub>), and the other current source sinks current from the selected negative analog input (AIN<sub>N</sub>). In case of an open circuit in the sensor, these burn-out current sources pull the positive input towards AVDD and the negative input towards AVSS, resulting in a full-scale reading. A full-scale reading indicates that the sensor is open or a wire break condition has occurred.



**Figure 24. Burn-Out Current Sources for Sensor Diagnostic**

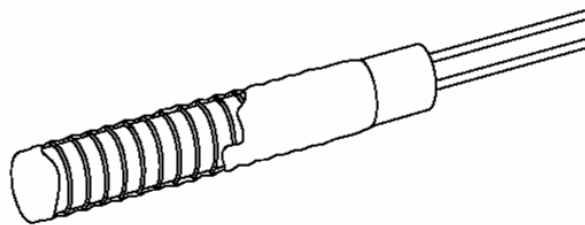
**NOTE:** Do not leave burn-out current sources active during normal measurements, since burn-out current sources will corrupt the readings.

## 5.2 RTD Input Channel

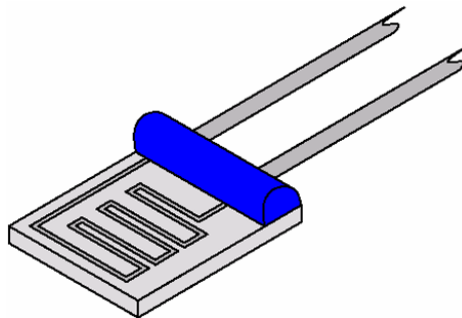
### 5.2.1 Resistance Temperature Detector (RTD) – “Back to Basics”

A Resistance Temperature Detector (RTD) is a sensing element used to measure the temperature as the element's resistance changes with changes in temperature. RTDs have been constantly in use for many years to measure the temperature in laboratories and industries. The relationship between an RTD's resistance and temperature is highly predictable and allows accurate and repeatable temperature measurement over wide ranges.

RTDs are constructed in two common configurations – wire wound RTDs and thin metal film RTDs (see [Figure 25](#) and [Figure 26](#)). Wire wound type RTDs are made by inserting helical sensing wire into a packed powder-filled insulating mandrel to provide a strain-free sensing element. Thin film RTDs are made by depositing a thin layer of metal (for example, platinum) in a resistance pattern on a ceramic substrate. The thin metal film RTDs appear to have an advantage over wire wound configurations in terms of ruggedness, vibration resistance, cost, size, and response.



**Figure 25. Wire Wound RTD**

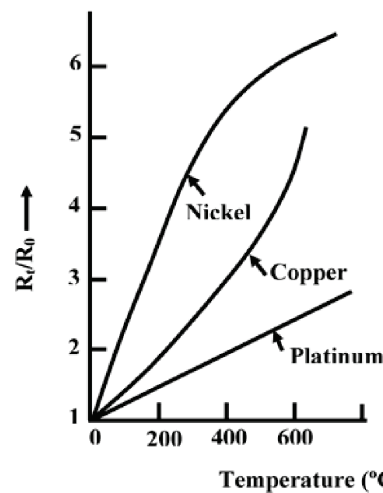


**Figure 26. Thin Film RTD**

The basic principle for RTD operation is that all the metals have positive change resistance with increase in temperature. Metals having high resistivity, high melting point, and high corrosion resistance are generally preferred for making RTDs and allow using less of the metal material to achieve high nominal resistance value.

**Table 4. Metals and Their Resistivity**

METAL	RESISTIVITY ( $\Omega$ /CMF) CMF = CIRCULAR MIL FOOT
Platinum (Pt)	59
Nickel (Ni)	36
Tungsten (W)	30
Gold (Au)	13
Copper (Cu)	9.26
Silver (Ag)	8.8



**Figure 27. RTD Metal Resistance versus Temperature**

Gold and silver are less preferred for RTD sensing elements, as they have low resistivity. Copper is sometimes used as an RTD element for temperature measurement up to approximately 100°C. Copper's linearity and low cost make copper a more cost-effective alternative. RTDs using copper as the sensing element are larger in size because copper's lower resistivity forces use of longer wire to wind as a sensor. Tungsten has relatively higher resistivity compared to gold, silver, and copper. Tungsten's use is restricted to extremely high temperature applications. Tungsten is a fragile (breakable) material, which makes machining or construction more difficult.

The most commonly used RTDs are made of either platinum, nickel, or nickel alloys. Nickel-based sensors used in cost-effective applications (like consumer goods) have a nonlinear response and also have a tendency to drift over time.

By far, platinum is the best material for RTDs because of the high resistivity and long-term stability. Platinum follows a more linear resistance-temperature relationship compared to other metals. The unique properties of platinum make platinum the material of choice for temperature standards over the range of -200°C to 850°C. As a noble metal (chemically inert), platinum is less susceptible to contamination. Platinum is one of the leading choices for a temperature measurement task. Platinum RTDs are typically available in 100 Ω (PT100), 200 Ω (PT200), 500 Ω (PT500), and 1000 Ω (PT1000) nominal resistance values at 0°C. Historically, PT100 is the most popular. However, higher-valued RTDs such as PT200, PT500, or PT1000 can be used for increased sensitivity and resolution at a small extra cost.

RTDs are built to conform to certain standards like the European standard (DIN-IEC-60751), the American standard (ASTM 1137), or the International Temperature Scale (ITS-90). For PT100 RTD, the DIN-IEC-60751 standard defines a base resistance of 100 Ω at 0°C and a temperature coefficient of resistance ( $\alpha$ ) of 0.00385 Ω/Ω/°C between 0°C to 100°C. The American standard defines a base resistance of 100 Ω at 0°C and a temperature coefficient of resistance ( $\alpha$ ) of 0.003911 Ω/Ω/°C between 0 and 100°C. The ITS-90 standard defines a base resistance of 100 Ω at 0°C and a temperature coefficient of resistance ( $\alpha$ ) of 0.003925 Ω/Ω/°C between 0 and 100°C.

The three essential characteristics of an RTD are the following:

- Temperature coefficient of resistance – relationship between resistance and temperature
- Nominal resistance at 0°C; for example, PT100 RTD has 100 Ω resistance at 0°C
- Tolerance class – RTD accuracy



**Table 5. RTD Class and Tolerance Information**

TOLERANCE CLASS (DIN-IEC 60751)	TEMPERATURE RANGE of VALIDITY <sup>(1)</sup>		TOLERANCE VALUES (°C)	RESISTANCE at 0°C (Ω)	ERROR at 100°C (°C)	ERROR OVER WIRE-WOUND RANGE (°C)
	WIRE-WOUND	THIN-FILM				
AAA (1/10 DIN) <sup>(2)</sup>	0 to 100	0 to 100	$\pm(0.03 + 0.0005 \times T)$	$100 \pm 0.012$	0.08	0.08
AA (1/3DIN)	-50 to 250	0 to 150	$\pm(0.1 + 0.0017 \times T)$	$100 \pm 0.04$	0.27	0.525
A	-100 to 450	-30 to 300	$\pm(0.15 + 0.002 \times T)$	$100 \pm 0.06$	0.35	1.05
B	-196 to 600	-50 to 500	$\pm(0.3 + 0.005 \times T)$	$100 \pm 0.12$	0.8	3.3
C	-196 to 600	-50 to 600	$\pm(0.6 + 0.01 \times T)$	$100 \pm 0.24$	1.6	6.6

<sup>(1)</sup> Manufacturers may choose to guarantee operation over a wider temperature range than DIN-IEC60751 provides.

<sup>(2)</sup> AAA (1/10DIN) is not included in the DIN-IEC-60751 specification but is an industry accepted tolerance class for high-performance measurements.

The relationship between the resistance and temperature of platinum RTD is defined by a nonlinear mathematical model known as the Callendar-Van Dusen (CVD) equations. The coefficients in the Callendar-Van Dusen equations are defined by the IEC-60751 standard.

For  $T > 0^\circ\text{C}$ , the CVD equation is a second-order polynomial as given in [Equation 14](#):

$$\text{RTD}(T) = R_0 \times [1 + A(T) + B(T)^2] \quad (14)$$

For  $T < 0^\circ\text{C}$ , the CVD equation expands to a fourth-order polynomial as given in [Equation 15](#):

$$\text{RTD}(T) = R_0 \times [1 + A(T) + B(T)^2 + C(T)^3(T - 100)] \quad (15)$$

The linear approximation model is as follows:

$$\text{RTD}(T) = R_0 \times [1 + \alpha(T)]$$

where

- $T$  = Temperature of RTD element in  $^\circ\text{C}$
- $\text{RTD}(T)$  = resistance of RTD element as a function of temperature
- $R_0$  is the resistance of the RTD element at  $0^\circ\text{C}$
- $\alpha$  = Sensitivity of RTD element =  $0.00385 \Omega/\Omega/^\circ\text{C}$
- $A = 3.9083 \times 10^{-3} \text{ }^\circ\text{C}^{-1}$
- $B = -5.7750 \times 10^{-7} \text{ }^\circ\text{C}^{-2}$
- $C = -4.1830 \times 10^{-12} \text{ }^\circ\text{C}^{-4}$

The behavior of resistance for PT100 RTD from  $-200^{\circ}\text{C}$  to  $850^{\circ}\text{C}$  is shown in Figure 28.

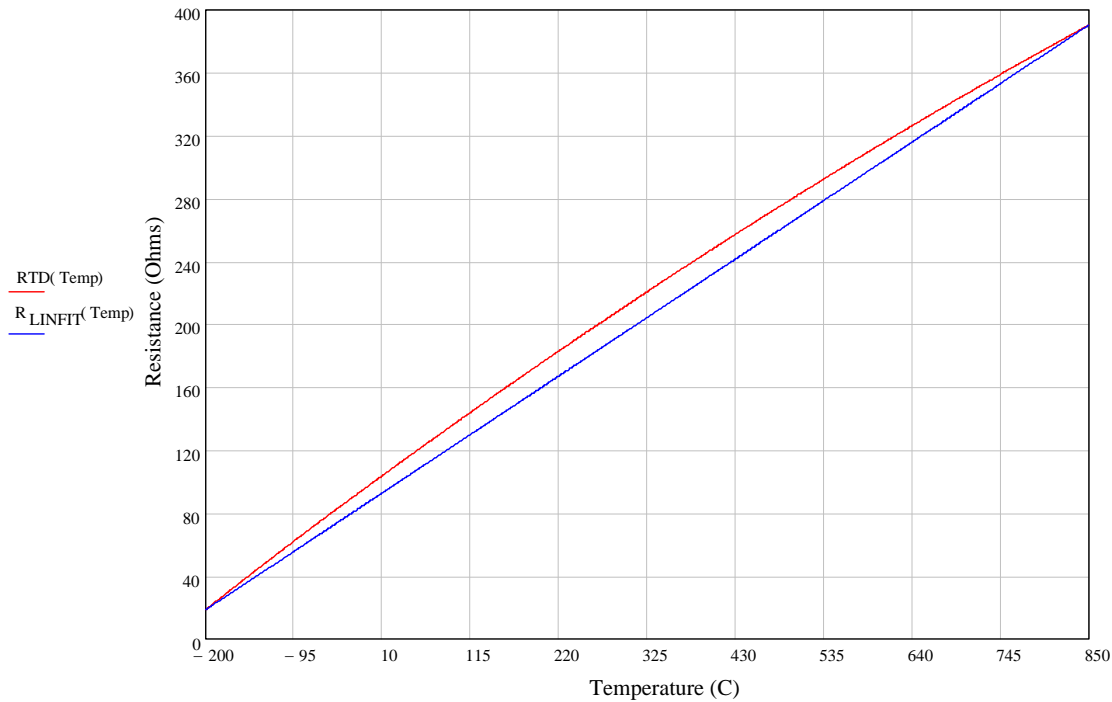


Figure 28. RTD Resistance and Linear Fit Line versus Temperature

The change in RTD resistance is piecewise linear over small temperature ranges. An end-point curve fitting shows RTDs have a second-order, nonlinearity of approximately 0.375% as shown in Figure 29 . To correct this nonlinearity error requires implementing a digital linearization technique.

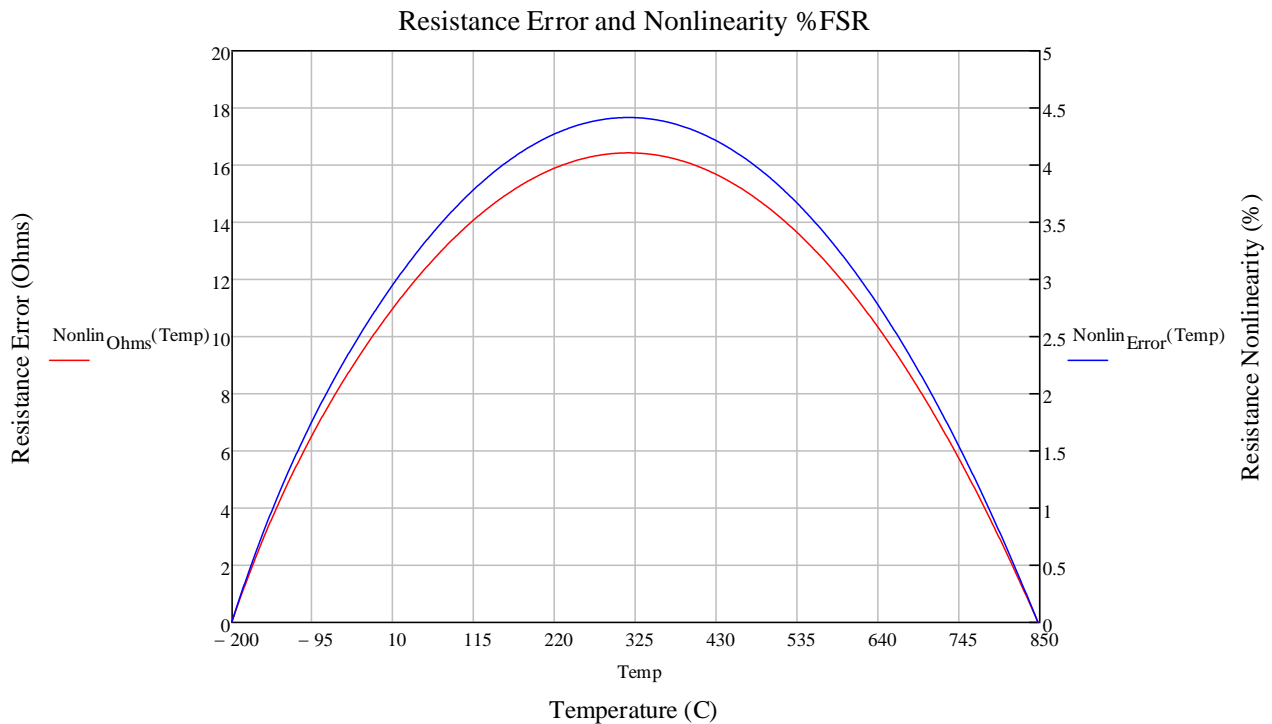


Figure 29. Resistance Error and Nonlinearity versus Temperature

The three techniques for RTD linearization are as follows:

1. Simple Linear Approximation Method
2. Piecewise Linear Approximation Method
3. Callendar-Van Dusen Equations Method

A brief comparison is also given in [Table 6](#).

**Table 6. Linear Approximation Methods**

METHOD	ADVANTAGE	DISADVANTAGE	OTHER REMARKS
Simple Linear Approximation	Easy to implement Fast execution Accurate over small temperature ranges Smaller code size	Least accurate over wide temperature range	Simple method when memory size is limited and temperature range is smaller
Piecewise Linear Approximation	Accuracy depends on the entries in the lookup table Fast execution	High accuracy More entries in lookup table Bigger code size	Most practical method implement by most of the embedded systems
Callendar-Van Dusen Equations	Most accurate	Extremely Processor Intensive Time consuming Requires Square root and Power functions on the processor	Not practical in most applications

This reference design implements the piecewise linear approximation method using the manufacturer's lookup table with more number of entries to achieve better accuracy.

### 5.2.2 RTD Resistance Measurement

The basic principle required for RTD measurement is based on Ohm's Law.

Ohm's law equation is as follows:

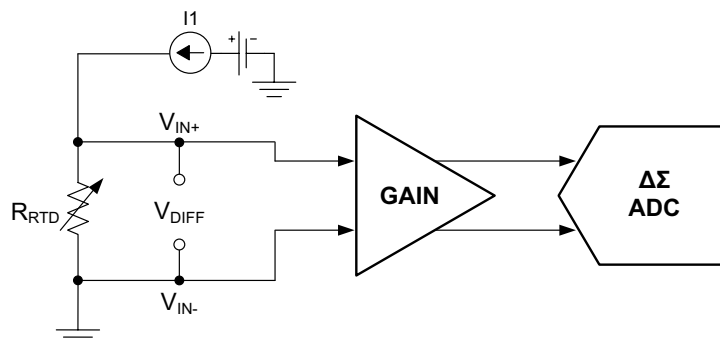
$$R = \frac{V}{I}$$

where

- R = Resistance of the RTD element
- I = Known excitation current
- V = Voltage across RTD element

(16)

As an RTD is a passive sensor, an RTD does not produce output on its own. An RTD requires a known constant current source for the RTD's excitation to produce a useful voltage output proportional to the resistance of the RTD. The resulting voltage output is then amplified and fed to an ADC for measurement. By this method, an unknown resistance of an RTD can be easily calculated and then transformed to temperature using a software algorithm. Depending on the nominal resistance of the RTD, different excitation currents can be used. The excitation current flow through an RTD should be minimized to avoid self-heating. In general, approximately 1 mA or less current is used.



**Figure 30. Simplified RTD Measurement Circuit**

The RTD is generally installed in plastic, food, petrochemical-processing equipment, gas exhausts, pipelines, stoves, and other places in industry. The measurement circuit inside a control room can be hundreds of feet away from the processing plant. Under such conditions, the measurement wires that lead to the sensor can be several ohms. The small resistance of the wire could add to the RTD resistance. Therefore, errors in resistance measurement can be caused. For example, a wire resistance of 0.5 Ω in each lead of a field-mounted RTD causes an  $(0.5 \Omega + 0.5 \Omega) / (0.385^\circ\text{C}/\Omega) = 2.6^\circ\text{C}$  error in measurement. RTDs are available in three different lead wire configurations: 2-wire, 3-wire, and 4-wire. Before discussing each configuration in detail, the background is given for a ratiometric measurement approach for RTDs, as this reference design also implements ratiometric measurement.

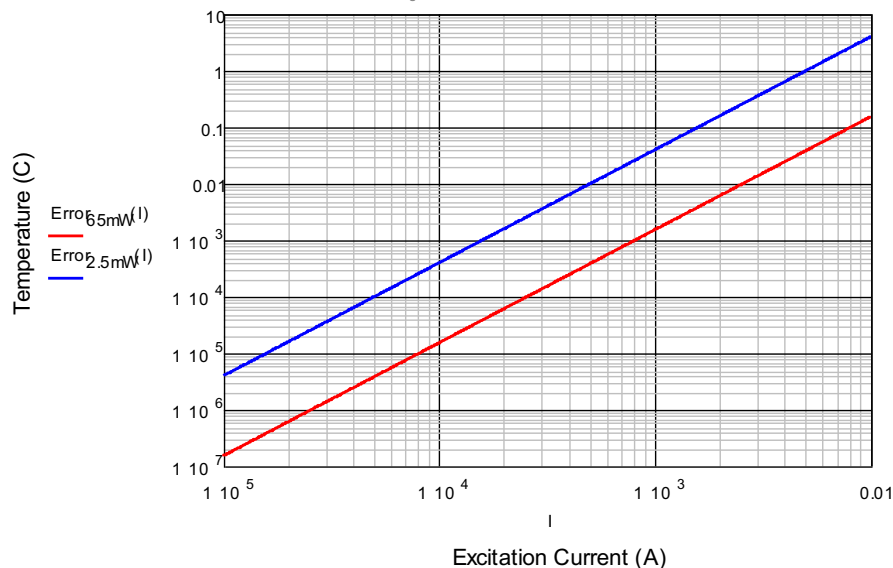
### 5.2.3 Self-Heating

Unlike thermocouples, RTDs are not self-powered. Therefore, RTD's need an excitation source. Excitation current flowing through the RTD produces a useful voltage that can be measured. Maximizing the excitation current appears desirable by augmenting system performance. The excitation current must be high enough so that voltage produced is greater than the peak-to-peak noise level of the ADC.

At the same time, care must be taken not to pass a large current through the RTD, since a large current can cause higher  $I^2R$  losses.  $I^2R$  losses lead to self-heating within the element. If the sensor is unable to dissipate the self-heat, the sensing element increases above ambient temperature, which can cause resistance of the RTD element to increase. Therefore, an artificially high temperature will be reported.

The errors due to self-heating cannot be easily corrected. These errors should be kept lower than 25% of the total error budget. The amount of self-heat generated also depends upon the sensor's thermal resistance, surroundings, and placement in an application. An RTD placed in a moving, fluid medium will not self-heat because the moving fluid will keep the RTD at the temperature of the fluid.

However, in open-air temperature measurements or other applications where the RTD is surrounded by an insulator, the RTD will self-heat and cause errors. Self-heating error is expressed in  $\text{mW}/^\circ\text{C}$ . The typical range of RTD self-heating coefficients is  $2.5 \text{ mW}/^\circ\text{C}$  for small elements to  $65 \text{ mW}/^\circ\text{C}$  for larger elements. Figure 31 displays the self-heating error in  $^\circ\text{C}$  versus applied excitation current for the range of RTD self-heating coefficients.



**Figure 31. Self Heating versus Excitation Current**

Typically, a good compromise is to make sure that RTD and current are scaled so the drift (due to self-heating) is significantly less than the errors associated with the RTD itself.

### 5.2.4 Ratiometric Measurement

Performing ratiometric measurement provides a significant advantage, where errors resulting from the absolute accuracy of the excitation current and errors due to excitation drift are virtually eliminated. In addition, the noise of the excitation source at the inputs is also reflected on the reference path of the ADC. In this way, the noise gets cancelled.

An ADC requires a reference voltage to convert the input voltage into digital output. In most applications, this reference is fixed and generated either internal or external to the ADC. The voltage reference has a direct influence on the accuracy of output. If the measurement can be arranged so that the ADC result is a ratio of the input and a precision element such as a resistor, then much higher precision results can be obtained.

In ratiometric configuration, the excitation current that flows through the RTD returns to ground through a low-side reference resistor,  $R_{REF}$ , as shown in Figure 32. The voltage developed across  $R_{REF}$  is fed into the positive and negative reference pins (REFP and REFN) of the ADC and the ADS1220 is configured to use this external reference voltage  $V_{REF}$  for the analog-to-digital conversions. The  $R_{REF}$  resistor and excitation current are sized to produce a 1.65 V external reference.  $R_{REF}$  should be selected as a low-tolerance, low-drift resistor for accurate results.

The voltage drop across the RTD and  $R_{REF}$  resistors is produced by the same excitation source. The ADC output code is a relationship between the input voltage and the reference voltage. Therefore, errors as a result of the absolute accuracy of the excitation current and errors because of excitation drift are virtually eliminated. As mentioned in the first paragraph in Section 5.2.4, the noise of the excitation source at the inputs is also reflected on the reference path of the ADC. In this way, the noise gets cancelled. Therefore, the system becomes immune to variations in the excitation.

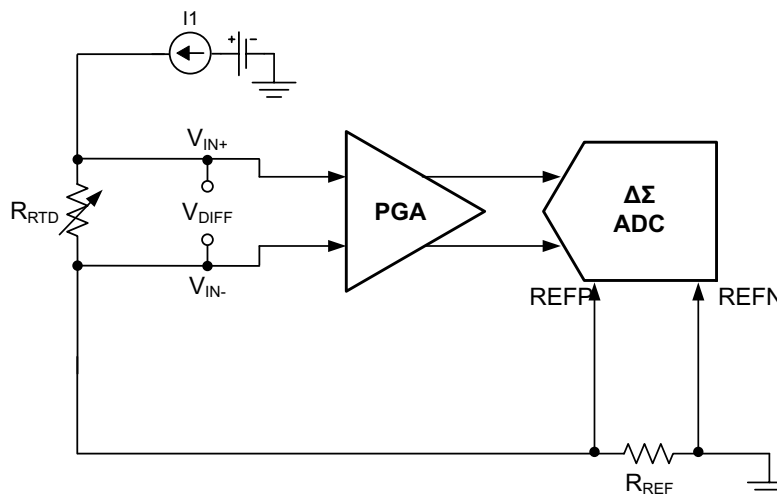


Figure 32. Simplified Circuit for RTD Ratiometric Measurement

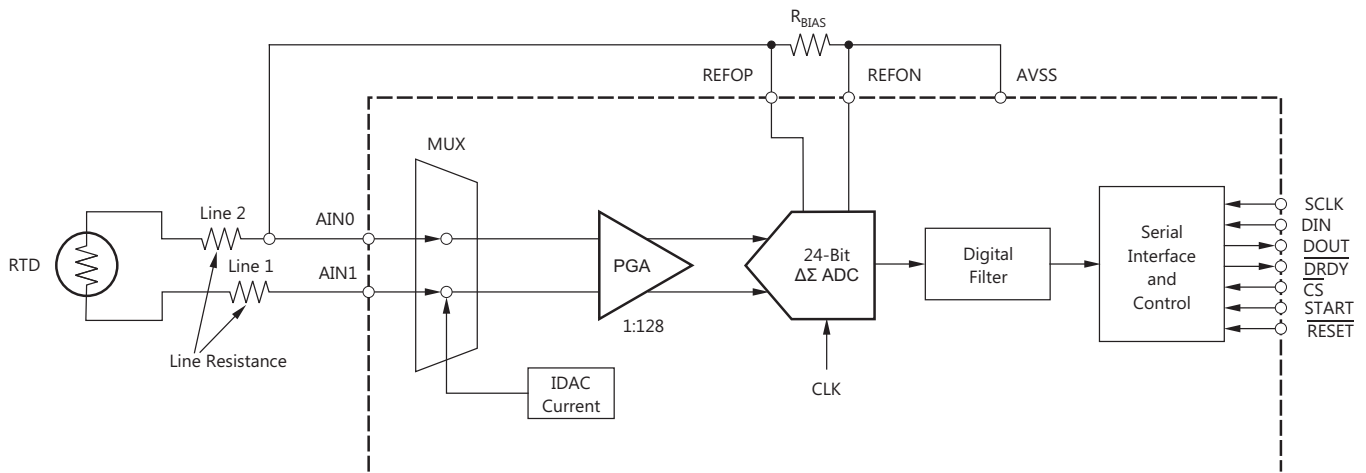
$$\text{ADC\_Output} = \frac{V_{IN} \times \text{GAIN} \times (2^{23} - 1)}{V_{REF}} \quad (17)$$

$$\text{ADC\_Output} = \frac{I_{DAC} \times \text{RTD} \times \text{GAIN} \times (2^{23} - 1)}{I_{DAC} \times R_{REF}} \quad (18)$$

$$\text{ADC\_Output} = \frac{\text{RTD} \times \text{GAIN} \times (2^{23} - 1)}{R_{REF}} \quad (19)$$

The accuracy of the measurement now depends only on the reference resistor. Therefore, the absolute accuracy and temperature drift of the excitation current does not matter. However, because the value of the reference resistor directly impacts the measurement result, the accuracy can be set to a higher level by choosing a high precision low drift reference resistor  $R_{REF}$ .

### 5.2.5 Two-Wire RTD Application



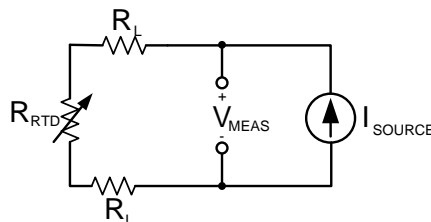
NOTE:  $R_{BIAS}$  should be as close to the ADC as possible.

**Figure 33. Two-Wire RTD Circuit**

The two-wire RTD connection is the simplest method for a remote connection. Figure 33 presents one possible RTD application. The ADS1220 current sources are connected to one of the terminals of the RTD lines by setting the appropriate bits in configuration register 2. The value of the current can be chosen by setting the IDAC [2:0]: IDAC current setting bits in configuration register 2. The voltage developed across the RTD is measured by connecting the RTD through the PGA to the ADC.

The voltage measured across the RTD is proportional to temperature (determined by the characteristics of the RTD). The  $R_{BIAS}$  value is selected according to the IDAC current source setting. The reference to the device is also derived from the IDAC. The appropriate external reference must be selected by setting the  $V_{REF}$  [1:0]: voltage reference selection bits in configuration register 2.  $R_{BIAS}$  determines the reference voltage to the ADC as well as the input common mode of the PGA. Both reference and input to the device are functions of the IDAC current in this topology. This ratiometric approach ensures a greater effective number of bits (ENOB) because the noise in the IDAC reflects in the reference as well as in the input, and therefore tends to cancel off.

The effect of the IDAC current temperature drift is also cancelled out in this ratiometric topology. However, a major limitation of the two-wire method is that the voltage drop across the line resistances adds up to the voltage drop across the RTD. Therefore, the sensor cannot be very far away from the measurement setup. The IDAC current mismatch drift in this topology also does not matter, because there is only one current path.



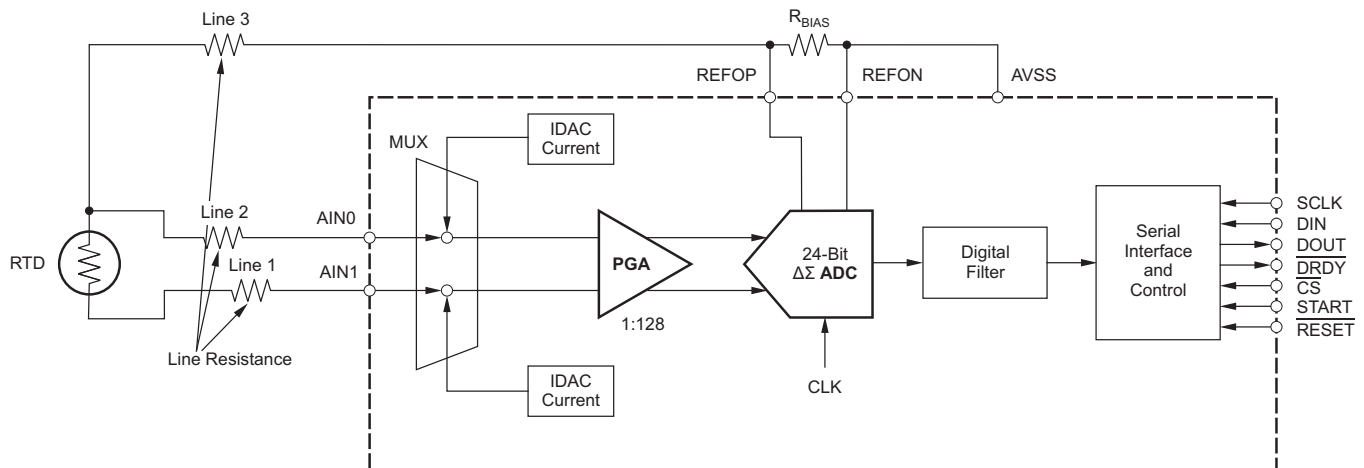
**Figure 34. Simplified Two-Wire RTD Configuration and Excitation**

$$V_{MEAS} = I_{SOURCE} \times R_{RTD} + 2 \times I_{SOURCE} \times R_L$$

$$V_{ERROR} = 2 \times I_{SOURCE} \times R_L \tag{20}$$

The two-wire RTD measurement is least accurate with longer lead wires resistance. Two-wire RTD measurement variation with temperature adds significant measurement error. The two-wire RTD measurement is used only when the sensor is located at a very short distance. Higher accuracy is not a concern in this case of short distance. Otherwise (in the case of long distance), the effect of lead wires cannot be eliminated.

### 5.2.6 Three-Wire RTD Application



A NOTE:  $R_{BIAS}$  should be as close to the ADC as possible.

Figure 35. Three-Wire RTD Circuit

For optimum performance in three-wire RTD applications, the two current sources of ADS1220 have been extremely closely matched. Figure 35 shows a typical implementation of a ratiometric 3-wire RTD measurement using two excitation-current sources integrated in the ADS1220, which excites the RTD as well as implements automatic RTD lead-resistance compensation. In order to implement a ratiometric 3-wire RTD measurement using the ADS1220, IDAC1 is routed to one of the excitation leads of the RTD, while IDAC2 is routed to the second excitation lead. Both currents have the same value, which is programmable by IDAC [2:0]: IDAC current setting bits in configuration register 2. The design of the ADS1220 ensures that both IDAC values are closely matched, even across temperature.

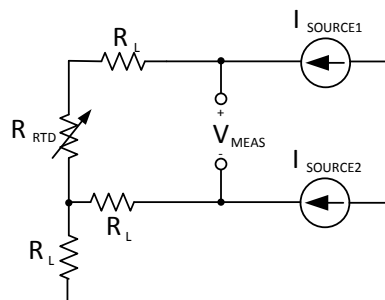


Figure 36. Simplified Three-Wire RTD Configuration and Excitation

Assuming that  $I_{SOURCE1} = I_{SOURCE2} = I$  and all lead wire resistances are equal.

$$V_{MEAS+} = I \times R_L + I \times R_{RTD} + 2 \times I \times R_L = I \times R_{RTD} + 3 \times I \times R_L$$

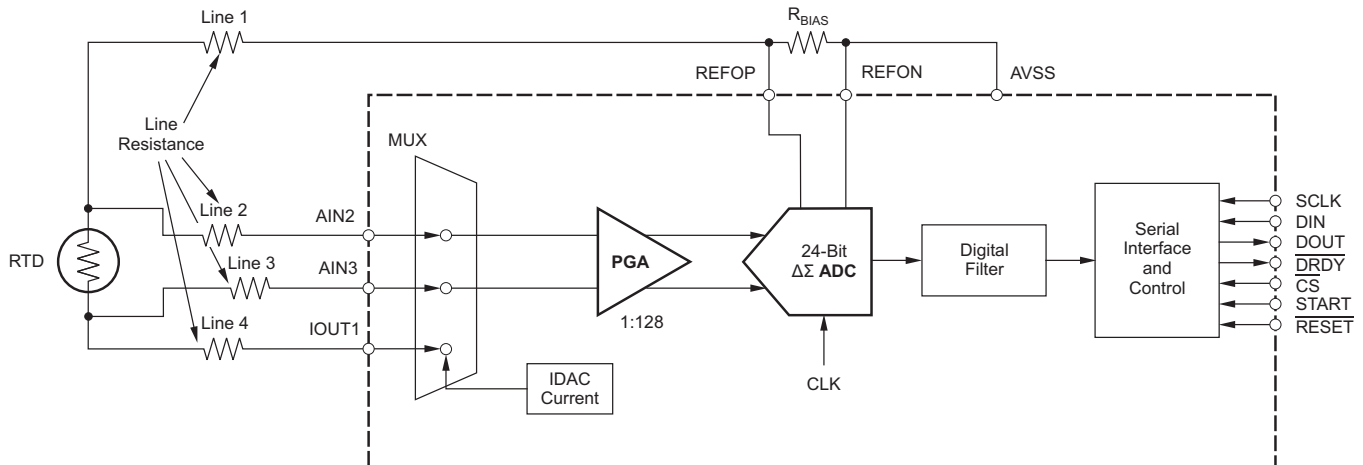
$$V_{MEAS-} = I \times R_L + 2 \times I \times R_L = 3 \times I \times R_L$$

$$V_{MEAS+} - V_{MEAS-} = I \times R_{RTD}$$

(21)

The 3-wire RTD configuration is widely used in industrial applications, because it saves cost by using three wires instead of four wires and provides accurate measurements. The 3-wire RTD configuration provides significant improvement over the 2-wire RTD approach, but the excitation current mismatches (offset and drift) and unequal lead wire resistances can introduce measurement error.

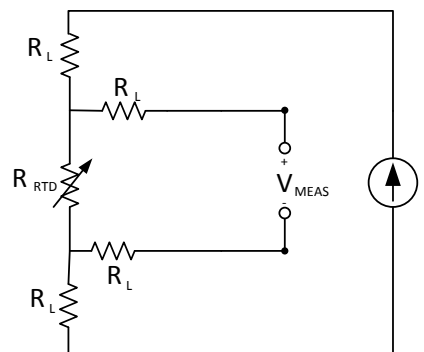
### 5.2.7 Four-Wire RTD Application



A NOTE:  $R_{BIAS}$  should be as close to the ADC as possible.

**Figure 37. Four-Wire RTD Circuit**

The 4-wire RTD approach as shown in [Figure 37](#) provides the highest level of accuracy because it isolates the excitation path of the RTD from the high impedance sensing path. The ADS1220 current sources are connected to one of the RTD line terminals by setting the appropriate I1MUX [2:0]: IDAC1 routing configuration bits and I2MUX [2:0]: IDAC2 routing configuration bits in configuration register 3. Line 4 of the RTD has been tied to the IOUT1 terminal of the device because Line 4 is not a sensing line, which saves an input channel in the device for other sensors. The current value can be chosen by setting IDAC [2:0]: IDAC current setting bits in configuration register 2. The voltage developed across the RTD is also measured by connecting the RTD through the PGA to the ADC. The voltage measured across the RTD is proportional to temperature (determined by the characteristics of the RTD). The value of  $R_{BIAS}$  is selected according to the IDAC current source setting. With ratiometric 4-wire configuration, a small cost is paid for extra wires to get the best accuracy measurements without the influence of the lead wire resistances, compared to the 2- and 3-wire configurations.



**Figure 38. Simplified Four-Wire RTD Configuration and Excitation**

$$V_{MEAS} = I \times R_{RTD} \quad (22)$$

In this way, the system errors are reduced to the measurement circuit accuracy.



### 5.2.8 Connecting Two-, Three-, and Four-Wire RTD Probes

This module is compatible with 2-, 3-, and 4-wire RTD probes. The connection diagrams for connecting to the module are shown in Figure 39. The designer just needs to connect jumper wires externally, as indicated in red color as shown in Figure 39. This arrangement does not call for any change in the hardware on the module. This arrangement is quite useful when the designer can access only the interface connectors.

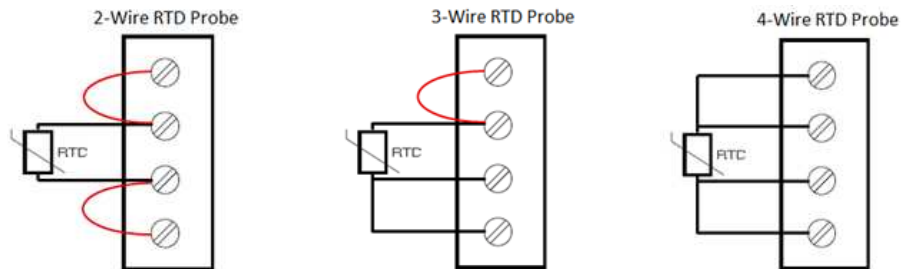


Figure 39. Different RTD Probe Connections

### 5.2.9 Three-Wire RTD Measurement

The ADS1220 integrates all necessary features (such as dual-matched programmable current sources, buffered reference inputs, PGA, and so forth) to ease the implementation of ratiometric 2-, 3-, and 4-wire RTD measurements. The 3-wire RTD configuration is very popular and the most commonly used for industrial temperature sensors. The design calculations are explained in the following paragraph. Figure 40 shows a typical implementation of a ratiometric 3-wire RTD measurement.

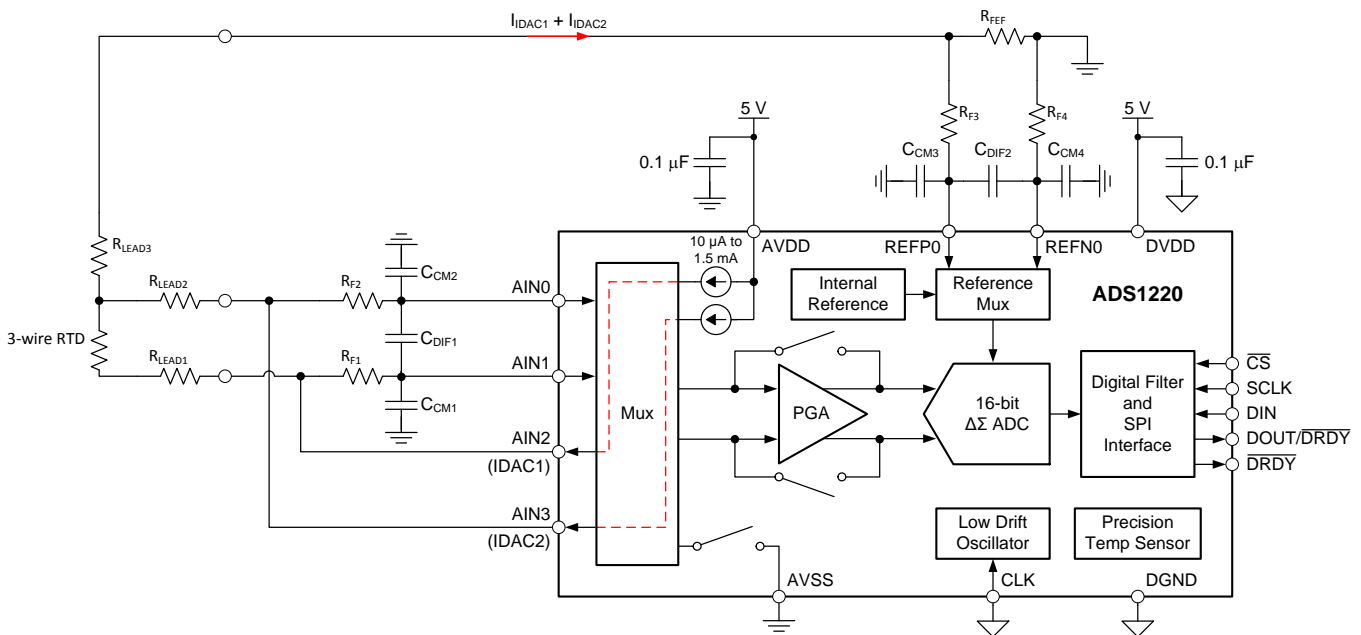


Figure 40. Three-Wire RTD Measurement Circuit Diagram

The ADS1220 features two IDAC current sources capable of outputting currents from 10  $\mu$ A to 1.5 mA. IDAC1 is routed to one of the excitation leads of the RTD, while IDAC2 is routed to the second excitation lead as shown in Figure 40 by the appropriate setting of I1MUX [2:0]: IDAC1 routing configuration bits and I2MUX [2:0]: IDAC2 routing configuration bits in configuration register 3. Both currents have the same value, which is programmable by bits IDAC [2:0] in the configuration register. The design of the ADS1220 ensures that both IDAC values are closely matched, even across temperature.

#### R<sub>REF</sub> and PGA Gain

The resistance of the PT100 changes from 18.52 Ω at -200°C to 390.481 Ω at 850°C. The line resistance  $R_{LEAD}$  depends on the distance of the sensor from the measurement setup. Assume  $R_{LEAD}$  is equal to 5 Ω. The positive resistance swing is from 100 Ω to 390.481 Ω, which is about 290.481 Ω. The negative resistance swing is from 100 Ω to 18.52 Ω, which is about 81.48 Ω. The IDAC current should be 1 mA or less to minimize the self-heating error. The IDAC current chosen is 500 μA.

Therefore, maximum and minimum input voltages to the PGA are 390.481 Ω × 500 μA = 195.2405 mV and 18.52 Ω × 500 μA = 9.26 mV, respectively. The external reference resistor,  $R_{REF}$ , serves two purposes. First, the external reference resistor sets the external reference voltage for ADC. Second, the external reference resistor determines the input common mode voltage of the PGA. It is a best practice to set the common mode voltage around mid-supply  $(AVDD - AVSS) / 2 = (5 V - 0 V) / 2 = 2.5 V$ . Therefore, the reference voltage chosen is 2.49 V, which also depends on an easily available resistance value and excitation current. The sum of both currents flows through a precision low-drift reference resistor,  $R_{REF}$ . The voltage,  $V_{REF}$ , generated across the reference resistor is given in Equation 23.

$$V_{REF} = (IDAC1 + IDAC2) \times R_{REF} \tag{23}$$

Because  $IDAC1 = IDAC2 = 500 \mu A$ ,

$$V_{REF} = 2 \times IDAC1 \times R_{REF} \tag{24}$$

Solving for  $R_{REF}$ :

$$R_{REF} = \frac{V_{REF}}{2 \times IDAC1} = \frac{2.49 V}{2 \times 500 \mu A} = 2.49 K \tag{25}$$

Then, find out the PGA gain:

$$GAIN_{PGA} = \frac{V_{REF}}{V_{IN_{MAX}}} = \frac{2.49 V}{195.2405 mV} = 12.75 V/V \tag{26}$$

The closest gain supported by the PGA is 8 V/V.

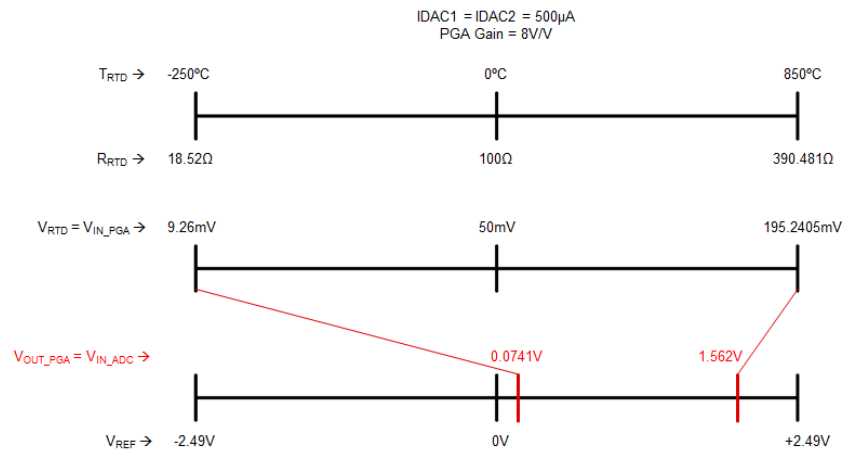
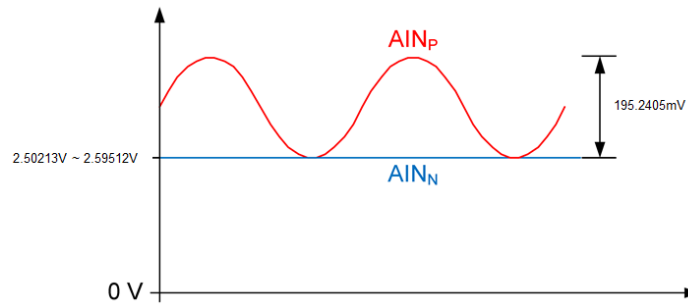


Figure 41. PGA Gain

### Common Mode Input Voltage

The signal of an RTD is of a pseudo-differential nature. The negative input must be biased at a voltage other than 0 V and the positive input can then swing up to 195.2405 mV above the negative input.



**Figure 42. Pseudo-Differential Input Signal**

$$V_{\text{CMI}} = \text{IDAC1} \times R_L + \frac{\text{IDAC1} \times R_{\text{RTD}}}{2} + 2 \times \text{IDAC1} \times (R_L + R_{\text{REF}})$$

where

- IDAC1 = IDAC2
- $R_L = 5 \Omega$  (depends on length of lead wires) (27)

The output common mode of the PGA,  $V_{\text{CMO}}$ , is the same as the input common mode  $V_{\text{CMI}}$ . The PGA output can swing between 0.2 V and 4.8 V. The maximum output differential voltage is 2.49 V. Therefore, the output common mode of the PGA can vary from  $(0.2 \text{ V} + 1.245 \text{ V}) = 1.445 \text{ V}$  to  $(4.8 \text{ V} - 1.245 \text{ V}) = 3.555 \text{ V}$ , so that the output does not saturate. The input common mode can vary between 1.445 V and 3.555 V. In this case, the  $V_{\text{CMI}}$  varies between 2.50213 V to 2.59512 V, which is well within the range of 1.445 V to 3.555 V.

### IDAC Compliance Voltage

While designing the circuit, care should also be taken to meet the compliance voltage requirement of the IDACs. The IDACs require a minimum headroom of  $(\text{AVDD} - 0.9 \text{ V})$  in order to operate accurately.

$$\text{AVSS} + \text{IDAC1} \times (R_{\text{LEAD1}} + R_{\text{RTD}}) + (\text{IDAC1} + \text{IDAC2}) \times (R_{\text{LEAD3}} + R_{\text{REF}}) \leq \text{AVDD} - 0.9 \text{ V}$$

where

- IDAC1 = IDAC2 = 500  $\mu\text{A}$
- $R_{\text{LEAD1}} = R_{\text{LEAD3}} = 5 \Omega$
- $R_{\text{RTD}} (\text{max}) = 390.481 \Omega$
- $R_{\text{REF}} = 2.49 \text{ K}\Omega$

then

- $2.69274 \text{ V} \leq 4.1 \text{ V}$  (28)

In 3-wire RTD configuration, the measurement error resulting from the voltage drop across the RTD lead resistance is compensated, as long as the lead resistance values and the IDAC values are well matched.

Implementing a 2- or 4-wire RTD measurement is very similar to the 3-wire RTD measurement, except that only one IDAC is required.

### 5.2.10 IDAC Multiplex Chopping Technique

The two current sources must be perfectly matched to successfully cancel the lead resistances of the RTD wires. While initial matching of the current sources is important, any remaining mismatch in the two sources can be minimized by using a multiplexer to swap, or “chop,” the two current sources between the two inputs. Taking a measurement in both configurations and averaging the two readings will greatly reduce the effects of mismatched current sources. This design uses a digitally-controlled multiplexer in the ADS1220 to implement this technique.

Sample 1: Measurement with normal current routing as shown in Figure 43.

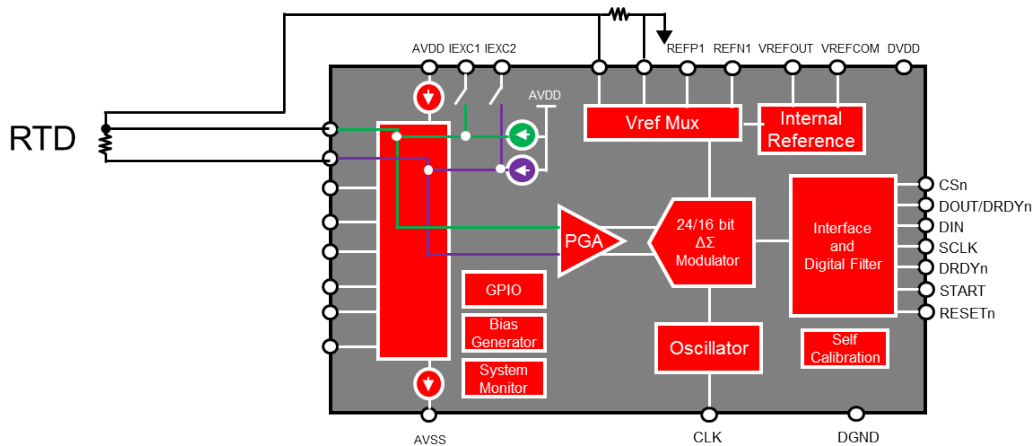


Figure 43. Excitation Current Chopping → Sample 1

Sample 2: Measurement with swapped current routing as shown in Figure 44.

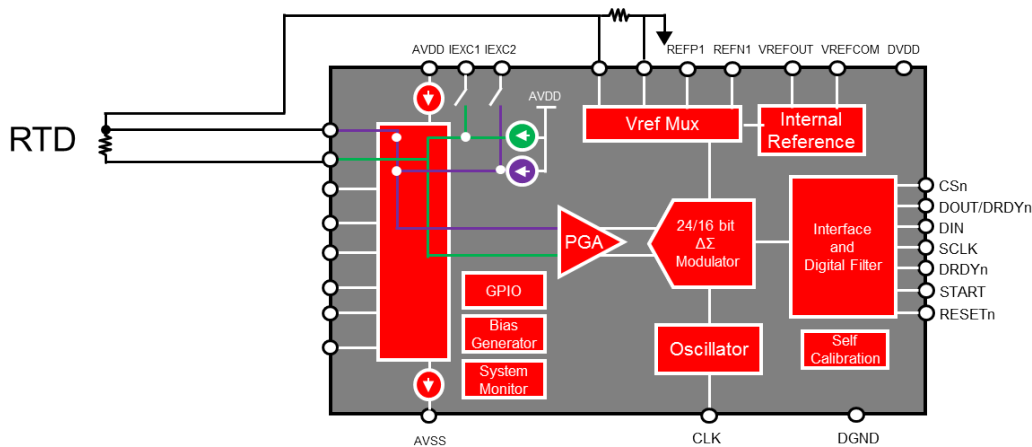


Figure 44. Excitation Current Chopping → Sample 2

$$\text{Mismatch corrected reading} = 0.5 \times (\text{Sample 1} + \text{Sample 2}) \quad (29)$$

### 5.2.11 Noise Considerations and Input Filter

RTD voltage output signals are typically in the millivolt range, which makes them susceptible to noise. A first-order differential and common-mode RC filter ( $R_{F1}$ ,  $R_{F2}$ ,  $C_{DIF1}$ ,  $C_{CM1}$ ,  $C_{CM2}$ ) is placed on the ADC inputs, as well as on the reference inputs ( $R_{F3}$ ,  $R_{F4}$ ,  $C_{DIF2}$ ,  $C_{CM3}$ ,  $C_{CM4}$ ) to eliminate high-frequency noise in RTD measurements. For best performance, it is recommended to match the corner frequencies of the input and reference filters. More detailed information on matching the input and reference filters can be found in the application report, *RTD Ratiometric Measurements and Filtering Using the ADS1148 and ADS1248 Family of Devices*, [SBAA201](#).

The differential filters chosen for this application were designed to have a  $-3$  dB corner frequency at least 10 times larger than the bandwidth of ADC. The selected ADS1220 sampling rate of 20 SPS results in a  $-3$  dB bandwidth of 13.1 Hz. The cut off frequency chosen for this design is higher to account for a faster sampling rate. For proper operation, the differential cutoff frequencies of the reference and input low-pass filters must be well matched. Matching the frequencies can be difficult because, as the resistance of the RTD changes over the span of the measurement, the filter cutoff frequency changes as well. To mitigate this effect, the two resistors used in the input filter ( $R_{I1}$  and  $R_{I2}$ ) are chosen to be more than an order of magnitude larger than the RTD. Limiting the resistors to at most 20 k $\Omega$  keeps DC offset errors low due to input bias current.

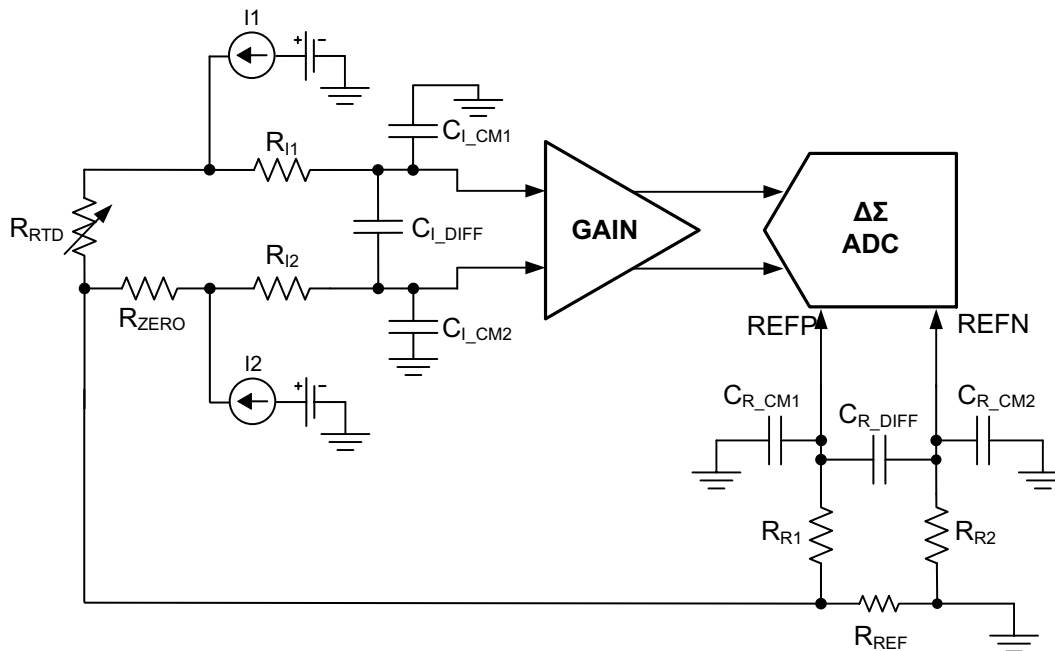


Figure 45. Common Mode and Differential Mode Filters on RTD Input and Reference

$$R_{I1} = R_{I2} = 4.12 \text{ K}$$

$$C_{I\_DIFF} = 0.047 \text{ } \mu\text{F}$$

The  $-3$  dB cutoff frequency of differential input filter at  $186 \text{ } \Omega$  RTD resistance (at mid-scale temperature) can be calculated as given in [Equation 30](#).

$$F_{-3\text{ dB}_I\_DIFF} = \frac{1}{2 \times \pi \times C_{I\_DIFF} \times (R_{I1} + R_{RTD} + R_{I2})}$$

$$F_{-3\text{ dB}_I\_DIFF} \approx 402.1 \text{ Hz} \quad (30)$$

To ensure that mismatch of the common-mode filtering capacitors is not translated to a differential voltage, the common-mode capacitors ( $C_{I\_CM1}$  and  $C_{I\_CM2}$ ) are chosen to be 10 times smaller than the differential capacitor. This common-mode capacitors' size results in a common-mode cutoff frequency that is roughly 10 times larger than the differential filter, making the matching of the common-mode cutoff frequencies less critical.

$$C_{I\_CM1} = C_{I\_CM2} = 4700 \text{ pF}$$

Although it is not always possible to exactly match the corner frequencies of all the filters, a good compromise is to attempt to balance the corner frequencies of the input path differential filter and the reference path differential filter, because these filters have a dominant effect in the performance.

$$R_{R1} = R_{R2} = 4.7 \text{ K}$$

$$C_{R\_DIFF} = 0.033 \text{ } \mu\text{F}$$

The  $-3$  dB cutoff frequency of differential reference filter can be calculated as given in [Equation 31](#).

$$F_{-3\text{ dB}_R\_DIFF} = \frac{1}{2 \times \pi \times C_{R\_DIFF} \times (R_{R1} + R_{REF} + R_{R2})}$$

$$F_{-3\text{ dB}_R\_DIFF} \approx 405.83 \text{ Hz} \quad (31)$$

To ensure that mismatch of the common-mode filtering capacitors is not translated to a differential voltage, the common-mode capacitors (CR\_CM1 and CR\_CM2) were chosen to be 10 times smaller than the differential capacitor. This common-mode capacitors' size results in a common-mode cutoff frequency that is roughly 10 times larger than the differential filter, making the matching of the common-mode cutoff frequencies less critical.

$$CR\_CM1 = CR\_CM2 = 3300 \text{ pF}$$

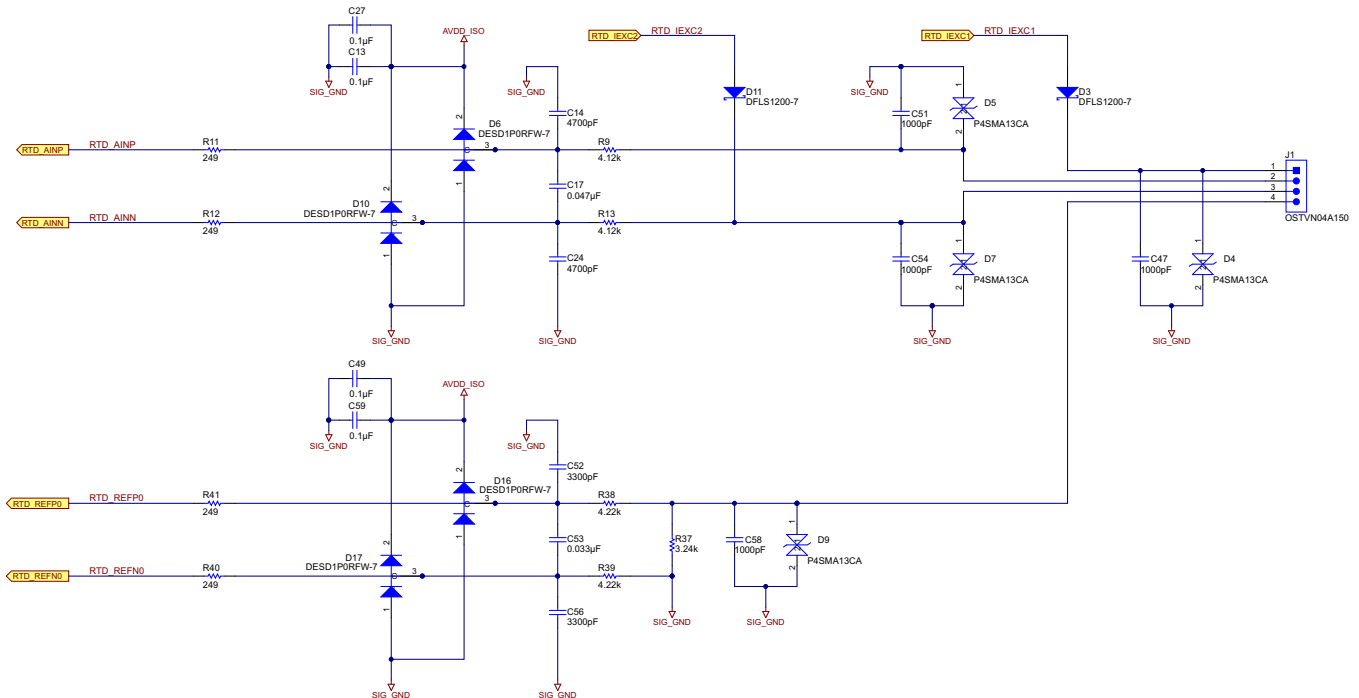


Figure 46. Common Mode and Differential Mode Filters Implemented in Design for RTD

The device uses a linear-phase finite impulse response (FIR) digital filter that performs both filtering and decimation of the digital data stream coming from the modulator. The digital filter is automatically adjusted for the different data rates and always settles within a single cycle. Only at data rates of 5 SPS and 20 SPS can the filter be configured to reject 50-Hz or 60-Hz line frequencies or to simultaneously reject 50 Hz and 60 Hz. Two bits (50/60[1:0]) in the configuration register are used to configure the filter accordingly.

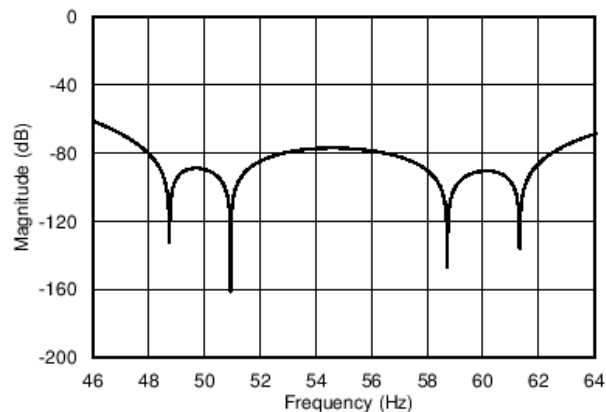


Figure 47. Details View of 50 Hz and 60 Hz Simultaneous Rejection at 20 SPS Data Rate

### 5.2.12 Piecewise Linear Approximation Method

RTD manufacturers usually provide a lookup table that offer excellent accuracy for linearization of a specific type of thermocouple. The granularity on these lookup tables is also very precise—approximately 1°C for each lookup value. To save microcontroller memory and development time, an interpolation technique applied to these values can be used. An example of this method when converting from voltage to temperature with eight lookup table entries is shown in Figure 48.

To perform a linear interpolation using a lookup table, first compare the measured RTD resistance to values given in the lookup table, until the lookup table value exceeds the measured value that is being converted.

Then, use Equation 32 to convert the measured RTD resistance to temperature, where  $R_{LT}$  is the resistance lookup table array, and  $T_{LT}$  is the temperature lookup table array. This operation involves four additions, one multiplication, and one division step, respectively. This operation can be done easily on most 16- and 32-bit microcontrollers.

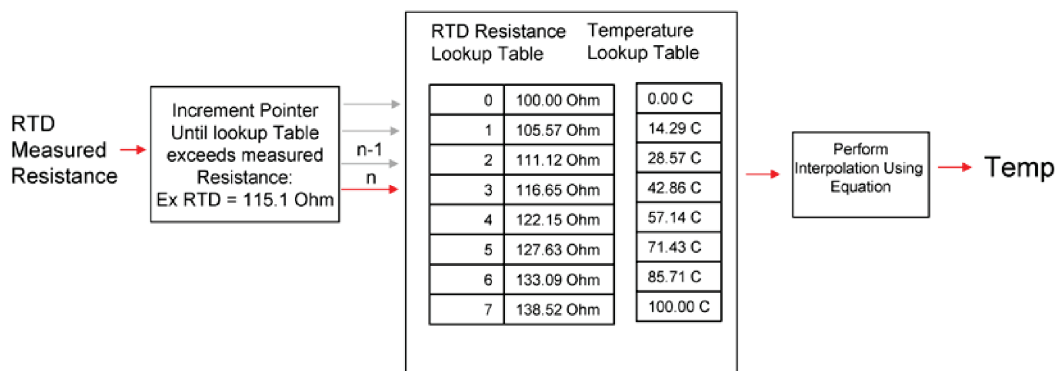


Figure 48. V-to-T Conversion Block Diagram for RTD

$$T = T_{LT} [n - 1] + (T_{LT} [n] - T_{LT} [n - 1]) \left( \frac{R_{IN} - R_{LT} [n - 1]}{R_{LT} [n] - R_{LT} [n - 1]} \right) \tag{32}$$

There is a trade-off between memory size and the piecewise linear approximation method’s accuracy. The more entries on the lookup table, the more accurate the results are. However, the larger number of entries on the lookup table uses more memory space.

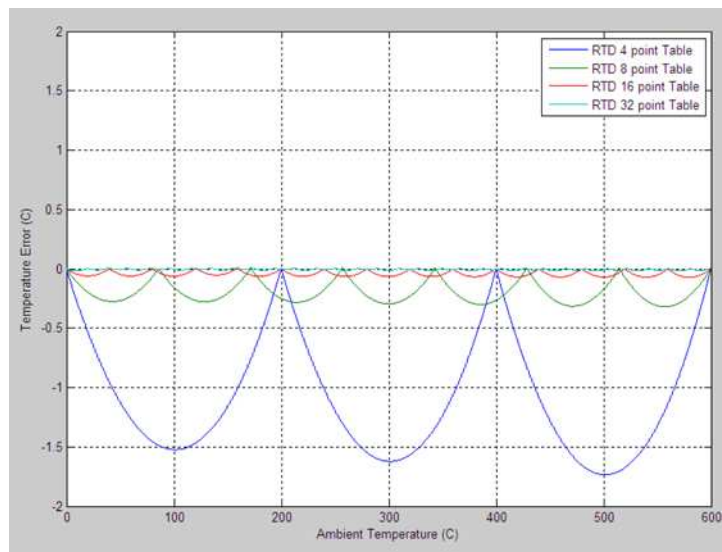


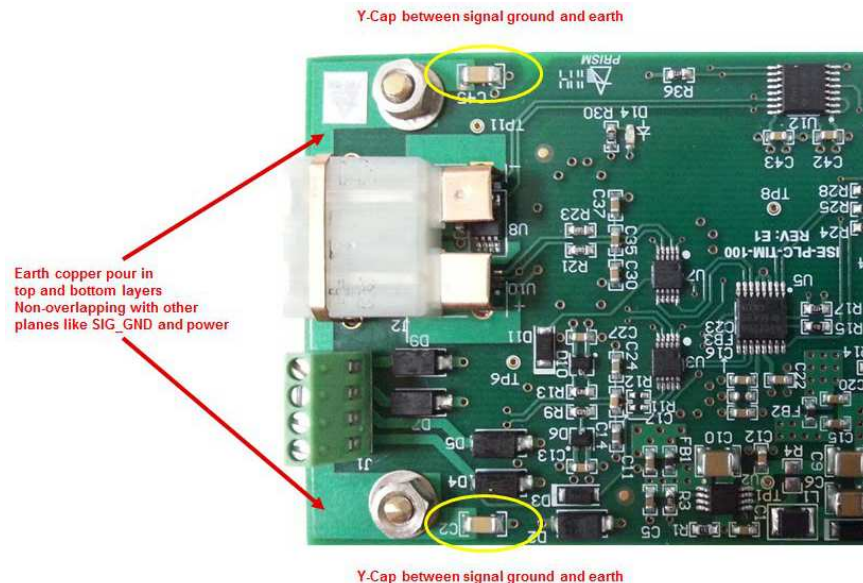
Figure 49. Temperature Error versus Temperature Using Different Sizes of lookup Table

## 6 Protection

In industrial and automotive environments, electronic devices can be subjected to high-voltage transients and overvoltage events very often. Transient voltage can cause severe damage and failure of the device. Overcoming unwanted damaging transient threats is one of the biggest challenges in the design. Therefore, adding robust EMC protection externally becomes a necessity. In the event that the device is exposed to transients on the inputs in excess of its ratings, external transient absorbers (Zener, TVS diodes and/or ESD diodes) are required. The TVS diode basically safeguards sensitive devices and circuitry by clamping the voltage level and diverting transient energy away from the device being protected when a trigger voltage is reached.

The following paragraph describes the case of 1 KV (CM) at 8/20  $\mu$ s surge on the input lines.

The front end protection circuit consists of a P4SMA13CA TVS diode with 1000 pF/100 V Y-cap in parallel. Apart from that, three more 1000 pF/2 kV Y-caps have been placed at three different locations on the board. Transient events like ESD, Surge, and EFT bursts are wideband phenomena with spectral components up to hundreds of MHz and appear as common-mode pulses to the inputs. The Y-caps provide a quick and low impedance return path to these fast transients. These Y-caps work in tandem with the TVS diode, anytime 1000 pF/100 V Y-cap start charging and 1000 pF/100 V Y-cap voltage exceeds breakdown voltage of the TVS diode. The TVS diode acts immediately and clamps the voltage to the safe limits.



**Figure 50. Placement Y-Cap Between Signal Ground and Earth**

$$\text{Pulse Current} = I_P = \frac{(1000 \text{ V} - V_C)}{Z_s + R_s}$$

where

- $V_C$  is the clamping voltage of TVS at  $I_P$
- $Z_s$  is the source impedance of pulse generator
- $R_s$  is the external series filter resistance
- $Z_s = 42 \Omega$
- $R_s = 0 \Omega$

(33)

$$\text{Clamping Voltage} = V_C = \frac{I_P}{I_{PP(\text{MAX})}} [V_C(\text{MAX}) - V_{BR(\text{MAX})}] + V_{BR(\text{MAX})}$$

(34)

$$\text{Pulse Power Dissipation} = P_P = V_C \times I_P$$

(35)

For P4SMA13CA TVS (Rating:  $V_R = 11.1 \text{ V}$ ,  $V_C(\text{MAX}) = 18.2 \text{ V}$  at  $I_{PP(\text{MAX})} = 22.5 \text{ V}$ ,  $P_{PP(\text{MAX})} = 400 \text{ Watts}$  at 10/1000  $\mu$ s or 1.8 KWatts at 8/20  $\mu$ s and maximum leakage current = 1  $\mu$ A)



Use the TVS ratings to solve Equation 33, Equation 34, and Equation 35 for  $I_p$ ,  $V_C$  and  $P_p$ :

$$I_p \approx 23.37 \text{ A}$$

$V_C \approx 18.38 \text{ V}$ , which is still greater than the absolute maximum rating of ADS1220

$$P_p = V_C \times I_p \approx 430 \text{ Watts, which is less 1.8 KWatts at } 8/20 \mu\text{s}$$

**Table 7. ABSOLUTE MAXIMUM RATINGS**

		VALUE		UNIT
		MIN	MAX	
AVDD to AVSS		-0.3	7	V
DVDD to DGND		-0.3	7	V
AVSS to DGND		-2.8	0.3	V
Analog input voltage	AIN0/REFP1, AIN1, AIN2, AIN3/REFN1, REFPO, REFNO	AVSS - 0.3	AVDD + 0.3	V
Digital input voltage	$\overline{CS}$ , SCLK, DIN, DOUT/ $\overline{DRDY}$ , $\overline{DRDY}$ , CLK	DGND - 0.3	DVDD + 0.3	V
Analog input current	Momentary	-100	100	mA
	Continuous	-10	10	

In the second stage, the circuit uses a DESD1P0RFW-7 ESD diode to clamp the input to the power supply rail during the transient event and a series resistor of 499  $\Omega$  in thermocouple input path (4.12 K and 4.7 K for the RTD) to limit the current.

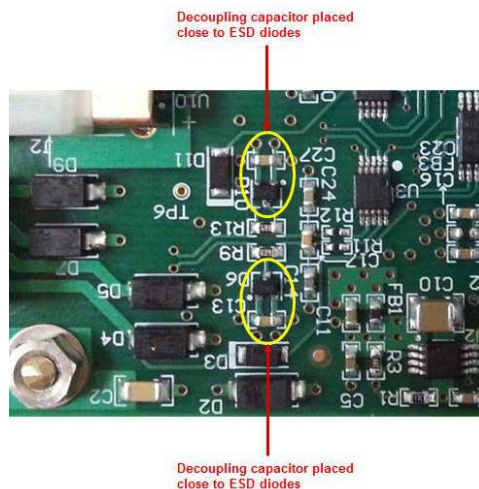
$$\text{Maximum Current through ESD diode} = \frac{\text{TVS Clamping Voltage} - \text{AVDD}}{\text{Series Resistance}} = \frac{18.38 \text{ V} - 5 \text{ V}}{499 \Omega} \approx 27 \text{ mA} \quad (36)$$

Based on the DESD1P0RFW-7 ESD diode datasheet, the DESD1P0RFW-7 ESD diode clamping voltage is less than 1.2 V at 27 mA forward current. Therefore, the input is clamped at (5 V + 1.2 V) = 6.2 V, which is still higher than 5.3 V (AVDD + 0.3 V = absolute maximum rating of ADS1220).

To mitigate the higher voltage, one more series resistance of 249  $\Omega$  has been introduced as shown in Figure 51.

$$\text{Analog Input Current} = \frac{6.2 \text{ V} - 5.3 \text{ V}}{249 \Omega} = 3.9 \text{ mA} \quad (37)$$

The analog input current of 3.9 mA is less than 10 mA maximum rating of the device. Decoupling capacitors of 0.1  $\mu\text{F}$  have also been placed near each ESD diode power supply pin. During a transient event, it is likely that power supply may rise above 5 V and exceed the device's maximum rating. To take care of such a situation, the PTZTE255.1B - 5.4 V Zener diode is used on the power supply rail.



**Figure 51. Placement of De-Coupling Capacitor Near ESD Diodes**

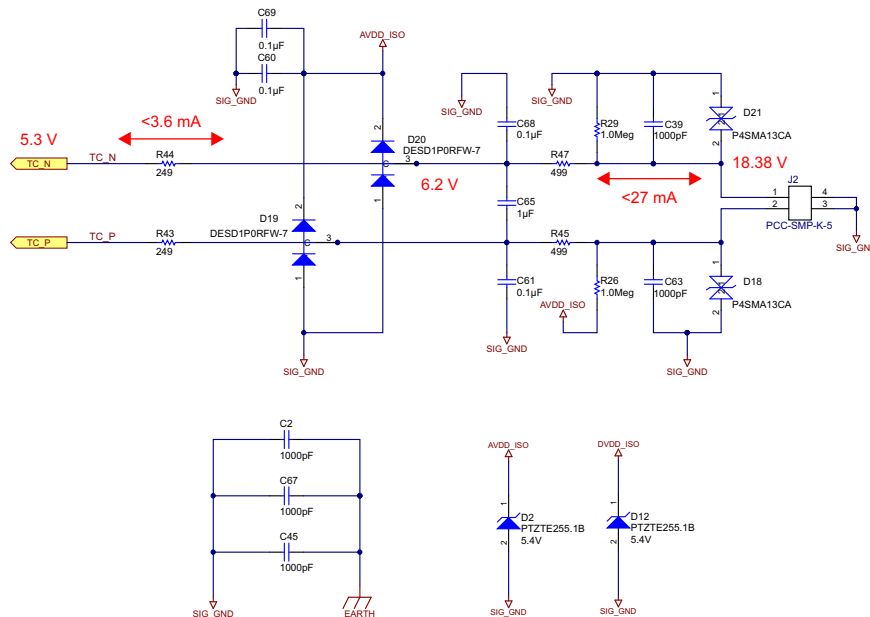


Figure 52. Protection Circuitry Implemented in the Design

Adding external protection devices like Schottky, Sener, TVS, and ESD diodes also adds leakage current path in the sensor signal chain. Therefore, it is always important to choose low leakage protection devices in order to achieve high accuracy

## 7 Power Supply Design and Isolation

The power supply input to the temperature sensor interface module is approximately 24-V DC  $\pm$  20%. The expected outputs required for proper operation are non-isolated 3.3 V/50 mA and isolated 5 V/100 mA as shown in Figure 53.

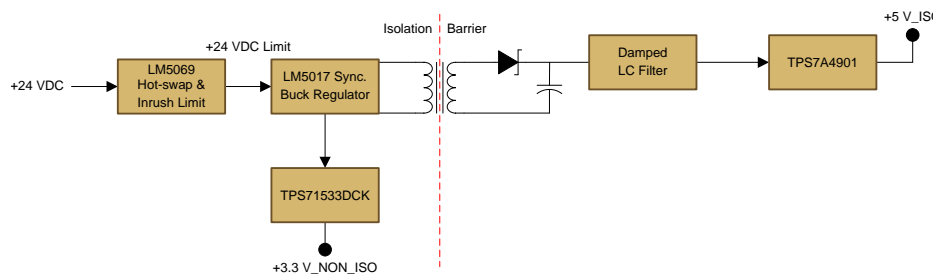


Figure 53. Power Tree

The front-end consists of an LM5069 positive hot swap controller providing intelligent control of the power supply connections during insertion and removal of the module from a live system backplane or other "hot" power sources. The LM5069 provides in-rush current control to limit system voltage droop and transients. The current limit and power dissipation in the external series pass N Channel MOSFET are programmable, ensuring operation within the Safe Operating Area (SOA).

### Current Limit

$$\text{Desired Current Limit Threshold (I}_{\text{LIMIT}}) = \frac{55 \text{ mV}}{R16 \text{ (in m}\Omega)} = \frac{55 \text{ mV}}{15 \text{ m}\Omega} = 2.75 \text{ A} \tag{38}$$

For proper operation of the device, R16 must be smaller than 100 m $\Omega$ .

**NOTE:** The current sense resistor (R16) must be placed near to LM5069 and connected using the Kelvin Connection as shown in Figure 54.

Kelvin Sense Connection

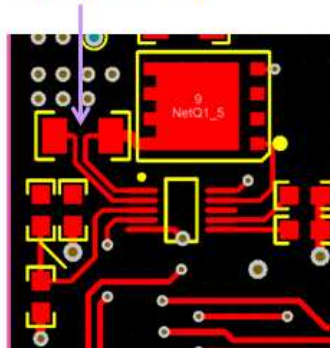


Figure 54. Kelvin Sense Connection for Sense Resistor

UVLO and OVLO

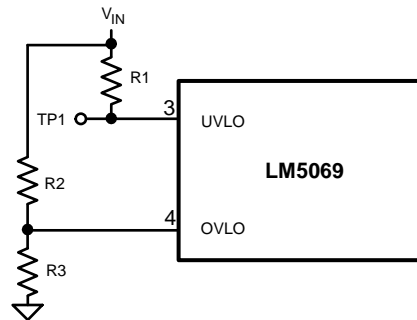


Figure 55. UVLO & OVLO Using External Resistors

Choose the upper and lower UVLO thresholds:

$$R1 = \frac{V_{UVH} - V_{UVL}}{21 \mu A} = \frac{1.5 V}{21 \mu A} = 71.5 K \tag{39}$$

$$R4 = \frac{2.5 V \times R1}{V_{UVL} - 2.5 V} = \frac{2.5 V \times 71.5 K}{14.66 V - 2.5 V} = 14.7 K \tag{40}$$

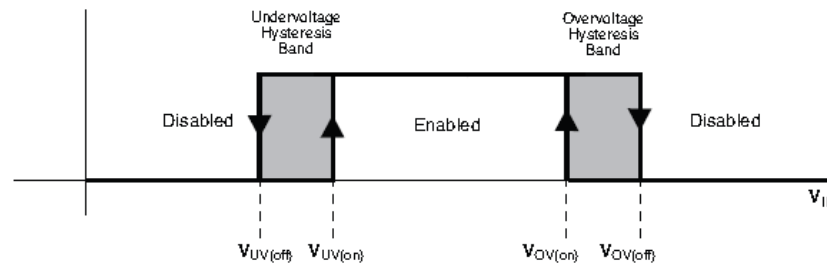
Therefore,  $V_{UVH} = 16.1 V$  and  $V_{UVL} = 14.66 V$  with hysteresis of 1.5 V that keeps the device from responding to power-on glitches during start up.

Choose the upper and lower OVLO thresholds:

$$R2 = \frac{V_{OVH} - V_{OVL}}{21 \mu A} = \frac{2 V}{21 \mu A} = 95.3 K \tag{41}$$

$$R3 = \frac{2.5 V \times R2}{V_{OVL} - 2.5 V} = \frac{2.5 V \times 95.3 K}{34.27 V - 2.5 V} = 7.5 K \tag{42}$$

Therefore,  $V_{OVH} = 34.27 V$  and  $V_{OVL} = 31.77 V$  with hysteresis of 2 V.


**Figure 56. UVLO and OVLO Hysteresis**

Refer to LM5069 datasheet [SNVS452D](#) and LM5069EVAL evaluation board [SNVA184B](#) for device operation, design procedure, and recommended PCB layout guidelines.

To protect against transients and ground loops, the field side or the sensor side is galvanically isolated from the control side. The LM5017 device has been used to generate two supplies, nonisolated 3.3 V and isolated 5 V, from 24-V DC input. The LM5017 is a synchronous buck (step-down) regulator with integrated MOSFETs. The isolated Fly-Buck topology uses a smaller transformer for power transfer from primary and secondary. In the Fly-Buck, the regulation is done on the primary side. Therefore, no opto-coupler or auxiliary winding is needed, resulting in smaller size and a more cost effective solution.

When the circuit is in regulation, the buck switch is turned on each cycle for a time determined by  $R_{ON}$  and  $V_{IN}$  according to [Equation 43](#).

$$T_{ON} = \left( \frac{10^{-10} \times R_{ON}}{V_{IN}} \right) = \left( \frac{10^{-10} \times 137 \text{ K}}{24 \text{ V}} \right) = 0.571 \mu\text{sec} \quad (43)$$

The operating frequency can be calculated with [Equation 44](#):

$$F_{SW} = \frac{V_{OUT}}{10^{-10} \times R_{ON}} = \frac{7 \text{ V}}{10^{-10} \times 137 \text{ K}} = 511 \text{ KHz} \quad (44)$$

The non-isolated output voltage ( $V_{CC\_NON\_ISO}$ ) is set by two external resistors ( $R_8$  and  $R_{10}$ ). The regulated output voltage is calculated in [Equation 45](#):

$$V_{CC\_NON\_ISO} = 1.225 \times \left( \frac{R_8}{R_{10}} + 1 \right) = 1.255 \times \left( \frac{46.4 \text{ K}}{10 \text{ K}} + 1 \right) = 6.91 \text{ V} \quad (45)$$

$V_{CC\_NON\_ISO}$  is given to TPS71533DCK LDO that generates  $3.3 \text{ V}_{NON\_ISO}$  and is capable of delivering 50 mA of output current.  $3.3 \text{ V}_{NON\_ISO}$  is then used to power-up one EEPROM and two digital isolators.

### Selection of rectifier diode D1

The reverse bias voltage across D1 when the high side buck switch is on:

$$V_{D1} = \frac{N_S}{N_P} V_{IN\_MAX} = 1 \times 32 = 32 \text{ V} \quad (46)$$

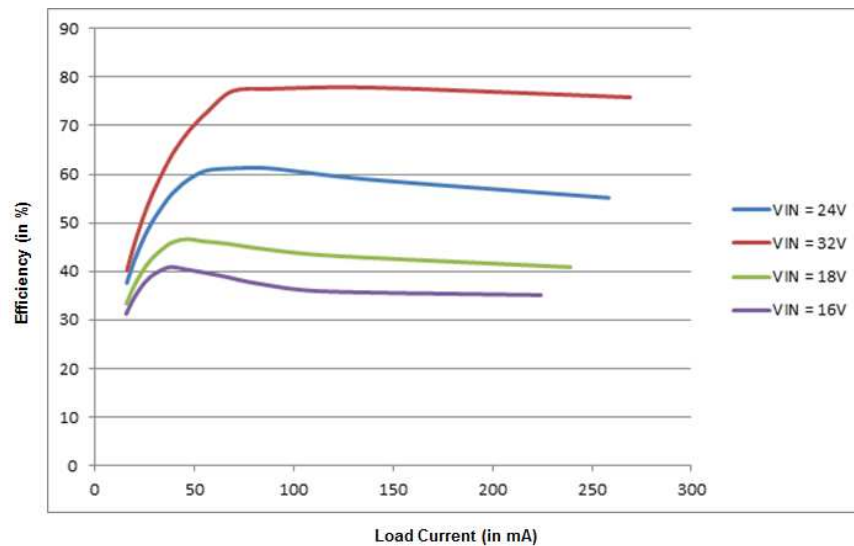
Therefore, the PIV for the selected diode must be greater than the 32 V.

Rectified output (+ $V_{CC\_ISO}$ ) on the secondary side will be:

$$+V_{CC\_ISO} = \frac{N_S}{N_P} \times V_{CC\_NON\_ISO} - V_{F\_D1} = 6.91 - 0.4 \text{ V} = 6.51 \text{ V} \quad (47)$$

D15 is an optional diode connected between  $V_{CC\_NON\_ISO}$  and VCC regulator output. When  $V_{CC\_NON\_ISO}$  is  $> V_{CC}$ , the VCC is supplied from  $V_{CC\_NON\_ISO}$ , which results in reduced losses in the VCC regulator inside the IC.

The efficiency curve for LM5017 is also given in [Figure 57](#).



**Figure 57. Efficiency versus Load Current Graph for LM5017**

Refer to the LM5017 datasheet [SNVS783G](#), and *AN-2292 Designing an Isolated Buck (Fly-Buck) Converter* [SNVA674](#) for device operation, design procedure, and recommended PCB layout guidelines.

It is generally not recommended to power-up ADCs directly from the switching regulator output because the switching regulator output always contains ripple noise due to switching frequency and high-frequency noise. Rapid transitions in the voltage or currents cause high-frequency noise. Applying the switching regulator output directly to the ADC would kill the ADC's performance. Therefore, it is always best practice to power-up ADCs from a low noise LDO with high PSRR. The LDO selected for the design is TPS7A4901. TPS7A4901 supports up to 36 V of input voltage and has an ultra-low noise of 15.4  $\mu\text{V}_{\text{RMS}}$  and 72 dB PSRR. The low-frequency ripple noise from the switching regulator can adequately be attenuated by the TPS7A4901. Typically, PSRR of LDOs is high at lower frequencies, tends to decrease at higher frequencies, and becomes zero above a few MHz. Therefore, it is important to add at least a single damped LC filter right at the LDO input to prevent the noise coupling through the LDO to the ADC.

The TPS7A4901 comes from a series of high-voltage, ultra-low noise LDOs that are ideal for precision applications. A resistor divider at the LDO output sets the output voltage ( $V_{\text{LDO\_OUT}}$ ) proportional to the LDO's internal reference voltage ( $V_{\text{LDO\_REF}}$ ). For this device,  $V_{\text{LDO\_REF}} = 1.194 \text{ V}$ . In order to set  $V_{\text{LDO\_OUT}}$  to the desired 5 V, the resistor divider components are selected as:

$$V_{\text{LDO\_OUT}} = V_{\text{LDO\_REF}} \times \left[ \frac{R3}{R1} + 1 \right]$$

where

- $R3 = 47.5 \text{ K}$

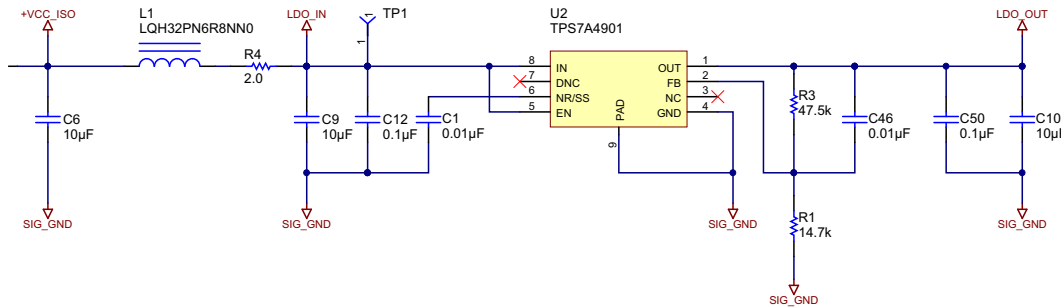
and

- $R1 = 14.7 \text{ K}$

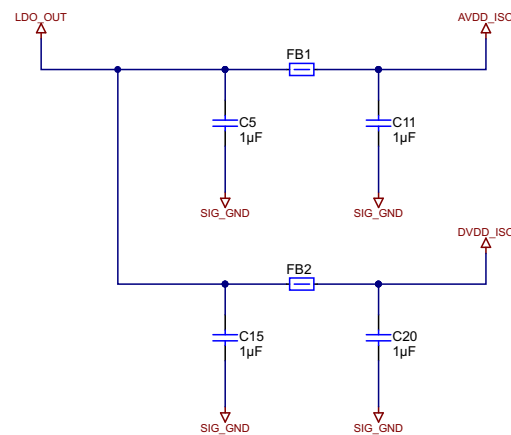
then

- $V_{\text{LDO\_OUT}} = 5 \text{ V}$

(48)


**Figure 58. LC Filter and LDO Implemented in Design**

ADS1220 has a separate analog supply (AVDD) and digital supply (DVDD). Both are generated using 5 V  $V_{LDO\_OUT}$  but are separated from each other using ferrite beads to prevent digital switching noise from entering in to the AVDD pin of the ADC.

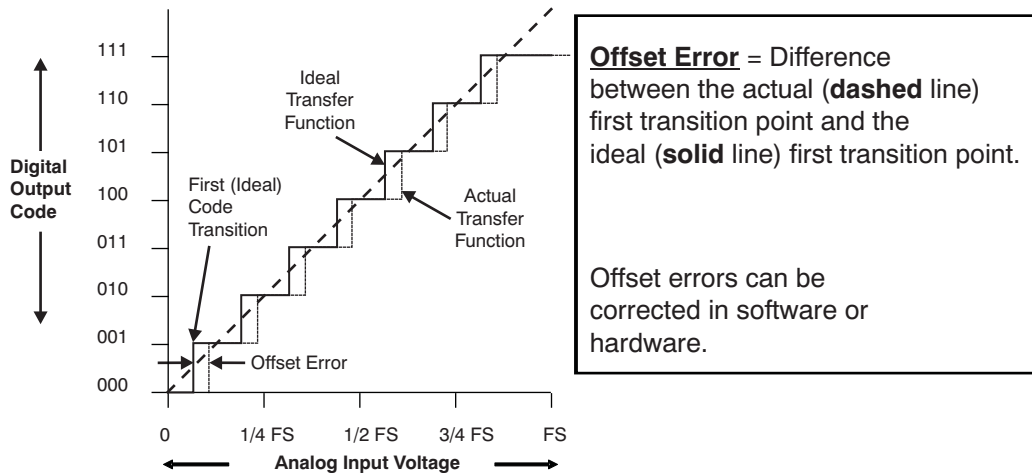

**Figure 59. AVDD and DVDD Separated by Ferrite Bead**

## 8 Test Setup, Calibration, Histogram, Verification, and Measured Performance

### 8.1 Offset Calibration

It is recommended to run an offset calibration routine before performing any measurements or when changing the gain of the PGA to compensate for the offset related PGA and ADC within the ADS1220 device. The internal offset of the ADS1220 can be measured by shorting the inputs to mid-supply by setting MUX [3:1] bits to 1110 in configuration register 0. The TIVA microcontroller (on the base board) then takes multiple readings (32 readings as implemented in the firmware) from the ADS1220 with the inputs shorted, averaging the results to reduce the effect of noise and store the average value in the TIVA microcontroller memory. When measuring the sensor signal, the microcontroller then subtracts the stored offset value from each ADS1220 reading to get an offset compensated result (OCR) as shown in [Equation 49](#). The offset calibration for thermocouple and RTD input channels is done in the same method as internal to the ADS1220.

$$\text{OCR} = \text{RAW\_CODE}_{\text{ADC}} - \text{OFFSET\_COUNTS} \quad (49)$$



In this graph, FS means Full Scale.

Figure 60. Offset Error

```

506
507
508 * Name: offset_calib_ADS1220
509 * Brief: Used for the calibration of the ADC
510 * Short: ADMP and AINN-N with AD0=AD55/2 for calibration
511 * offset will be calculated by measuring the differential voltage between AINP and AINN
512 * Parameter: spiBase : Base address of the SSI
513 * I2C_base : Base address of the I2C
514 * slot : Slot information
515 * Return: None
516
517 void offset_calib_ADS1220(unsigned int spiBase, unsigned int I2C_base, unsigned char slot)
518 {
519     // Return if there is an error
520     if(Error_status)
521         return;
522
523     uint8_t i=0, j=0;
524     uint64_t ADCdata=0;
525     uint32_t spi_temp;
526     unsigned char temp_array[10]=(0);
527     if(slot == SLO1)
528     {
529         for(i=0; i<8; i++)
530             Offset_ADS1220_SLO1[i] = 0;
531     }
532     else if(slot == SLO2)
533     {
534         for(i=0; i<8; i++)
535             Offset_ADS1220_SLO2[i] = 0;
536     }
537
538     // Copy all the register Values into temp register
539     temp_array[5] = 0x23;
540     Set_CS_Low(slot);
541     spi_Bulk_read_write(&temp_array[5], 5, spiBase);
542     Set_CS_High(slot);
543
544     for(i=0; i<8; i++)
545     {
546         ADCdata =0;
547         // write the hard code Value into the registers for calibration
548         temp_array[0] = 0x43;
549         temp_array[1] = 0xE0 | (i<<1);
550         temp_array[2] = 0x00;
551         temp_array[3] = 0x18;
552         temp_array[4] = 0x00;
553     }
554 }
555
556
557
558
559
560
561
562
563
564
565
566
567
568
569
570
571
572
573
574
575
576
577
578
579
580
581
582
583
584
585
586
587
588
589
590
591
592
593
594
595
596
597
598
599
600
601
602
603
604
605
606
607
608
609
610
611
612
613
614
615
616
617
618
619
620
621
622
623
624
625
626
627
628
629
630
631
632
633
634
635
636
637
638
639
640
641
642
643
644
645
646
647
648
649
650
651
652
653
654
655
656
657
658
659
660
661
662
663
664
665
666
667
668
669
670
671
672
673
674
675
676
677
678
679
680
681
682
683
684
685
686
687
688
689
690
691
692
693
694
695
696
697
698
699
700
701
702
703
704
705
706
707
708
709
710
711
712
713
714
715
716
717
718
719
720
721
722
723
724
725
726
727
728
729
730
731
732
733
734
735
736
737
738
739
740
741
742
743
744
745
746
747
748
749
750
751
752
753
754
755
756
757
758
759
760
761
762
763
764
765
766
767
768
769
770
771
772
773
774
775
776
777
778
779
780
781
782
783
784
785
786
787
788
789
790
791
792
793
794
795
796
797
798
799
800
801
802
803
804
805
806
807
808
809
810
811
812
813
814
815
816
817
818
819
820
821
822
823
824
825
826
827
828
829
830
831
832
833
834
835
836
837
838
839
840
841
842
843
844
845
846
847
848
849
850
851
852
853
854
855
856
857
858
859
860
861
862
863
864
865
866
867
868
869
870
871
872
873
874
875
876
877
878
879
880
881
882
883
884
885
886
887
888
889
890
891
892
893
894
895
896
897
898
899
900
901
902
903
904
905
906
907
908
909
910
911
912
913
914
915
916
917
918
919
920
921
922
923
924
925
926
927
928
929
930
931
932
933
934
935
936
937
938
939
940
941
942
943
944
945
946
947
948
949
950
951
952
953
954
955
956
957
958
959
960
961
962
963
964
965
966
967
968
969
970
971
972
973
974
975
976
977
978
979
980
981
982
983
984
985
986
987
988
989
990
991
992
993
994
995
996
997
998
999
1000
1001
1002
1003
1004
1005
1006
1007
1008
1009
1010
1011
1012
1013
1014
1015
1016
1017
1018
1019
1020
1021
1022
1023
1024
1025
1026
1027
1028
1029
1030
1031
1032
1033
1034
1035
1036
1037
1038
1039
1040
1041
1042
1043
1044
1045
1046
1047
1048
1049
1050
1051
1052
1053
1054
1055
1056
1057
1058
1059
1060
1061
1062
1063
1064
1065
1066
1067
1068
1069
1070
1071
1072
1073
1074
1075
1076
1077
1078
1079
1080
1081
1082
1083
1084
1085
1086
1087
1088
1089
1090
1091
1092
1093
1094
1095
1096
1097
1098
1099
1100
1101
1102
1103
1104
1105
1106
1107
1108
1109
1110
1111
1112
1113
1114
1115
1116
1117
1118
1119
1120
1121
1122
1123
1124
1125
1126
1127
1128
1129
1130
1131
1132
1133
1134
1135
1136
1137
1138
1139
1140
1141
1142
1143
1144
1145
1146
1147
1148
1149
1150
1151
1152
1153
1154
1155
1156
1157
1158
1159
1160
1161
1162
1163
1164
1165
1166
1167
1168
1169
1170
1171
1172
1173
1174
1175
1176
1177
1178
1179
1180
1181
1182
1183
1184
1185
1186
1187
1188
1189
1190
1191
1192
1193
1194
1195
1196
1197
1198
1199
1200
1201
1202
1203
1204
1205
1206
1207
1208
1209
1210
1211
1212
1213
1214
1215
1216
1217
1218
1219
1220
1221
1222
1223
1224
1225
1226
1227
1228
1229
1230
1231
1232
1233
1234
1235
1236
1237
1238
1239
1240
1241
1242
1243
1244
1245
1246
1247
1248
1249
1250
1251
1252
1253
1254
1255
1256
1257
1258
1259
1260
1261
1262
1263
1264
1265
1266
1267
1268
1269
1270
1271
1272
1273
1274
1275
1276
1277
1278
1279
1280
1281
1282
1283
1284
1285
1286
1287
1288
1289
1290
1291
1292
1293
1294
1295
1296
1297
1298
1299
1300
1301
1302
1303
1304
1305
1306
1307
1308
1309
1310
1311
1312
1313
1314
1315
1316
1317
1318
1319
1320
1321
1322
1323
1324
1325
1326
1327
1328
1329
1330
1331
1332
1333
1334
1335
1336
1337
1338
1339
1340
1341
1342
1343
1344
1345
1346
1347
1348
1349
1350
1351
1352
1353
1354
1355
1356
1357
1358
1359
1360
1361
1362
1363
1364
1365
1366
1367
1368
1369
1370
1371
1372
1373
1374
1375
1376
1377
1378
1379
1380
1381
1382
1383
1384
1385
1386
1387
1388
1389
1390
1391
1392
1393
1394
1395
1396
1397
1398
1399
1400
1401
1402
1403
1404
1405
1406
1407
1408
1409
1410
1411
1412
1413
1414
1415
1416
1417
1418
1419
1420
1421
1422
1423
1424
1425
1426
1427
1428
1429
1430
1431
1432
1433
1434
1435
1436
1437
1438
1439
1440
1441
1442
1443
1444
1445
1446
1447
1448
1449
1450
1451
1452
1453
1454
1455
1456
1457
1458
1459
1460
1461
1462
1463
1464
1465
1466
1467
1468
1469
1470
1471
1472
1473
1474
1475
1476
1477
1478
1479
1480
1481
1482
1483
1484
1485
1486
1487
1488
1489
1490
1491
1492
1493
1494
1495
1496
1497
1498
1499
1500
1501
1502
1503
1504
1505
1506
1507
1508
1509
1510
1511
1512
1513
1514
1515
1516
1517
1518
1519
1520
1521
1522
1523
1524
1525
1526
1527
1528
1529
1530
1531
1532
1533
1534
1535
1536
1537
1538
1539
1540
1541
1542
1543
1544
1545
1546
1547
1548
1549
1550
1551
1552
1553
1554
1555
1556
1557
1558
1559
1560
1561
1562
1563
1564
1565
1566
1567
1568
1569
1570
1571
1572
1573
1574
1575
1576
1577
1578
1579
1580
1581
1582
1583
1584
1585
1586
1587
1588
1589
1590
1591
1592
1593
1594
1595
1596
1597
1598
1599
1600
1601
1602
1603
1604
1605
1606
1607
1608
1609
1610
1611
1612
1613
1614
1615
1616
1617
1618
1619
1620
1621
1622
1623
1624
1625
1626
1627
1628
1629
1630
1631
1632
1633
1634
1635
1636
1637
1638
1639
1640
1641
1642
1643
1644
1645
1646
1647
1648
1649
1650
1651
1652
1653
1654
1655
1656
1657
1658
1659
1660
1661
1662
1663
1664
1665
1666
1667
1668
1669
1670
1671
1672
1673
1674
1675
1676
1677
1678
1679
1680
1681
1682
1683
1684
1685
1686
1687
1688
1689
1690
1691
1692
1693
1694
1695
1696
1697
1698
1699
1700
1701
1702
1703
1704
1705
1706
1707
1708
1709
1710
1711
1712
1713
1714
1715
1716
1717
1718
1719
1720
1721
1722
1723
1724
1725
1726
1727
1728
1729
1730
1731
1732
1733
1734
1735
1736
1737
1738
1739
1740
1741
1742
1743
1744
1745
1746
1747
1748
1749
1750
1751
1752
1753
1754
1755
1756
1757
1758
1759
1760
1761
1762
1763
1764
1765
1766
1767
1768
1769
1770
1771
1772
1773
1774
1775
1776
1777
1778
1779
1780
1781
1782
1783
1784
1785
1786
1787
1788
1789
1790
1791
1792
1793
1794
1795
1796
1797
1798
1799
1800
1801
1802
1803
1804
1805
1806
1807
1808
1809
1810
1811
1812
1813
1814
1815
1816
1817
1818
1819
1820
1821
1822
1823
1824
1825
1826
1827
1828
1829
1830
1831
1832
1833
1834
1835
1836
1837
1838
1839
1840
1841
1842
1843
1844
1845
1846
1847
1848
1849
1850
1851
1852
1853
1854
1855
1856
1857
1858
1859
1860
1861
1862
1863
1864
1865
1866
1867
1868
1869
1870
1871
1872
1873
1874
1875
1876
1877
1878
1879
1880
1881
1882
1883
1884
1885
1886
1887
1888
1889
1890
1891
1892
1893
1894
1895
1896
1897
1898
1899
1900
1901
1902
1903
1904
1905
1906
1907
1908
1909
1910
1911
1912
1913
1914
1915
1916
1917
1918
1919
1920
1921
1922
1923
1924
1925
1926
1927
1928
1929
1930
1931
1932
1933
1934
1935
1936
1937
1938
1939
1940
1941
1942
1943
1944
1945
1946
1947
1948
1949
1950
1951
1952
1953
1954
1955
1956
1957
1958
1959
1960
1961
1962
1963
1964
1965
1966
1967
1968
1969
1970
1971
1972
1973
1974
1975
1976
1977
1978
1979
1980
1981
1982
1983
1984
1985
1986
1987
1988
1989
1990
1991
1992
1993
1994
1995
1996
1997
1998
1999
2000
2001
2002
2003
2004
2005
2006
2007
2008
2009
2010
2011
2012
2013
2014
2015
2016
2017
2018
2019
2020
2021
2022
2023
2024
2025
2026
2027
2028
2029
2030
2031
2032
2033
2034
2035
2036
2037
2038
2039
2040
2041
2042
2043
2044
2045
2046
2047
2048
2049
2050
2051
2052
2053
2054
2055
2056
2057
2058
2059
2060
2061
2062
2063
2064
2065
2066
2067
2068
2069
2070
2071
2072
2073
2074
2075
2076
2077
2078
2079
2080
2081
2082
2083
2084
2085
2086
2087
2088
2089
2090
2091
2092
2093
2094
2095
2096
2097
2098
2099
2100
2101
2102
2103
2104
2105
2106
2107
2108
2109
2110
2111
2112
2113
2114
2115
2116
2117
2118
2119
2120
2121
2122
2123
2124
2125
2126
2127
2128
2129
2130
2131
2132
2133
2134
2135
2136
2137
2138
2139
2140
2141
2142
2143
2144
2145
2146
2147
2148
2149
2150
2151
2152
2153
2154
2155
2156
2157
2158
2159
2160
2161
2162
2163
2164
2165
2166
2167
2168
2169
2170
2171
2172
2173
2174
2175
2176
2177
2178
2179
2180
2181
2182
2183
2184
2185
2186
2187
2188
2189
2190
2191
2192
2193
2194
2195
2196
2197
2198
2199
2200
2201
2202
2203
2204
2205
2206
2207
2208
2209
2210
2211
2212
2213
2214
2215
2216
2217
2218
2219
2220
2221
2222
2223
2224
2225
2226
2227
2228
2229
2230
2231
2232
2233
2234
2235
2236
2237
2238
2239
2240
2241
2242
2243
2244
2245
2246
2247
2248
2249
2250
2251
2252
2253
2254
2255
2256
2257
2258
2259
2260
2261
2262
2263
2264
2265
2266
2267
2268
2269
2270
2271
2272
2273
2274
2275
2276
2277
2278
2279
2280
2281
2282
2283
2284
2285
2286
2287
2288
2289
2290
2291
2292
2293
2294
2295
2296
2297
2298
2299
2300
2301
2302
2303
2304
2305
2306
2307
2308
2309
2310
2311
2312
2313
2314
2315
2316
2317
2318
2319
2320
2321
2322
2323
2324
2325
2326
2327
2328
2329
2330
2331
2332
2333
2334
2335
2336
2337
2338
2339
2340
2341
2342
2343
2344
2345
2346
2347
2348
2349
2350
2351
2352
2353
2354
2355
2356
2357
2358
2359
2360
2361
2362
2363
2364
2365
2366
2367
2368
2369
2370
2371
2372
2373
2374
2375
2376
2377
2378
2379
2380
2381
2382
2383
2384
2385
2386
2387
2388
2389
2390
2391
2392
2393
2394
2395
2396
2397
2398
2399
2400
2401
2402
2403
2404
2405
2406
2407
2408
2409
2410
2411
2412
2413
2414
2415
2416
2417
2418
2419
2420
2421
2422
2423
2424
2425
2426
2427
2428
2429
2430
2431
2432
2433
2434
2435
2436
2437
2438
2439
2440
2441
2442
2443
2444
2445
2446
2447
2448
2449
2450
2451
2452
2453
2454
2455
2456
2457
2458
2459
2460
2461
2462
2463
2464
2465
2466
2467
2468
2469
2470
2471
2472
2473
2474
2475
2476
2477
2478
2479
2480
2481
2482
2483
2484
2485
2486
2487
2488
2489
2490
2491
2492
2493
2494
2495
2496
2497
2498
2499
2500
2501
2502
2503
2504
2505
2506
2507
2508
2509
2510
2511
2512
2513
2514
2515
2516
2517
2518
2519
2520
2521
2522
2523
2524
2525
2526
2527
2528
2529
2530
2531
2532
2533
2534
2535
2536
2537
2538
2539
2540
2541
2542
2543
2544
2545
2546
2547
2548
2549
2550
2551
2552
2553
2554
2555
2556
2557
2558
2559
2560
2561
2562
2563
2564
2565
2566
2567
2568
2569
2570
2571
2572
2573
2574
2575
2576
2577
2578
2579
2580
2581
2582
2583
2584
2585
2586
2587
2588
2589
2590
2591
2592
2593
2594
2595
2596
2597
2598
2599
2600
2601
2602
2603
2604
2605
2606
2607
2608
2609
2610
2611
2612
2613
2614
2615
2616
2617
2618
2619
2620
2621
2622
2623
2624
2625
2626
2627
2628
2629
2630
2631
2632
2633
2634
2635
2636
2637
2638
2639
2640
2641
2642
2643
2644
2645
2646
2647
2648
2649
2650
2651
2652
2653
2654
2655
2656
2657
2658
2659
2660
2661
2662
2663
2664
2665
2666
2667
2668
2669
2670
2671
2672
2673
2674
2675
2676
2677
2678
2679
2680
2681
2682
2683
2684
2685
2686
2687
2688
2689
2690
2691
2692
2693
2694
2695
2696
2697
2698
2699
2700
2701
2702
2703
2704
2705
2706
2707
2708
2709
2710
2711
2712
2713
2714
2715
2716
2717
2718
2719
2720
2721
2722
2723
2724
2725
2726
2727
2728
2729
2730
2731
2732
2733
2734
2735
2736
2737
2738
2739
2740
2741
2742
2743
2744
2745
2746
2747
2748
2749
2750
2751
2752
2753
2754
2755
2756
2757
2758
2759
2760
2761
2762
2763
2764
2765
2766
2767
2768
2769
2770
2771
2772
2773
2774
2775
2776
2777
2778
2779
2780
2781
2782
2783
2784
2785
2786
2787
2788
2789
2790
2791
2792
2793
2794
2795
2796
2797
2798
2799
2800
2801
2802
2803
2804
2805
2806
2807
2808
2809
2810
2811
2812
2813
2814
2815
2816
2817
2818
2819
2820
2821
2822
2823
2824
2825
2826
2827
2828
2829
2830
2831
2832
2833
2834
2835
2836
2837
2838
2839
2840
2841
2842
2843
2844
2845
2846
2847
2848
2849
2850
2851
2852
2853
2854
2855
2856
2857
2858
2859
2860
2861
2862
2863
2864
2865
2866
2867
2868
2869
2870
2871
2872
2873
2874
2875
2876
2877
2878
2879
2880
2881
2882
2883
2884
2885
2886
2887
2888
2889
2890
2891
2892
2893
2894
2895
2896
2897
2898
2899
2900
2901
2902
2903
2904
2905
2906
2907
2908

```

## 8.2 RTD Input Channel Testing

### 8.2.1 Noise Histogram

The peak-to-peak noise of the acquisition system can be approximated from an output code histogram. The RTD was replaced with a high precision resistor of 0.01% tolerance. ADS1220 was configured for a data rate of 20 SPS. Then, 1000 samples were recorded by the TIVA MCU to generate the histogram plot shown in Figure 62. The peak-to-peak spread of the codes in the histogram is roughly 70 codes. Equation 50 calculates the Least-Significant Bit (LSB) size of the ADC, which is then used to translate the peak-to-peak noise voltage in Equation 51.

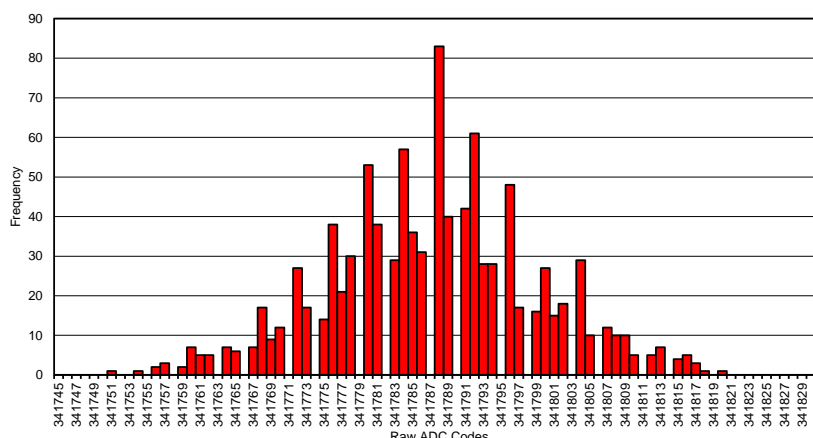


Figure 62. Raw ADC Code Distribution Histogram for RTD Input

$$1\text{LSB} = \frac{2 \times V_{\text{REF}} / \text{PGA}}{2^{24} - 1} = \frac{2 \times 2.49\text{V} / 8}{2^{24} - 1} = 37.104 \text{ nV} \quad (50)$$

$$\text{Input Referred Noise (PP)} = \text{ADC Code Spread} \times 1\text{LSB} = 70 \times 37.104 \text{ nV} = 2.5973 \text{ } \mu\text{V} \quad (51)$$

The noise can be further reduced by applying averaging or filtering in the software. The peak-to-peak input referred noise of the ADC can be used to calculate the total noise in degrees Celsius as given in Equation 52.

$$\text{Noise Free Resolution} = \frac{\text{Peak - to - Peak Input Referred Noise}}{\text{PT100 Sensitivity} \times \text{Excitation Current}} = \frac{2.5973 \text{ } \mu\text{V}}{0.385 \text{ } \Omega / \text{ } ^\circ\text{C} \times 500 \text{ } \mu\text{A}} = 0.0135 \text{ } ^\circ\text{C} \quad (52)$$

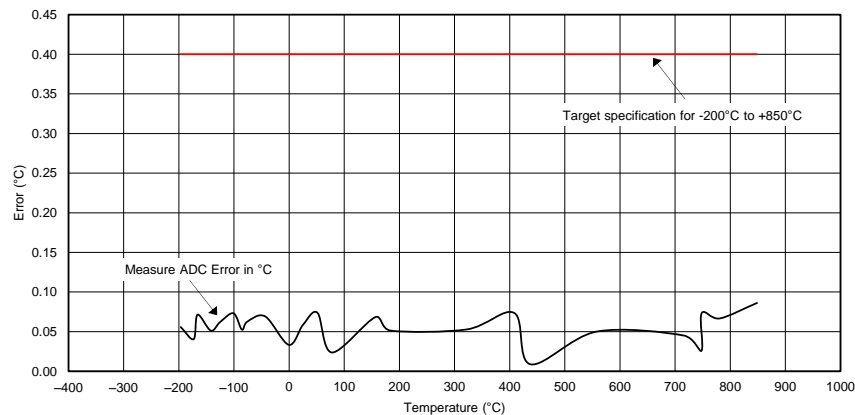
### 8.2.2 Measured ADC Error for RTD Input

To emulate RTD for testing, several high precision resistors (with 0.01% and/or 0.05% tolerance) and their combinations have been used. Their resistance values have been measured again using four wires (4W) resistance measurement method by 6½ digits multimeter and recorded. These measured resistance values are treated as precision reference and converted to their corresponding reference temperatures using the manufacturer's lookup table. Then, precision resistors are connected to the J1 connector. Firmware running in the TIVA MCU based I/O controller evaluation platform controls the ADS1220 to take measurements. The TIVA MCU based I/O controller evaluation platform also sends the measured resistance and corresponding temperature to the GUI for display. Table 8 captures the reference values, measured values, and measurement errors.



**Table 8. Measured ADC Error of RTD Input**

(A)	(B)	(C)	(D)	(E)
PRECISION RESISTANCE VALUES MEASURED BY 6½ DIGIT MULTIMETER (4 WIRE METHOD)	REFERENCE TEMPERATURE CORRESPONDING TO MEASURED RESISTANCE, CALCULATED USING PT100 LOOKUP TABLE LINEAR INTERPOLATION	MEASURED RTD RESISTANCE BY ADC AFTER OFFSET CALIBRATION AND IDAC CHOPPING	CALCULATED TEMPERATURE BY RUNNING PT100 LOOKUP TABLE LINEAR INTERPOLATION ON MEASURED RTD RESISTANCE	MEASURED ADC ERROR (E =  D – B )
20.02	-196.5349	19.996	-196.5907	0.0558
30.06	-173.0238	30.043	-173.0643	0.0405
33.026	-166.0095	32.996	-166.081	0.0714
43.06	-141.9756	43.039	-142.0268	0.0512
49.894	-125.3952	49.868	-125.4571	0.0619
59.932	-100.8	59.902	-100.8732	0.0732
66.078	-85.58	66.057	-85.6325	0.0525
69.953	-75.9425	69.928	-76.005	0.0625
82.954	-43.3231	82.927	-43.3923	0.0692
99.81	-0.4872	99.797	-0.5205	0.0333
109.962	25.5949	109.939	25.5359	0.059
120.01	51.6053	119.982	51.5316	0.0737
130.03	77.7105	130.021	77.6868	0.0237
159.89	156.8684	159.864	156.8	0.0684
169.93	183.9189	169.911	183.8676	0.0514
219.94	322.25	219.921	322.1972	0.0528
249.96	408.3529	249.935	408.2794	0.0735
259.97	437.6176	259.967	437.6088	0.0088
259.97	437.6176	259.965	437.6029	0.0147
299.86	557.25	299.844	557.2	0.05
350.01	715.2903	349.996	715.2452	0.0452
359.94	747.7097	359.932	747.6839	0.0258
360.07	748.1333	360.048	748.06	0.0733
369.99	780.9333	369.97	780.8667	0.0667
390.07	848.5862	390.045	848.5	0.0862

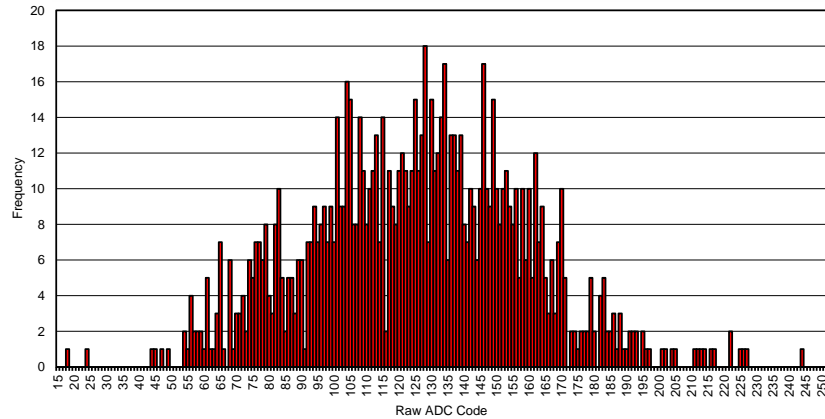

**Figure 63. Measured Error of RTD Input across Temperature Range of -200°C to 850°C**

The overall accuracy can be further improved by calibration at the system level.

### 8.3 Thermocouple Input Channel Testing

#### 8.3.1 Noise Histogram

Both the pins of the thermocouple connector shorted together generating 0 mV differential input voltage. ADS1220 was configured for the data rate of 20 SPS. Then, 1000 samples were recorded by the TIVA MCU to generate the histogram plot shown in Figure 64. The peak-to-peak spread of the codes in the histogram is roughly 226 codes. Equation 53 calculates the Least-Significant Bit (LSB) size of the ADC, which is then used to translate the peak-to-peak noise voltage in Equation 54.



**Figure 64. Raw ADC Code Distribution Histogram for Thermocouple Input**

$$1\text{LSB} = \frac{2 \times V_{\text{REF}} / \text{PGA}}{2^{24} - 1} = \frac{2 \times 2.048\text{V} / 32}{2^{24} - 1} = 7.63 \text{ nV} \quad (53)$$

$$\text{Input Referred Noise (PP)} = \text{ADC Code Spread} \times 1\text{LSB} = 226 \times 7.63 \text{ nV} = 1.7244 \mu\text{V} \quad (54)$$

The peak-to-peak input referred noise of the ADC can be used to calculate the total noise in degrees Celsius as given in Equation 55.

$$\text{Noise Free Resolution} = \frac{\text{Peak - to - Peak Input Referred Noise}}{\text{K - Type Thermocouple Sensitivity}} = \frac{1.7244 \mu\text{V}}{40.6 \mu\text{V} / ^\circ\text{C}} = 0.0425 ^\circ\text{C} \quad (55)$$

#### 8.3.2 Measured ADC Error for Thermocouple Input

It is not always possible to test the module with a thermocouple over the entire temperature range in the laboratory. In order to test the module over the entire temperature range in the laboratory, a thermocouple may be replaced with a precision source meter capable of generating all the voltages accurately as produced by the thermocouple itself. The control stations (which contain electronic modules performing control and monitoring tasks) maintain a controlled environment where temperature may vary from 0°C to 60°C. In order to simulate the actual environment where the module is to be used, the module is kept inside a thermal chamber, as shown in Figure 65. This test setup is expected to reveal inaccuracies that arise because of changes to the system board temperature, cold junction temperature, and ADS1220 parameters. The results shown in Figure 66 indicate an approximately 0.8°C drift when the system temperature is varied from 0°C to 60°C. These results include errors as a result of ADS1220 internal reference drift, temperature sensor error, and isothermal errors.

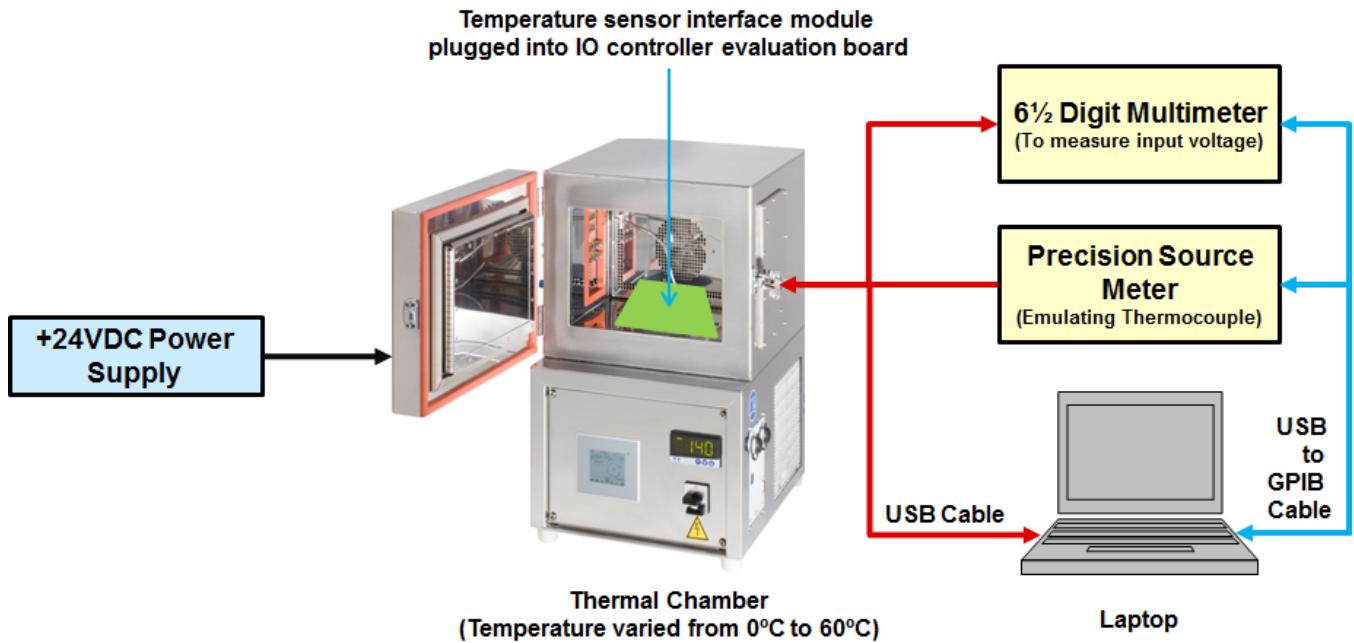


Figure 65. Thermocouple Test Setup with Varying Cold Junction Temperature

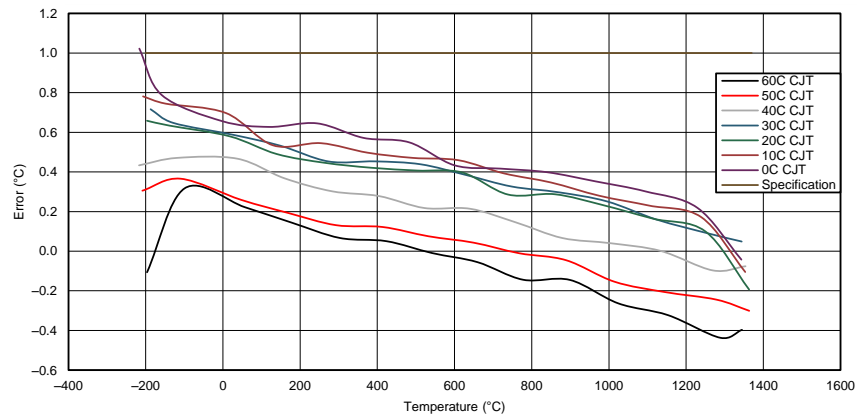


Figure 66. Measured Error of Thermocouple Input across Temperature Range of -200°C to 1372°C

The overall accuracy can be further improved by calibration at system level using a thermal bath and a thermocouple calibrator.

## 9 Bill of Materials

To download the bill of materials (BOM), see the design files at [TIDA-00018](#). Table 9 shows the BOM for the Temperature Sensor Interface Module for Programmable Logic Controllers (PLC).

**Table 9. BOM**

FITTED	DESCRIPTION	DESIGNATOR	MANUFACTURER	PART NUMBER	QUANTITY	RoHS	PACKAGE REFERENCE
Fitted	CAP, CERM, 0.01uF, 50V, +/-10%, X7R, 0603	C1, C4, C38, C46	Kemet	C0603C103K5RACTU	4	Y	0603
Fitted	CAP, CERM, 1000pF, 2KV 10% X7R 1206	C2, C19, C45, C67	Johanson Dielectrics Inc	202R18W102KV4E	4	Y	1206
Fitted	CAP, CERM, 0.47uF, 100V, +/-10%, X7R, 0805	C3	MuRata	GRM21BR72A474KA73L	1	Y	0805
Fitted	CAP, CERM, 1uF, 25V, +/-10%, X7R, 0603	C5, C11, C15, C20, C25, C31, C48, C65	TDK	C1608X7R1E105K080AB	8	Y	0603
Fitted	CAP, CERM, 10uF, 25V, +/-20%, X7R, 1210	C6, C9, C10	TDK	C3225X7R1E106M	3	Y	1210
Fitted	CAP, CERM, 0.1uF, 50V, +/-10%, X7R, 0603	C7	AVX	06035C104KAT2A	1	Y	0603
Fitted	CAP, CERM, 3300pF, 50V, +/-10%, X7R, 0603	C8	MuRata	GRM188R71H332KA01D	1	Y	0603
Fitted	CAP, CERM, 0.1uF, 50V, +/-10%, X7R, 0603	C12, C50	MuRata	GRM188R71H104KA93D	2	Y	0603
Fitted	CAP, CERM, 0.1uF, 50V, +/-10%, X7R, 0603	C13, C16, C22, C23, C26, C27, C28, C33, C34, C36, C40, C41, C42, C43, C44, C49, C55, C57, C59, C60, C61, C62, C64, C66, C68, C69	Kemet	C0603C104K5RACTU	26	Y	0603
Fitted	CAP, CERM, 4700pF, 50V, +/-10%, X8R, 0603	C14, C24	TDK	C1608X8R1H472K	2	Y	0603
Fitted	CAP, CERM, 0.047uF, 50V, +/-10%, X7R, 0603	C17	TDK	C1608X7R1H473K	1	Y	0603
Fitted	CAP, CERM, 10uF, 35V, +/-20%, X7R, 1210	C18	Taiyo Yuden	GMK325AB7106MM-T	1	Y	1210
Fitted	CAP, CERM, 2.2uF, 100V, +/-10%, X7R, 1210	C21	MuRata	GRM32ER72A225KA35L	1	Y	1210
Fitted	CAP, CERM, 1000pF, 100V, +/-20%, X7R, 0603	C29	AVX	06031C102MAT2A	1	Y	0603
Fitted	CAP, CERM, 0.47uF, 25V, +/-10%, X7R, 0603	C32	MuRata	GRM188R71E474KA12D	1	Y	0603
Fitted	CAP, CERM, 1uF, 25V, +/-10%, X7R, 0603	C37	MuRata	GRM188R71E105KA12D	1	Y	0603
Fitted	CAP CER 1000PF 100V 10% X7R 1206	C39, C47, C51, C54, C58, C63	Yageo	CC1206KRX7R0BB102	6	Y	1206
Fitted	CAP, CERM, 3300pF, 50V, +/-10%, X7R, 0603	C52, C56	Kemet	C0603C332K5RACTU	2	Y	0603

**Table 9. BOM (continued)**

FITTED	DESCRIPTION	DESIGNATOR	MANUFACTURER	PART NUMBER	QUANTITY	RoHS	PACKAGE REFERENCE
Fitted	CAP. CERM, 0.033uF, 50V, +/- 10%, X7R, 0603	C53	MuRata	GRM188R71H333KA61D	1	Y	0603
Fitted	Diode, Schottky, 200V, 1A, PowerDI123	D1, D3, D11	Diodes Inc.	DFLS1200-7	3	Y	PowerDI123
Fitted	DIODE ZENER 5.4V 1W PMDS	D2, D12	Rohm Semiconductor	PTZTE255.1B	2		DO-214AC, SMA
Fitted	TVS DIODE 11.1VWM 18.2VC SMD	D4, D5, D7, D9, D18, D21	Littelfuse Inc	P4SMA13CA	6		SMA
Fitted	Diode, P-N, 70V, 0.2A, SOT-323	D6, D10, D16, D17, D19, D20	Diodes Inc	DESD1P0RFW-7	6	Y	SOT-323
Fitted	LED SmartLED Green 570NM	D8, D13, D14	OSRAM	LG L29K-G2J1-24-Z	3		0603
Fitted	Diode, Schottky, 45V, 0.1A, SOD-523	D15	Diodes Inc.	SDM10U45-7-F	1	Y	SOD-523
Fitted	FERRITE CHIP 1000 OHM 100MA 0603	FB1, FB2, FB3, FB4, FB5, FB6	Murata Electronics North America	BLM18HG102SN1D	6	Y	0603
Fitted	CONN TERM BLOCK 2.54MM 4POS PCB	J1	On Shore Technology Inc	OSTVN04A150	1	Y	Header 4x1 keyed
Fitted	Circuit board mini connectors, type K	J2	OMEGA	PCC-SMP-K-5	1		
Fitted	Receptacle, 0.8mm, 25x2, SMT	J3	Samtec	ERF8-025-05.0-L-DV-K-TR	1	Y	25x2 Socket Strip
Fitted	Inductor, Wirewound, Ferrite, 6.8uH, 0.85A, 0.24 ohm, SMD	L1	MuRata	LQH32PN6R8NN0	1	Y	1210
Fitted	MOSFET, N-CH, 60V, 50A, SON 5x6mm	Q1	Texas Instruments Inc	CSD18537NQ5A	1	Y	SON 5x6mm
Fitted	RES, 14.7k ohm, 1%, 0.1W, 0603	R1	Yageo America	RC0603FR-0714K7L	1	Y	0603
Fitted	RES, 110k ohm, 1%, 0.1W, 0603	R2	Vishay-Dale	CRCW0603110KFKEA	1	Y	0603
Fitted	RES, 47.5k ohm, 1%, 0.1W, 0603	R3	Yageo America	RC0603FR-0747K5L	1	Y	0603
Fitted	RES, 2.0 ohm, 5%, 0.125W, 0805	R4	Panasonic	ERJ-6GEYJ2R0V	1	Y	0805
Fitted	RES, 75.0k ohm, 1%, 0.1W, 0603	R5	Vishay-Dale	CRCW060375K0FKEA	1	Y	0603
Fitted	RES, 6.34k ohm, 1%, 0.1W, 0603	R6	Vishay-Dale	CRCW06036K34FKEA	1	Y	0603
Fitted	RES, 137k ohm, 1%, 0.1W, 0603	R7	Vishay-Dale	CRCW0603137KFKEA	1	Y	0603
Fitted	RES, 46.4k ohm, 1%, 0.1W, 0603	R8	Yageo America	RC0603FR-0746K4L	1	Y	0603
Fitted	RES, 4.12k ohm, 0.1%, 0.1W, 0603	R9, R13	Susumu Co Ltd	RG1608P-4121-B-T5	2	Y	0603
Fitted	RES, 10.0k ohm, 0.1%, 0.1W, 0603	R10	Yageo America	RT0603BRD0710KL	1	Y	0603
Fitted	RES 249 OHM 1/10W 1% 0402 SMD	R11, R12, R40, R41, R43, R44	Panasonic Electronic Components	ERJ-2RKF2490X	6	Y	0402
Fitted	RES, 300 ohm, 5%, 0.1W, 0603	R14, R20, R30	Vishay-Dale	CRCW0603300RJNEA	3	Y	0603
Fitted	RES, 47 ohm, 5%, 0.1W, 0603	R15, R24, R25, R27, R28	Vishay-Dale	CRCW060347R0JNEA	5	Y	0603
Fitted	RES, 0.02 ohm, 1%, 1W, 1206	R16	Susumu Co Ltd	PRL1632-R020-F-T1	1	Y	1206

**Table 9. BOM (continued)**

FITTED	DESCRIPTION	DESIGNATOR	MANUFACTURER	PART NUMBER	QUANTITY	RoHS	PACKAGE REFERENCE
Fitted	RES, 4.7k ohm, 5%, 0.1W, 0603	R17, R35, R36	Yageo America	RC0603JR-074K7L	3	Y	0603
Fitted	RES, 71.5k ohm, 1%, 0.1W, 0603	R18	Vishay-Dale	CRCW060371K5FKEA	1	Y	0603
Fitted	RES, 56k ohm, 5%, 0.1W, 0603	R19	Yageo America	RC0603JR-0756KL	1	Y	0603
Fitted	RES, 14.7k ohm, 1%, 0.1W, 0603	R22	Vishay-Dale	CRCW060314K7FKEA	1	Y	0603
Fitted	RES, 1.00k ohm, 1%, 0.1W, 0603	R23	Vishay-Dale	CRCW06031K00FKEA	1	Y	0603
Fitted	RES, 1.0Meg ohm, 5%, 0.1W, 0603	R26, R29	Vishay-Dale	CRCW06031M00JNEA	2	Y	0603
Fitted	RES, 1.5k ohm, 5%, 0.063W, 0402	R31, R32, R33, R34	Vishay-Dale	CRCW04021K50JNED	4	Y	0402
Fitted	RES 2.49K OHM 1/4W 0.1% 1206	R37	Vishay-Dale	TNPW12062K49BEEA	1	Y	1206
Fitted	RES, 4.70k ohm, 0.1%, 0.1W, 0603	R38, R39	Susumu Co Ltd	RG1608P-472-B-T5	2	Y	0603
Fitted	RES, 95.3k ohm, 1%, 0.1W, 0603	R42	Vishay-Dale	CRCW060395K3FKEA	1	Y	0603
Fitted	RES, 499 ohm, 1%, 0.1W, 0603	R45, R47	Vishay-Dale	CRCW0603499RFKEA	2	Y	0603
Fitted	RES, 7.50k ohm, 1%, 0.1W, 0603	R46	Vishay-Dale	CRCW06037K50FKEA	1	Y	0603
Fitted	TRANSFORMER, ER9.5 PACKAGE, 260uH	T1	WURTH ELEKTRONIK	750342304	1	Y	ER9.5
Fitted	100V, 600mA Constant On-Time Synchronous Buck Regulator, DDA0008B	U1	Texas Instruments Inc	LM5017MRE/NOPB	1	Y	DDA0008B
Fitted	IC REG LDO ADJ .15A 8MSOP	U2	Texas Instruments Inc	TPS7A4901DGNR	1	Y	MSOP8
Fitted	1-O DUAL SPDT ANALOG SWITCH 5-V/3.3-V 2-CHANNEL 2:1 MULTIPLEXER/DE MULTIPLEXER, DGS0010A	U3, U7	Texas Instruments Inc	TS5A23159DGS	2	Y	DGS0010A
Fitted	50 mA, 24 V, 3.2-mA Supply Current Low-Dropout Linear Regulator, DCK0005A	U4	Texas Instruments Inc	TPS71533DCK	1	Y	DCK0005A
Fitted	low power, low noise analog to digital converter	U5	Texas Instruments Inc	ADS1220IPWR	1		TSSOP
Fitted	Positive High Voltage Hot Swap / Inrush Current Controller with Power Limiting, 10-pin MSOP, Pb-Free	U6	National Semiconductor	LM5069MM-2/NOPB	1	Y	MUB10A
Fitted	IC, 0.5 ° C Digital Out Temperature Sensor	U8	Texas Instruments Inc	TMP275AIDGK	1		MSOP-8
Fitted	4242-VPK Small-Footprint and Low-Power Quad Channels Digital Isolators, DBQ0016A	U9	Texas Instruments Inc	ISO7141CCDBQ	1	Y	DBQ0016A

**Table 9. BOM (continued)**

FITTED	DESCRIPTION	DESIGNATOR	MANUFACTURER	PART NUMBER	QUANTITY	RoHS	PACKAGE REFERENCE
Fitted	1.5V, Multi-Gain Analog Temperature Sensor with Class-AB Output, 5-pin SC-70, Pb-Free	U10	National Semiconductor	LM94022QBIMG/NOPB	1	Y	MAA05A
Fitted	IC DGTL ISO 3CH I2C 8SOIC	U11	Texas Instruments Inc	ISO1541DR	1	Y	8-SOIC
Fitted	IC I/O EXPANDER I2C 8B 16TSSOP	U12	Texas Instruments Inc	TCA6408APWR	1	Y	16-TSSOP
Fitted	IC, EEPROM, 2KBIT, 1MHZ, SOIC-8	U13	Atmel	AT24C02C-SSHM-B	1	Y	SOIC-8
Not Fitted	CAP, CERM, 0.1uF, 50V, +/-10%, X7R, 0603	C30	Kemet	C0603C104K5RACTU	0	Y	0603
Not Fitted	CAP, CERM, 1uF, 25V, +/-10%, X7R, 0603	C35	TDK	C1608X7R1E105K080AB	0	Y	0603
Not Fitted	RES, 499 ohm, 1%, 0.1W, 0603	R21	Vishay-Dale	CRCW0603499RFKEA	0	Y	0603

## 10 Schematics

To download the Schematics, see the design files at [TIDA-00018](http://TIDA-00018).

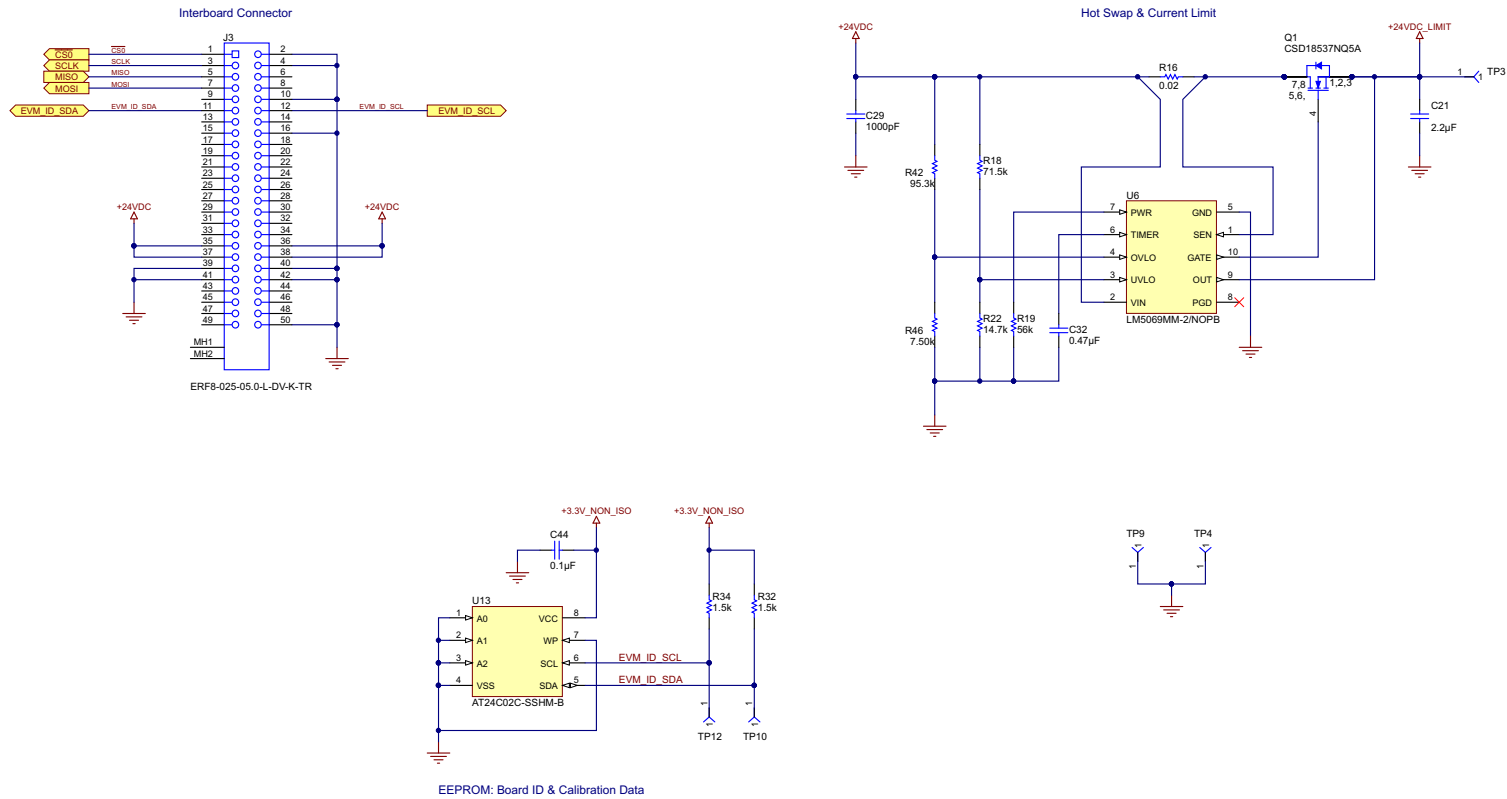


Figure 67. Schematic Sheet 3



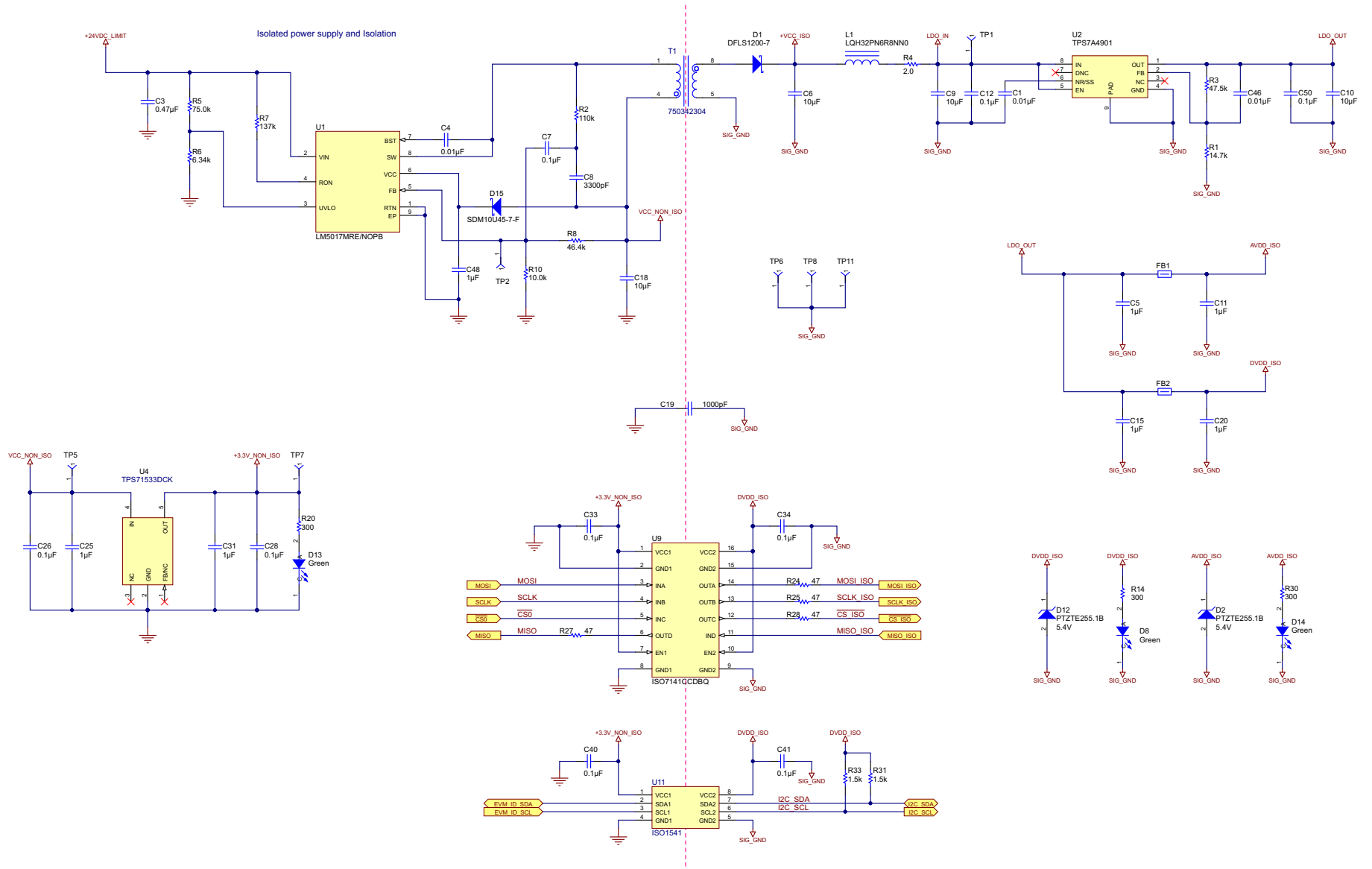
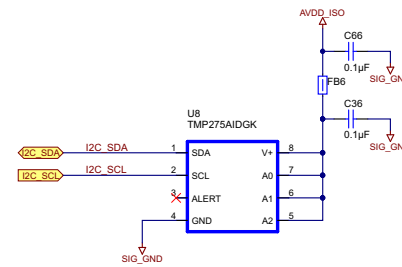
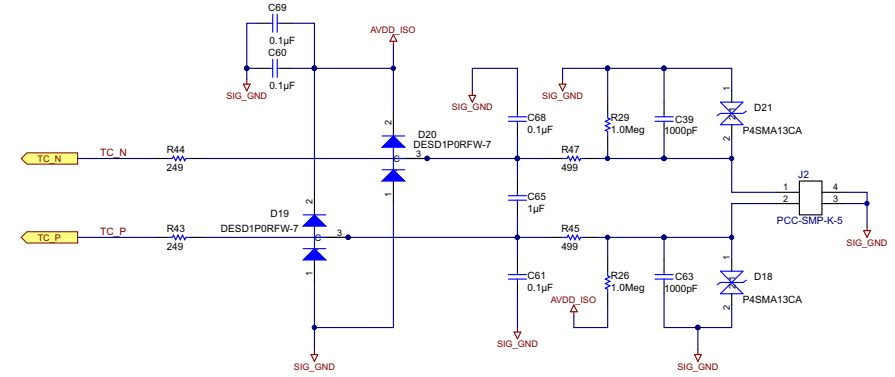
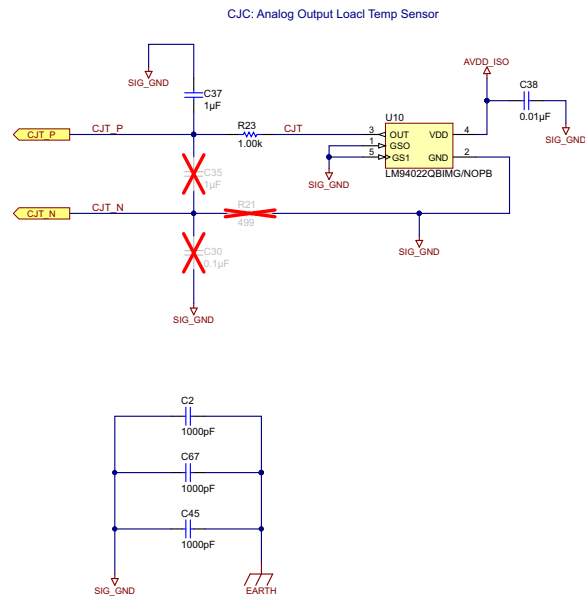


Figure 68. Schematic Sheet 4



CJC: Digital Output Load Temp Sensor

Figure 69. Schematic Sheet 5

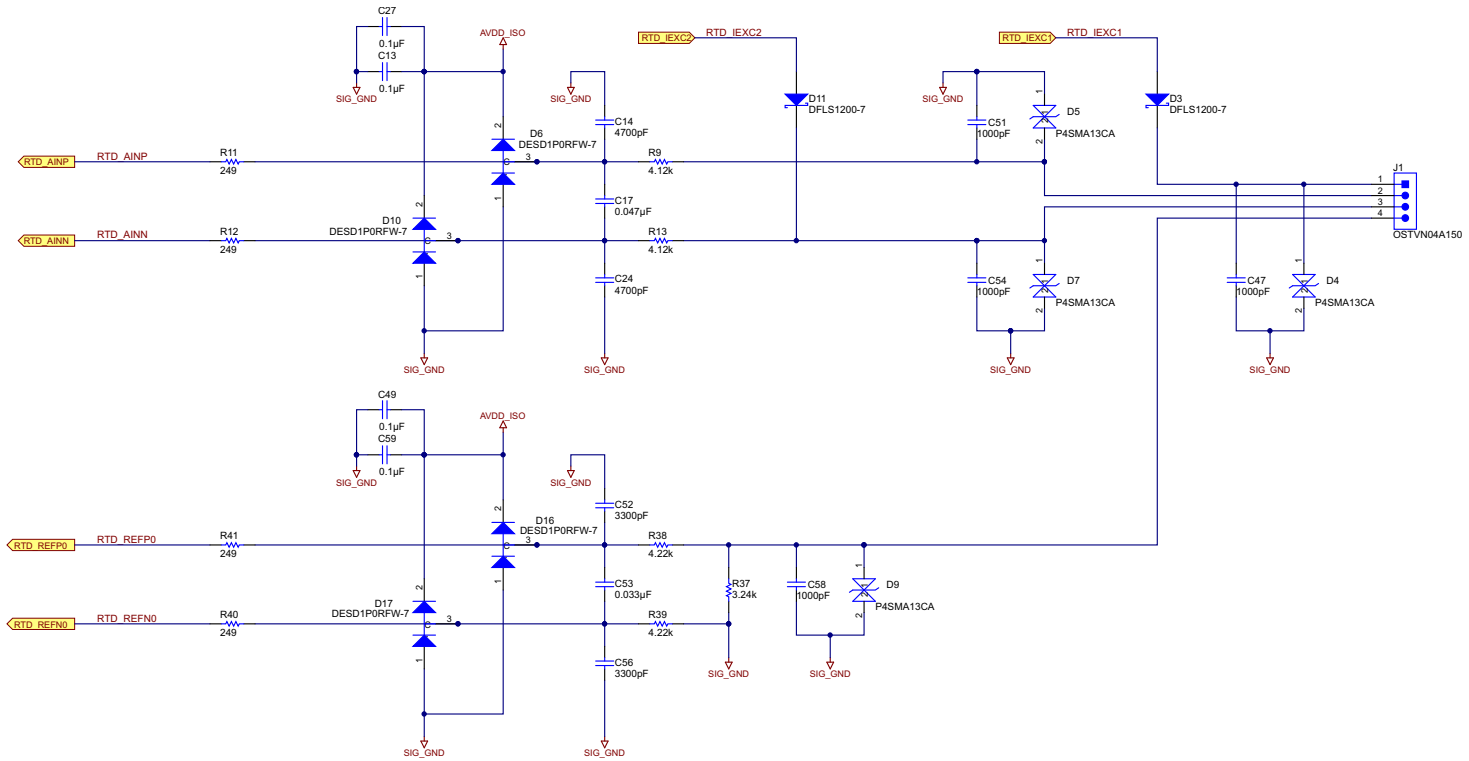


Figure 70. Schematic Sheet 6

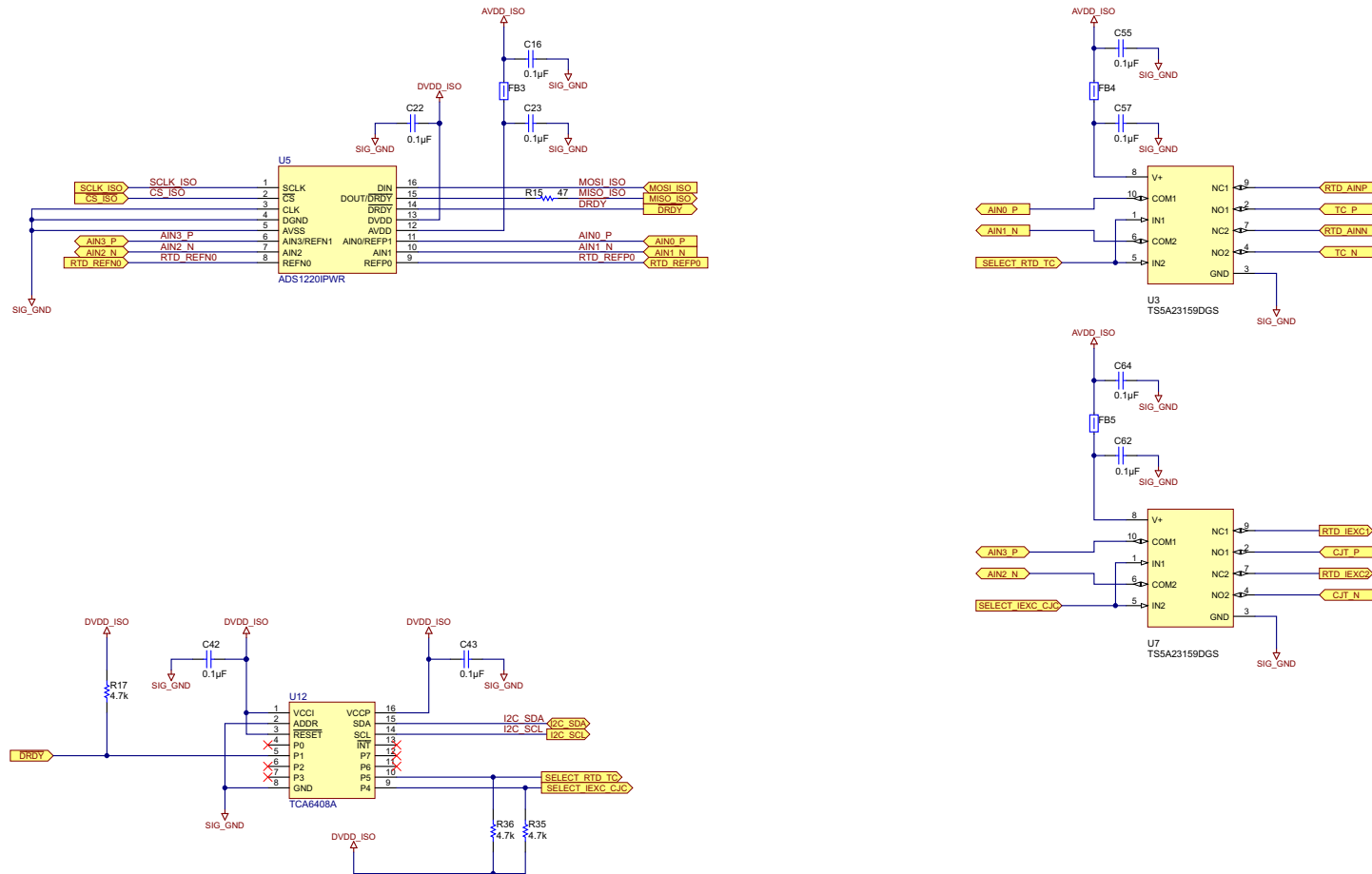


Figure 71. Schematic Sheet 7

## 11 PCB Layer Plots

To download the PCB Layer Plots, see the design files at [TIDA-00018](#).

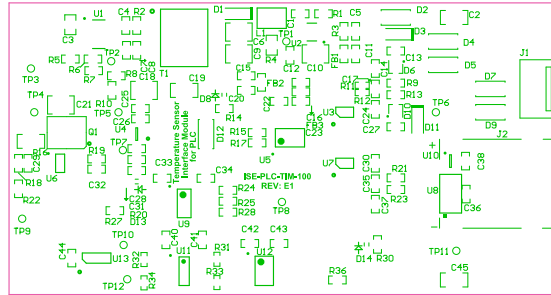


Figure 72. Top Overlay

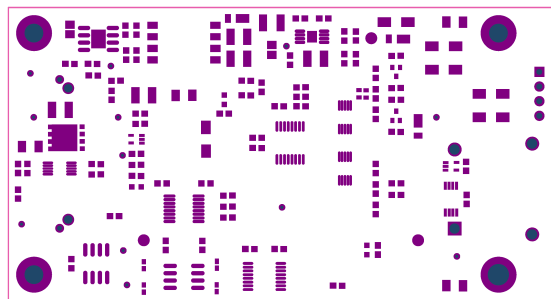


Figure 73. Top Solder

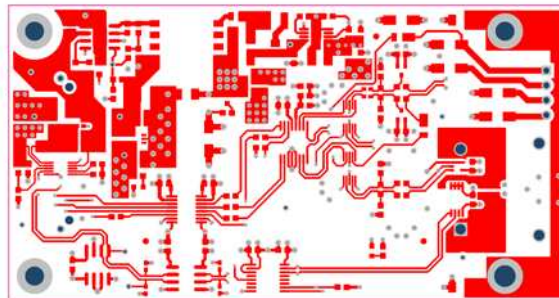


Figure 74. Top Layer

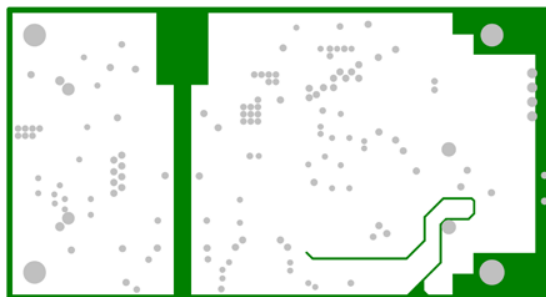
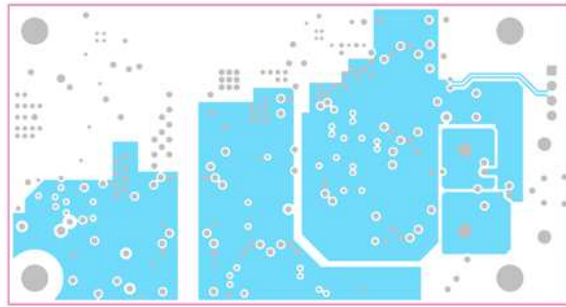
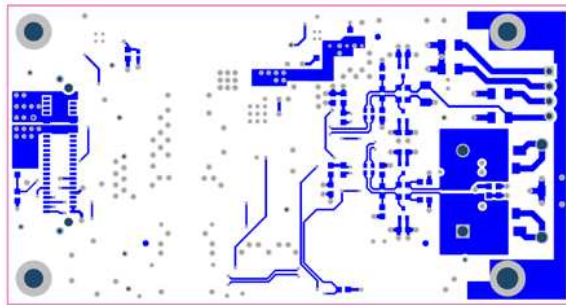


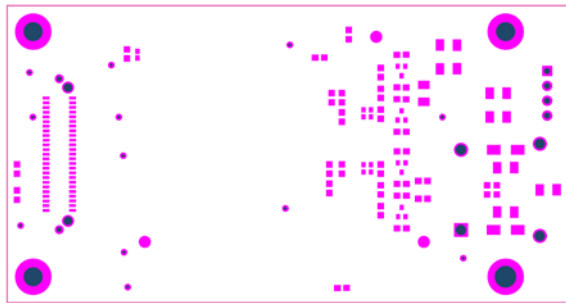
Figure 75. Negative GND Plane



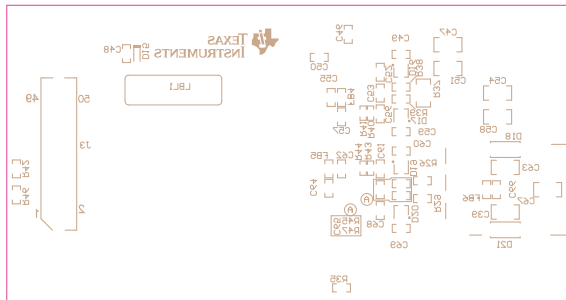
**Figure 76. Power Layer**



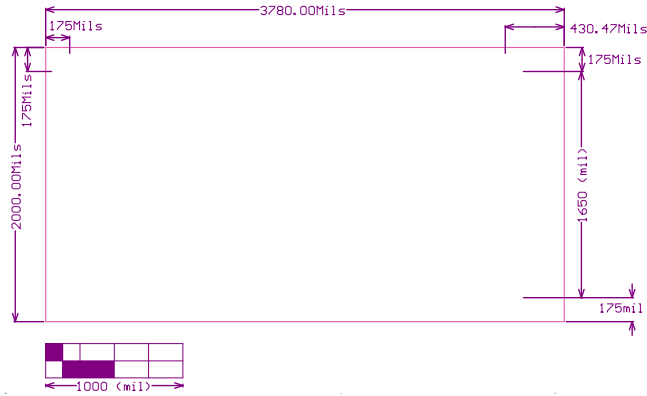
**Figure 77. Bottom Layer**



**Figure 78. Bottom Solder**



**Figure 79. Bottom Overlay**



**Figure 80. Board Dimensions**

## 12 Conclusion

Temperature sensors (such as thermocouples and RTDs) have their own advantages and disadvantages, even when they are widely used across the industrial sector. Thermocouples and RTDs generally have long wires running to a monitoring room or station. Thermocouples and RTDs generate weak analog output signals, which make measurement more difficult. *Clearly, it requires precise sensor excitation, high resolution, low noise, low drift, low power, and small size  $\Delta\Sigma$  ADC to perform the temperature sensing task.* ADS1220 becomes an ideal choice for the DC sensing application as ADS1220 is equipped with two differential or four single-ended inputs, a highly flexible input multiplexer, a low noise PGA, two programmable excitation current sources, an internal reference, an internal oscillator, a low side bridge switch, and a precision internal temperature sensor. ADS1220 has a SPI™ compatible interface and is easy to program and use. This Industrial TI Design shows how ADS1220 can be used with thermocouple and RTD in different configurations. This reference design is an effort to provide sufficient information to users who wish to develop a precision temperature measurement solution using ADS1220.

## 13 References

1. *TIDA-0095 RTD Temperature Transmitter for 2-Wire, 4 to 20-mA Current Loop Systems*, [TIDU182](#) Application Report
2. *RTD Ratiometric Measurements and Filtering Using the ADS1148 and ADS1248 Family of Devices*, Application Report [SBAA201](#)
3. *TI Precision Designs: 0-1A, Single-Supply, Low-Side, Current Sensing Solution*, [TIDU040](#)
4. *TI Precision Designs: Verified Design Hardware-Compensated Ratiometric 3-Wire RTD System, 0°C – 100°C, 0.005°C Error*, [TIPD152](#)
5. *TI Precision Designs: Ratiometric 3-Wire RTD Acquisition System, 0 °C – 100 °C, 0.005% FSR*, [SLAU520](#)
6. *Example Temperature Measurement Applications Using the ADS1247 and ADS1248*, Application Report [SBAA180](#)
7. *Signal Conditioning and Linearization of RTD Sensors*, 2011 Texas Instruments Technology Day Presentation, Collin Wells
8. <http://www.omega.com>
9. <https://www.wikipedia.org>

## 14 About the Author

**SHARAD YADAV** is a Systems Engineer at Texas Instruments India where he is responsible for developing reference design solutions for the industrial segment. Sharad has eight years of experience in high-speed digital, mixed-signal boards, low-noise analog, and EMC protection circuit design.

**SANKAR SADASIVAM** is Chief Technologist for Industrial Systems Engineering at Texas Instruments, where he is responsible for architecting and developing reference design solutions for the Industrial segment. Sankar brings to this role his extensive experience in Analog, RF, Wireless, Signal Processing, High-speed Digital and Power electronics. Sankar earned his Master of Science (MS) in Electrical Engineering from the Indian Institute of Technology, Madras.



## IMPORTANT NOTICE FOR TI REFERENCE DESIGNS

Texas Instruments Incorporated ("TI") reference designs are solely intended to assist designers ("Buyers") who are developing systems that incorporate TI semiconductor products (also referred to herein as "components"). Buyer understands and agrees that Buyer remains responsible for using its independent analysis, evaluation and judgment in designing Buyer's systems and products.

TI reference designs have been created using standard laboratory conditions and engineering practices. **TI has not conducted any testing other than that specifically described in the published documentation for a particular reference design.** TI may make corrections, enhancements, improvements and other changes to its reference designs.

Buyers are authorized to use TI reference designs with the TI component(s) identified in each particular reference design and to modify the reference design in the development of their end products. HOWEVER, NO OTHER LICENSE, EXPRESS OR IMPLIED, BY ESTOPPEL OR OTHERWISE TO ANY OTHER TI INTELLECTUAL PROPERTY RIGHT, AND NO LICENSE TO ANY THIRD PARTY TECHNOLOGY OR INTELLECTUAL PROPERTY RIGHT, IS GRANTED HEREIN, including but not limited to any patent right, copyright, mask work right, or other intellectual property right relating to any combination, machine, or process in which TI components or services are used. Information published by TI regarding third-party products or services does not constitute a license to use such products or services, or a warranty or endorsement thereof. Use of such information may require a license from a third party under the patents or other intellectual property of the third party, or a license from TI under the patents or other intellectual property of TI.

TI REFERENCE DESIGNS ARE PROVIDED "AS IS". TI MAKES NO WARRANTIES OR REPRESENTATIONS WITH REGARD TO THE REFERENCE DESIGNS OR USE OF THE REFERENCE DESIGNS, EXPRESS, IMPLIED OR STATUTORY, INCLUDING ACCURACY OR COMPLETENESS. TI DISCLAIMS ANY WARRANTY OF TITLE AND ANY IMPLIED WARRANTIES OF MERCHANTABILITY, FITNESS FOR A PARTICULAR PURPOSE, QUIET ENJOYMENT, QUIET POSSESSION, AND NON-INFRINGEMENT OF ANY THIRD PARTY INTELLECTUAL PROPERTY RIGHTS WITH REGARD TO TI REFERENCE DESIGNS OR USE THEREOF. TI SHALL NOT BE LIABLE FOR AND SHALL NOT DEFEND OR INDEMNIFY BUYERS AGAINST ANY THIRD PARTY INFRINGEMENT CLAIM THAT RELATES TO OR IS BASED ON A COMBINATION OF COMPONENTS PROVIDED IN A TI REFERENCE DESIGN. IN NO EVENT SHALL TI BE LIABLE FOR ANY ACTUAL, SPECIAL, INCIDENTAL, CONSEQUENTIAL OR INDIRECT DAMAGES, HOWEVER CAUSED, ON ANY THEORY OF LIABILITY AND WHETHER OR NOT TI HAS BEEN ADVISED OF THE POSSIBILITY OF SUCH DAMAGES, ARISING IN ANY WAY OUT OF TI REFERENCE DESIGNS OR BUYER'S USE OF TI REFERENCE DESIGNS.

TI reserves the right to make corrections, enhancements, improvements and other changes to its semiconductor products and services per JESD46, latest issue, and to discontinue any product or service per JESD48, latest issue. Buyers should obtain the latest relevant information before placing orders and should verify that such information is current and complete. All semiconductor products are sold subject to TI's terms and conditions of sale supplied at the time of order acknowledgment.

TI warrants performance of its components to the specifications applicable at the time of sale, in accordance with the warranty in TI's terms and conditions of sale of semiconductor products. Testing and other quality control techniques for TI components are used to the extent TI deems necessary to support this warranty. Except where mandated by applicable law, testing of all parameters of each component is not necessarily performed.

TI assumes no liability for applications assistance or the design of Buyers' products. Buyers are responsible for their products and applications using TI components. To minimize the risks associated with Buyers' products and applications, Buyers should provide adequate design and operating safeguards.

Reproduction of significant portions of TI information in TI data books, data sheets or reference designs is permissible only if reproduction is without alteration and is accompanied by all associated warranties, conditions, limitations, and notices. TI is not responsible or liable for such altered documentation. Information of third parties may be subject to additional restrictions.

Buyer acknowledges and agrees that it is solely responsible for compliance with all legal, regulatory and safety-related requirements concerning its products, and any use of TI components in its applications, notwithstanding any applications-related information or support that may be provided by TI. Buyer represents and agrees that it has all the necessary expertise to create and implement safeguards that anticipate dangerous failures, monitor failures and their consequences, lessen the likelihood of dangerous failures and take appropriate remedial actions. Buyer will fully indemnify TI and its representatives against any damages arising out of the use of any TI components in Buyer's safety-critical applications.

In some cases, TI components may be promoted specifically to facilitate safety-related applications. With such components, TI's goal is to help enable customers to design and create their own end-product solutions that meet applicable functional safety standards and requirements. Nonetheless, such components are subject to these terms.

No TI components are authorized for use in FDA Class III (or similar life-critical medical equipment) unless authorized officers of the parties have executed an agreement specifically governing such use.

Only those TI components that TI has specifically designated as military grade or "enhanced plastic" are designed and intended for use in military/aerospace applications or environments. Buyer acknowledges and agrees that any military or aerospace use of TI components that have **not** been so designated is solely at Buyer's risk, and Buyer is solely responsible for compliance with all legal and regulatory requirements in connection with such use.

TI has specifically designated certain components as meeting ISO/TS16949 requirements, mainly for automotive use. In any case of use of non-designated products, TI will not be responsible for any failure to meet ISO/TS16949.